Aligned Polymer Scaffolds in Periodontal Tissue Engineering

Thesis submitted for the Degree of Doctor of Philosophy

Dalal Hazam Alotaibi

SCHOOL OF CLINICAL DENTISTRY
UNIVERSITY OF SHEFFIELD
UNITED KINGDOM

MAY 2014

وَقُلْ رَبِّ ارْحَمْهُمَا كَمَا رَبَّيَانِي صَغِيرًا

To my parents, Hazam and Sara.

Acknowledgments

I wish to express my sincere gratitude to my lead supervisor Dr. Aileen Crawford for her continuous guidance, support, and help throughout this study. Also, I would like to thank Prof. Gareth Griffiths and Prof. Paul Hatton for their contribution as my co-supervisors. They were all a source of great encouragement for me, and I feel very privileged for working with this supervisory team.

My special thanks to all the laboratory staff for their invaluable guidance, direction, training and scientific expertise during my PhD studies. My thanks go to all of my colleagues and friends, especially for their cooperation and support during this journey. I would also like to acknowledge the financial support and funding obtained from the Saudi Ministry for Higher Education and King Saud University.

My gratitude goes to Dr. Graham Riley for welcoming me into his laboratory at the University of East Anglia and his important contribution to the mechanical loading experiments. My gratitude is also extended to Dr. K Legerlotz and Dr. E Jones for assistance and training provided in the mechanical loading systems used. Thanks also to Fahad Alhakami for his technical advice and expertise in qRT-PCR. Thank you to Nada Alhindi for her friendship, and to all my lovely friends in office at the school for sharing the experience.

My deep gratitude to my parents Hazam and Sara, and my brothers and sisters, Nouf, Bader, Amal, Amjad , Abdullah, Mohammed, Ebtesam and Saud , for their support, motivation, inspiration and love that encouraged me to undertake and complete this PhD. I will be forever in debt to my sister Nouf, for she has been always a role model to follow. I would like to thank my nephews, Mohammed, Omar and Majed for brining joy to my life with their stories and laughs. I would also love to extend thanks to my friends Abeer, Hind, Lubna and Seba who contributed by their love and encouragement. Thank you to Dr. Manosur Assery for his guidance and help throughout my carrier.

Above all, I am thankful to Allah Almighty for His unlimited blessings.

Abstract

Periodontal disease is characterised by progressive gingival inflammation and degradation of the periodontal ligament (PDL) and alveolar bone. Recently, a limited number of studies have started to consider the use of tissue engineering approaches to facilitate periodontal tissue regeneration. Within the wider field of the skeletal bioengineering, research has been directed towards fabrication of aligned-fibre scaffolds and devices for reconstruction of larger ligaments and tendons for use in orthopaedic indications. Mechanical loading and growth factors are also known to influence the quality of engineered load-bearing musculoskeletal tissues; and it is increasingly being acknowledged that appropriate biomechanical cues are essential for appropriate organisation of the extracellular matrix (ECM). The aims of this study were to evalute the effect of fibre-alignment on cell behaviour and investigate the effect of either mechanical loads or growth factors on the quality of the resultant tissue engineered PDL tissue. Synthetic and natural scaffolds were prepared in aligned and random-fibre forms, and human periodontal ligament fibroblasts (HPDLFs) were cultured on these scaffolds and their biological responses were investigated. In aligned-fibre constructs, histochemical and immunochemical staining showed that HPDLFs were elongated in shape and oriented along the long-axis of the fibres and showed evidence of increased ECM deposition. Gene expression data showed that HPDLFs on aligned-fibre scaffolds expressed a more ligament-like phenotype, indicated by an increased expression of collagen type I (COL1A1) and periostin (POSTN) genes over the 20 days culture period. The results showed that static mechanical strain up-regulated the ligamentous genes namely; collagen type I, periostin and scleraxis (SCXA) with greater expression observed in aligned-fibre constructs. These effects were more marked in the aligned-fibre scaffolds. In contrast, Emdogain® (EMD) was found to promote the osteoblastic phenotype of HPDLFs as indicated by the up-regulation of alkaline phosphatase (ALPL) gene expression in the engineered tissue, while transforming growth factor beta 1 (TGF-β1) had more effect on the ligamentous genes (COL1A1, POSTN). This effect of EMD was also potentiated by the fibre-alignment of the scaffolds. EMD and TGF-β1 were observed to have a limited effect on HPDLF proliferation in the aligned-fibre constructs by day 14 of incubation regardless of whether EMD and TGF-β1 were added alone or in combination with each other. Although the exact mechanism by which EMD and TGF-β1 affected cell behaviour is unknown, the data suggested that their effects were heavily dependent on the cell phenotype and stage of differentiation which, in turn was greatly influenced by the alignment of the scaffold fibres. In conclusion, 3D tissue engineered PDL constructs, with good biological quality, can be developed using aligned-fibre scaffolds. These constructs have great potential for us as an *in vitro* model to study PDL regeneration and repair processes and ultimately, may inform research directed at new clinical applications.

Table of Content

List of Abbreviations

µg	Microgram
µl	Micro litre
µm	Micrometre
ACTA2	Actin alpha 2
ADM	Acellular dermal matrix
ALPL	Alkaline phosphatase
Ang	Angiotensinogen
ATP	Adenosine triphosphate
b-FGF	Basic fibroblast growth factor
BGLAP	Bone gamma-carboxyglutamate protein
BMPs	Bone morphogenetic proteins
BMSSCs	Bone marrow stromal stem cells
BSA	Bovine serum albumin
CAL	Clinical attachment loss
Cm	Centimetre
CO2	Carbon dioxide
COL1A1	Collagen type I alpha 1
DMEM	Dulbecco's modified eagle's medium
DNA	Deoxyribonucleic acid
DNase	Deoxyribonuclease
EDTA	Ethylenediamine tetraacetic acid
EGFR	Epidermal growth factor receptor
ERK	Extracellular signal-regulated kinase
FCS	Foetal calf serum
FDA	Food and Drug Administration
FFT	Fast Fourier Transform
FGF	Fibroblast growth factors
g	Gram
G	Gauge
GFs	Gingival fibroblasts
GTR	Guided tissue regeneration
H	Hour
HPDLFs	Human periodontal ligament fibroblasts
Hz	Hertz
IL1	Interleukin 1
IL6	Interleukin 6
IL8	Interleukin 8
JNK	c-Jun NH2-terminal kinase
kDa	kilodalton
kV	kilovolt
MAPKs	Mitogen-Activated Protein
MASH	Mathematics and Statistics Help
MeHA	Methacrylated hydroxylapatite
mg	Milligram
ml	Millilitre
mm	Millimetre
mM	Millimolar
mM	Milimolar
MMP	Matrix metalloproteinases

mRNA	Messenger RNA
MSCs	Mesenchymal stem cells
nm	Nanometre
ºC	Degree centigrade
BGLAP	Osteocalcin
OCT	Optimal cutting temperature
OPG	Osteoprotegerin
OPN	Osteopontin, known also as bone sialoprotein (BSP)
p	Probability
PBS	Phosphate buffered saline
PCL	Poly(e-caprolactone)
PDC	Copoly(ether)esterurethane
PDGFs	Platelet-derived growth factors
PDL	Periodontal ligament
PDLSCs	Periodontal ligament stem cells
PEO	Polyethylene oxide
PEUUR	Poly(ester urethane)urea elastomer
PGA	Poly glycolic acid
pH	Potential of hydrogen
PLA	poly lactic acid
PLLA	Poly(L-lactic acid)
PMMA	Poly(methyl methacrylate)
POSTN	Periostin
PPDLFs	Porcine periodontal ligament fibroblasts
PU	Polyurethane
qRT-PCR	Quantitative real time polymerase chain reaction
RANKL	Receptor activator of nuclear factor-jB ligand
RNA	Ribonucleic acid
RNase	Ribonuclease
RPDLFs	Rat periodontal ligament fibroblasts
rpm	Rounds per minute
RUNX2	Runt-related transcription factor 2
SCXA	Scleraxis homolog A
SD	Standard deviation
SEM	Scanning electron microscopy
TBS	Tris-buffered saline
TBST	Tris-buffered saline containing 0.05% Tween-20
TGF-β1	Transforming growth factor beta 1
TMJ	Temporomandibular joint
TnBP	Tributyl phosphate
TNF	Tumour necrosis factor
V	Voltage
VEGF	Vascular endothelial growth factor
vol/vol	Volume per unit volume
WB	Western blots
wt/vol	Weight per unit volume
α	Alpha
α-SMA	α-smooth muscle actin
β	Beta
β2M	Human beta-2-microglobulin

List of Figures

List of Tables

1. INTRODUCTION

The periodontal ligament (PDL) is a highly specialised connective tissue that supports and holds the teeth in place within the alveolar bone of the jaws. The extracellular matrix (ECM) of the PDL is composed mainly of collagen fibres that are arranged in parallel to each other and run between the alveolar bone and cementum. These collagen fibres are attached to the cementum and alveolar bone via partially mineralised fibres known as Sharpey's fibres. Besides the supporting and structural roles, it is well known that, in general, the extracellular matrix (ECM) of tissues is also a key regulator of cell phenotype and behaviour by providing molecular and topographical signals.

Periodontal disease is a chronic condition characterised by progressive gingival inflammation and degradation of the periodontal ligament and alveolar bone. However, current clinical periodontal treatments, including guided tissue regeneration, can provide acceptable clinical outcomes but do not predictably result in full regeneration of the lost periodontal structures, particularly the periodontal ligament. Full regeneration of periodontal ligament attachment remains a major clinical challenge. Recently, several studies have investigated the use of tissue engineering to facilitate periodontal tissue regeneration and to produce *in vitro* models for studying PDL repair and regeneration. Some interest has been directed towards the construction of aligned-fibre scaffolds which reflect the general topographic arrangement of collagen fibres in the native extracellular matrix of the

periodontal ligament. However, to my knowledge, there is no published work describing the impact of fibre-alignment on periodontal ligament cell activity and extracellular matrix production.

In general, application of appropriate biomechanical cues is essential for ECM organisation and alignment in engineered tissues. Appropriate mechanical loading has been recognised as critical elements in tissue engineering, especially when engineering load-bearing tissues such as ligaments and tendons. Application of appropriate biomechanical cues is essential for ECM organisation in engineered tissues. Applying mechanical loads and growth factors to tendons and ligaments may influence cell proliferation, differentiation, gene expression and protein synthesis. However, there have been few reported studies of the effects of mechanical loading on PDLF behaviour in 3D tissue engineered periodontal ligament constructs. Culture of cells in 3D can also influence their response to growth factor.

Therefore, this study was undertaken to develop a 3D tissue engineered model that resembles the native ECM of periodontal ligament tissue and investigate the effect of fibre-alignment of the scaffold component on PDLF behaviour and phenotype. In addition, the effect of both mechanical strain and growth factors, Emdogain® (EMD) and TGF-β1 on the tissue engineered periodontal ligament model was assessed.

2. LITERATURE REVIEW

2.1 Periodontium

The periodontium is a name given to the specialised tissues that surround and support the teeth in the jaws. The tissues that form the periodontium are the gingiva, periodontal ligament, cementum and alveolar bone (Figure 2-1).

2.1.1 Gingiva

In healthy periodontium the gingiva, which is composed of the overlying epithelium and the underlying connective tissue, forms a definite relationship to the tooth surface and alveolar bone (Bartold et al., 2000). The epithelium is classified into three functional types depending on its position: gingival, sulcuar, and junctional epithelium.

2.1.2 Cementum

The cementum is a mineralised avascular connective tissue that covers the root surfaces. It serves primarily as a site of attachment for the principle collagen fibres via Sharpey's fibres (Nanci, 2008). Cementum is formed simultaneously with the formation of root dentin and in the presence of the epithelial sheath of Hertwig (Bosshardt and Nanci, 2004). It is composed of about 50% mineral and 50% organic matrix. The predominant organic component is collagen type I, which constitutes about 95% of the organic matrix. Other types of collagens also associated with cementum include

Type III collagen, which is found during development and repair/regeneration of cementum, and type XII, a fibril-associated collagen.

Cementum also contains non-collagenous proteins such as osteocalcin, osteopontin, osteonectin, bone sialoprotein, cementum attachment protein (CAP) and cementum protein-23 (CP-23) (Alvarez-Pérez et al., 2006, Pitaru et al., 1995, Bosshardt et al., 1998, McKee et al., 1996). Studies have reported that these proteins play an important role in cementogenesis as well as in periodontal tissue development and regeneration (Shimonishi et al., 2007, Zeichner David, 2006, Saito et al., 2001). Unlike bone and tooth enamel, cementum is relatively permeable (Nanci, 2008, Hassell, 1993).

2.1.3 Alveolar Bone

The alveolar bone is anatomically consisted of the alveolar bone proper and the supporting alveolar bone. The alveolar bone proper is a thin dense compact bone with insert Sharpey's fibres. The supporting alveolar bone is composed of the facial and lingual compact bone and the cancellous trabeculae (Nanci, 2008).

Bone matrix is composed of organic collagen fibres, ground substance and inorganic substance. Mineral content provide stiffness and toughness of bone and collagen fibres provides tensile strength and flexibility. The organic matrix consists mainly of collagen type I and ground substance. Osteoblasts, osteocytes and osteoclasts are the main cells of bone. Also alveolar bone contains mesenchymal stem which concidered as a cell reservoir (Newman et al., 2011).

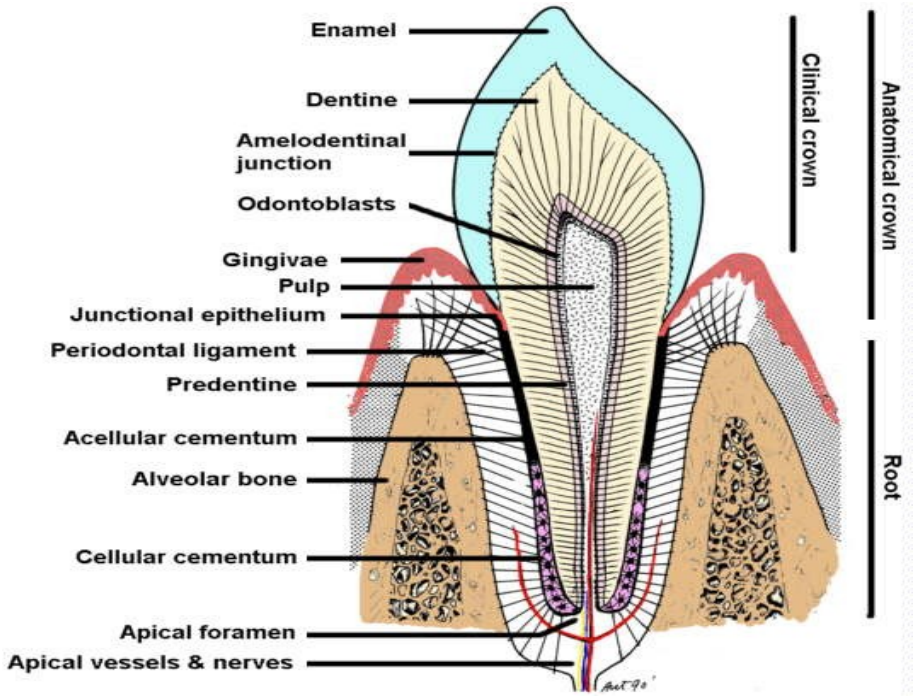

Figure 2-1: Schematic presentation of healthy periodontium (reprinted with permission from A. Jowett el al., 2000).

2.1.4 Periodontal Ligament (PDL)

The periodontal ligament is the soft specialised connective tissue located between the cementum and alveolar bone. The periodontal ligament is derived from the inner layer of the dental follicle (Nanci and Bosshardt, 2006). The main function of periodontal ligament is to support the tooth in the alveolar bone and absorb the masticatory forces and transmit them to the surronding alveolar bone. It also provides lymphatic drainage and blood vessels necessary for the nutrition of the cementum, bone, and gingiva. In addition, the periodontal ligament contains sensory receptors for the proper positioning of the jaws during mastication. It also, acts as a cell reservoir for

tissue homeostasis, repair and regeneration (Pitaru et al., 1987, Nanci, 2008).

The periodontal ligament made of cells and an extracellular matrix of collagenous and noncollagenous constituents. Fibroblasts and undifferentiated mesenchymal cells are known to be involved in periodontal regeneration (Nanci, 2008).

The collagen fibre bundles in the ligament and Sharpey's fibres are mainly composed of collagen type I and III (Huang et al., 1991, Wang et al., 1980). Collagen type V can be found either within the core or the spaces between the fibril bundles , and is implicated in the regulation of fibril diameter of collagen type I (Becker et al., 1991). In addition to collagen type V, the periodontal ligament also contains other minor collagens such as collagen type VI and XII (Becker et al., 1991, Karimbux et al., 1992). Several noncollagenous matrix proteins are also localised within the periodontal ligament e.g. proteoglycans (Hakkinen et al., 1993) and glycoproteins such as undulin, fibronectin and periostin (Zhang et al., 1993).

2.1.4.1 Periodontal Ligament Principal Fibres

The principal fibres of the periodontal ligament are dense collagen fibres thats arranged in bundles and insert into the cementum and bone forming Sharpey's fibres. They are classified into five groups and named based on their location and orientation namely, transseptal group, alveolar crest group, horizontal group and the oblique fibres. Their function is mainly to

retain the tooth in the socket and withstand vertical oriented forces (Newman et al., 2011).

2.1.4.2 Periodontal Ligament Cells

Periodontal Ligament Fibroblast (PDLFs)

Periodontal ligament connective tissues contain many different types of cells, of which the fibroblast is the most numerous. Morphologically, PDLFs are large spindled-shaped cells, with elongated appearance characteristic of fibroblast like cells when examined by both phase contrast or scanning electron microscopy (Somerman 1988, Kuru 1998). Usually PDLFs are aligned along the direction of the collagen fibres. The collagen fibrils are in constant remodelled by the fibroblasts, which are capable of synthesising and degrading collagen which play a major role in periodontal ligament regeneration (McCullouch and Knowles, 1993).

Although most fibroblasts appear similar microscopically e.g. gingival fibroblast (GFs) and PDLFs (Giannopoulou and Cimasoni 1996, Kuru 1998), heterogeneous cell populations exist within fibroblasts from different sources and within fibroblasts from the same source (Bellows et al., 1981, Mariotti and Cochran, 1990, Adams et al., 1993, Kaneda et al., 2006). Gingival fibroblasts and PDLFs are different in size, granularity, proliferative ability, enzyme activity, cell attachment, migration and expression of extracellular molecules (Ivanovski et al., 2001, Giannopoulou and Cimasoni, 1996, Kuru et al., 1998, Otsuka et al., 1988, Somerman et al., 1988).

PDLFs and GFs differ with respect to the production of extracellular matrix components. PDLFs express higher levels of collagen type I, III and fibronectin. They also express muscle differentiation markers mainly α-actin and smooth-muscle myosin more than gingival fibroblasts. Furthermore, PDLFs are unique cells as they display osteoblast-like characteristics, including osteocalcin production and high levels of alkaline phosphatase (Groeneveld et al., 1994, Kuru et al., 1998). Although some secreted matrix proteins and cytoskeletal proteins have been used to characterise PDLFs (Lekic et al., 1996, Groeneveld et al., 1993), there is no specific marker for the PDLF population.

Immunohistological studies showed that non-collagenous matrix proteins associated with mineralised tissue such as bone sialoprotein, osteopontin and osteocalcin, have a distinctive distribution within the periodontium.. Periodontal ligament fibroblasts demonstrated a higher gene expression of osteopontin, osteocalcin and bone sialoprotein compared to gingival fibroblasts (Ivanovski et al., 2001, Nohutcu et al., 1996).

Osteopontin is an adhesion molecule associated with mineralised tissues, but identified also in periodontal ligament (MacNeil et al., 1995). It is considered as an early marker of periodontal tissue regeneration that is linked with cell proliferation and migration in osteogenic and periodontal ligament cell populations (Lekic et al., 1996). Bone sialoprotein, an extracellular matrix protein of mineralised tissue, is expressed after cell proliferation at sites of mineralising bone formation (Lekic et al., 1996). Osteocalcin and bone sialoprotein are all secreted at different stages of

osteogenic cell differentiation (Boskey, 1996). The presence of these proteins supports the concept of osteogenic potential within a subpopulation of PDLFs (Cho et al., 1992, Inanc et al., 2006, Inanc et al., 2007).

Periostin was found to be expressed by PDLFs in the extracellular matrix (Horiuchi et al., 1999). It's expression in periodontal ligament is reported to increase under mechanical loading (Rios et al., 2008). Studies showed that periostin is also involved in the regulation of collagen type I fibrillogenesis and in the remodelling of the collagen matrix in periodontal ligament (Kii et al., 2006, Norris et al., 2007).

Mesenchymal Cells

In periodontal wound healing, the periodontal ligament can contribute not only in its repair but also in regenerate the lost bone and cementum. Recently, stem cells have been isolated from the human periodontal ligament (Seo et al., 2004).

2.2 Periodontal Disease

2.2.1 Definition

Periodontal disease is an inflammatory process that can lead to tooth loss. Gingivitis as an inflamation is assocaiated with changes in the gingival colour, contour and consistency. Gingivitis is a reversible condition if the etiological factors involved are removed.

Periodontitis is characterised by destruction and loss of connective tissue attachment and mineralised tissues. It can be either chronic or aggressive dependent upon the aetiology and the degree of destruction (Armitage, 2004). The severity of periodontal disease is dependent upon the amount of clinical attachment loss (CAL), where 1-2 mm CAL is slight, 3-4 mm CAL is moderate and more than 5 mm is severe periodontitis (Armitage, 1999).

2.2.2 Classification

The International Workshop for a Classification of Periodontal Diseases and Conditions held in 1999 classified periodontal disease into 8 main categories as listed below (Armitage, 1999):

- Gingival diseases
- Chronic periodontitis
- Aggressive periodontitis
- Periodontitis as a manifestation of systemic disease
- Necrotizing periodontal disease
- Abscesses of the periodontium
- Periodontitis associated with endodontic lesion
- Developmental or acquired deformities and conditions

Gingivitis and chronic periodontitis are the most common forms of periodontal disease.

2.2.3 Aetiology

The primary etiological factor of periodontal disease is bacteria. The bacteria involved in periodontal disease are largely gram-negative anaerobic bacilli with some anaerobic cocci and a large quantity of anaerobic spirochetes. The main organisms linked with periodontal lesions are *Porphyromonas gingivalis, Tanerella forsythensis, Aggregatibacter actinomycetemcomitans* and *Treponema denticola (Kilian et al., 2006)*. Although periodontal disease is mainly caused by bacteria, there are environmental factors, such as smoking, obesity, stress and genetic factors which can modulate the inflammatory response of the periodontal tissues (Stabholz et al., 2010). Smoking (Paulander et al., 2004), diabetes mellitus (Chavarry, 2009) and emotional stress (Peruzzo et al., 2007) are considered as risk factors for progression of periodontal disease. These factors can alter the immune response and impair the host's protective mechanisms against the bacterial insult (Kornman, 2008).

2.2.4 Periodontal Therapy

2.2.4.1 Control of Infection

Initial periodontal treatment aims at controlling the infection and eliminating the aetiological factors. This can be achieved by removal of dental plaque and calculus using scaling and root planing with or without conventional surgical approaches such as gingivectomy and open flap surgeries (Cionca et al., 2010). These treatment approaches can show successful clinical outcomes in terms of probing depth reduction and gain of clinical

attachment. However, at the histological level the healing was characterised by a long junctional epithelium and no formation of cementum or periodontal ligament (Caton and Greenstein, 1993). In some cases bone growth may occur, however, an epithelial lining was often interposed between the root surface and the newly formed bone (Caton and Greenstein, 1993).

2.2.4.2 Bone Graft

Bone grafts have been used for many years to treat the bone loss caused by periodontal disease. The concept of a bone graft is to fill the periodontal intrabony defect with one of a number of graft materials including autograft, allograft, xenograft and alloplastic material. These types of bone grafts can promote bone regeneration through the following mechanisms:

- Osteogenesis: the graft contain cells that form the bone matrix, leading to new bone formation.
- Osteoinduction: the graft release growth factors and signalling molecules promoting cells to form new bone.
- Osteoconduction: the graft acts as a scaffold for the host bone to grow on.

In a study with 9 month follow up, improved clinical measures were reported when autograft was used either alone, or in combination with guided tissue regeneration to treat deep intrabony defects, The authors concluded there was no statistically significant difference between the two treatment groups (Nygaard Østby et al., 2008). The patients were followed for 10 years and the results showed more favourable long term outcomes with the combined

therapy of bone and guided tissue regeneration (GTR) therapy compared to bone graft only (Nygaard Østby et al., 2010). Although using bone graft materials for periodontal defects results in some gain in clinical attachment and radiographic evidence of bone fill, histological evaluation reveals that these materials have little osteoinductive capacity and generally become encased in a dense fibrous connective tissue. Currently bone grafts are used mostly as scaffolds in combination with other treatment approaches such as GTR, and use of growth factors and enamel matrix derivatives (Anzai et al., 2010, Sowmya et al., 2010, Esposito et al., 2010).

2.2.4.3 Guided Tissue Regeneration (GTR)

The ultimate aim of periodontal treatments is to regenerate the lost periodontal ligament and supporting bone tissues. The nature of periodontal tissue healing depends mainly on the type of cells that repopulate the root surface at the healing time. Periodontal regeneration take place when the root surface is populated by the undifferentiated mesenchymal cells from the PDL. A novel procedure was proposed by Nyman et al., 1982 using a barrier membrane surgically placed between the connective tissue of the periodontal flap and the root surface in order to allow mesenchymal cells from PDL to repopulate the area. This approach was called guided tissue regeneration (GTR) (Karring et al., 1993, Nyman et al., 1982).

GTR showed improved clinical outcomes in terms of reduced probing depth and clinical attachment gain compared to the conventional open flap debridement. However, the results from GTR are not always predictable and

are very technique sensitive. GTR is still considered as a gold standard technique for periodontal regeneration. A recent study, of 10 years follow up, of deep infrabony defects treated with combined GTR therapy, reported long term improvement of periodontal defects with a significant probing depth reduction and probing bone gain (Nygaard Østby et al., 2010).

2.3 Periodontal Tissue Engineering

Periodontal tissue engineering is a relatively new field with enormous potential to overcome some of the shortcomings in the existing periodontal therapies. The aim of periodontal tissue engineering is to develop procedures and biomaterials to create a periodontal tissue graft *ex vivo* and implant it *in vivo* for the regeneration of functionally active periodontium. It involves three basic components namely: responsive progenitor cells, signalling molecules, and a suitable scaffold support for tissue growth. The cells synthesise extracellular matrix components while the scaffold provides a guide and acts as a 3D template for the new tissue. The function of signalling molecules (e.g. growth factors) is to induce and maintain the required cell phenotype and production of extracellular matrix needed for the developing tissue. A successful periodontal regeneration based on tissue engineering concepts, requires a delicate interaction between these factors (**Figure** 2-2) (Nygaard Østby et al., 2010). The major limitation in achieving periodontal regeneration is identifying the most appropriate form of progenitor cells, signalling molecules, and suitable scaffold support and

controlling the local factors that might impair their function, such as bacterial insult.

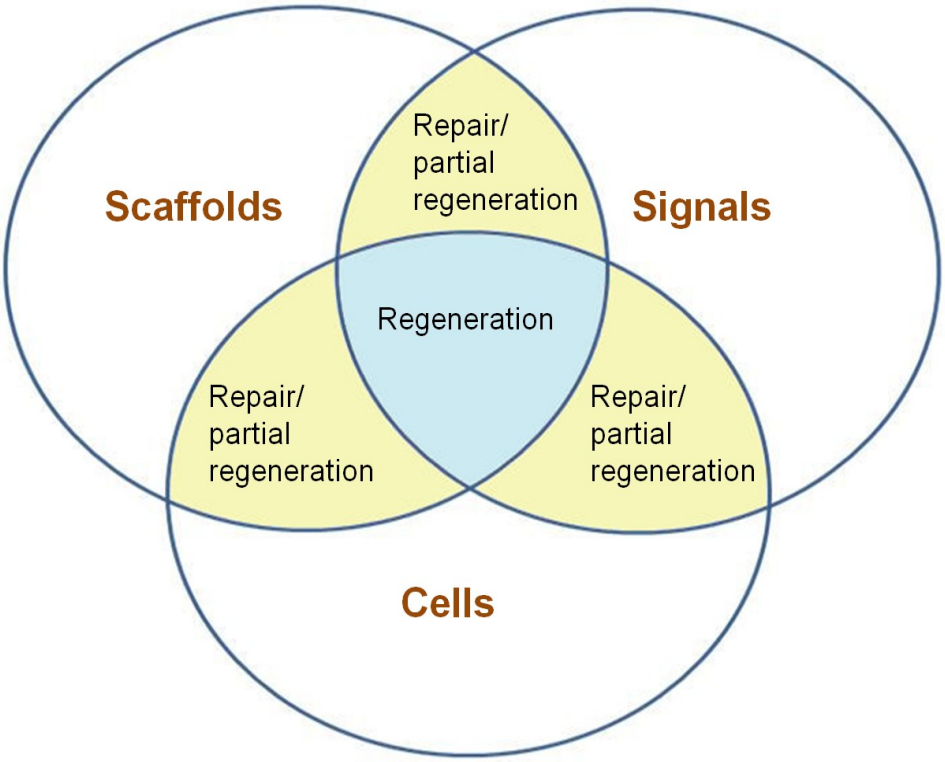

Figure 2-2: Schematic representation of the basic components required in periodontal tissue engineering. A combination of cells, scaffolds and signalling molecules are essential to regenerate the lost periodontal tissue.

2.3.1 Potential Cells for Periodontal Tissue Engineering

Cell sources available for tissue engineering may be classified into three main types on the basis of donor source: autologous (patient's own cells), allogenic (human donor) and xenogenic (animal origin). However, allogenic or xenogenic cells may not be the most desirable cells for periodontal regeneration for many reason such as potential immunogenicity and matrix

synthesis. Animal tissue can be useful sources for cells to create *ex vivo* models and testing scaffolds. Cells that could be utilised in periodontal tissue engineering are discussed in the following sections.

2.3.1.1 Stem Cells

Based on their potency to differentiate, stem cells can be classified into three types: totipotent (zygote), pluripotent (embryonic stem cells), and multipotent (e.g., mesenchymal stem cells). Although, embryonic stem cells have greater plasticity, their sourcing is controversial and they attract moral and legal issues, which currently limit their use in developing new therapies. Therefore, there is much attention directed to use of adult stem cells which retain the ability to self-renew, generate large numbers of progeny and are multipotent and able to differentiate into several mature cell types.

Mesenchymal stem cells (MSCs)

Adult stem cells are undifferentiated cells found in the tissues and organs of adults. Bone marrow is a rich source of haematopoietic stem cells and MSCs which are found in the stromal tissue of the bone marrow. Bone marrow-derived MSCs are also referred to as bone marrow stromal stem cells (BMSSCs). Much research is directed at using MSCs for tissue engineering as a relatively large biopsy can be obtained although potential donor site morbidity is a concern. Under appropriate conditions MSCs can differentiate into various lineages. Also, they exhibit extensive self-renewing potential. Kramer and co-workers reported an increased expression of osteocalcin and osteopontin by MSCs when they were co-cultured with

periodontal ligament. They concluded that factors released from the periodontal ligament may have induced the MSCs to develop periodontal ligament-like characteristics (Kramer et al., 2004). Evidence of regeneration of bone, cementum and periodontal ligament was observed in surgically-created periodontal defects treated with MSCs derived from bone marrow. These observations suggested a contribution of MSCs to periodontal tissue regeneration (Yang et al., 2010, Hasegawa et al., 2006). Therefore, MSCs can represent a potential source of cells for periodontal tissue engineering (Hasegawa et al., 2005, Zhao et al., 2008).

Periodontal ligament stem cells (PDLSCs)

MSC-like cell populations have been identified in many tissues, including adipose tissue, muscle, peripheral blood and periodontal ligament. The first report of isolation and identification of stem cells in human periodontal ligament was in 2004 (Seo et al., 2004). PDLSCs were isolated from the periodontal ligament tissue of extracted, normal, impacted third molars. Stem cells was founded in periodontal ligament cells and was determined using antibodies such as STRO-1 and CD146. the isolated cells with stemness properties was showen to differentiat into cementoblast-like cells, adipocytes and fibroblasts (Seo et al., 2004).

To assess whether PDLSCs contribute to periodontal tissue repair, the cells were transplanted into surgically created periodontal defects in immunocompromised rats. The transplanted human PDLSCs integrated into the PDL and attached to both the alveolar bone and cementum surfaces.

These observations emphasised the potential functional role of human PDLSC in periodontal regeneration (Seo et al., 2004).

In cell cultures derived from the PDL the ratio of cells expressing the stem cell marker, STRO-1 is variable. Cultured human periodontal ligament cells are reported to contain between 1.2% to 33.5% STRO-1-positive cells (Nagatomo et al., 2006, Itaya et al., 2009). Gay and co-workers reported that human periodontal tissue contains about 27% STRO-1 positive cells with only 3% strongly positive (Gay et al., 2007). The reason for this discrepancy is not clear. However, it has been reported that the ratio of stem cells marker's positive cells may change during culture as differentiation took place. Also, this may be as a results of the different techniques used such as fluorescence activated cell sorting or immunofluorescent analyses which could have differential sensitivities (Itaya et al., 2009).

Human PDLSCs, seeded in 3D biocompatible scaffolds *in vitro*, differentiated to osteoblasts and formed mineralised nodules when cultured in osteogenic medium (Trubiani et al., 2008). Therefore, periodontal ligament can be an efficient source of stem cells with a high expansion capacity and heterogeneous ability to differentiate into bone/ cementum-forming cells. In an animal model, PDLSCs were obtained from extracted teeth of miniature pigs, expanded *in vitro,* labelled with a membrane-binding fluorescent dye and transplanted into surgically created periodontal defects in the animals. After 12 weeks of transplantation, the labelled PDLSCs present in the newly formed alveolar bone tissue had differentiated to

osteoblasts, highlighting the contribution of PDLSCs in the periodontal tissue to regeneration (Liu et al., 2008). *In vivo* experiments performed by other investigators have showed that PDLSCs cultured *in vitro* can be successfully transplanted into periodontal defects to promote full periodontal regeneration (Hasegawa et al. 2005).

2.3.2 Scaffolds in Tissue Engineering

The scaffold is a temporary supporting structure acting as an artificial ECM for cells to grow on and form tissue. The scaffolds will physically support the implanted cells and allow them to proliferate, migrate, and differentiate in three dimensions. An ideal scaffold for tissue engineering, in theory, should have all the features of a native ECM and behave in the same manner under physiological conditions. Achieving this is very challenging as the native ECM is complex and tissue specific. Also, there is no clear understanding to date as to which exact features define the so-called ideal scaffold. However, the minimal requirements of a scaffold are that they should be non-antigenic, noncarcinogenic, biodegradable, non-toxic, sterilisable and have high cell/tissue biocompatibility. Most importantly a scaffold could potentially direct cell attachment, proliferation, and differentiation either by it's surface properties or by releasing incorporated molecules such as growth factors, hormones, and/or cytokines. *In vitro,* cells tend to lose their phenotype and de-differentiate. Therefore, constructing a scaffold with all the qualities of native ECM is likely to be useful in to developing and maintaining the characteristic phenotype, cell growth and in promoting biological function of the newly formed tissue.

2.3.2.1 Types of Scaffolds

A scaffold can be fabricated from either synthetic (e.g. polymers and ceramics) or natural material (e.g. collagen and gelatine). The selection of scaffold materials depends on the type of tissue to be engineered. The most common materials used for scaffold fabrication in tissue engineering are listed in Table 2-1.

Table 2-1: A broad classification of scaffolds used in tissue engineering.

Natural	Synthetic	Composite
Collagen Silk Chitosan Starch Alginate Hyaluronan Chondroitin Dextran Agar Cellulose	Polymers Polyglycolide (PGA) Polylactic acid (PLA) Polycaprolactone (PCL) Poly(Propylene Fumarate) (PPF) Poly(methyl methacrylate) (PMMA) Polyethylene (PE) Ceramic Bioinert ceramics (alumina and zirconia)	Combination of polymers and bioglass/ ceramics

2.3.2.2 Polymers as Scaffolds in Tissue Engineering

Polymers prepared from glycolic acid and lactic acid have found a multitude of uses in the medical devices industry beginning with biodegradable sutures which were first approved in the 1960s. Since that time, various products based on lactic and glycolic acid and on other materials, including poly(trimethylene carbonate) copolymers and poly(caprolactone) homo-polymers and copolymers have been used in medical devices.

Biodegradable polymers can be either natural or synthetic. Generally, synthetic polymers offer some advantages over natural materials as they can be tailored to give a wider range of properties than materials from natural sources.

Although the desired characteristics of a scaffold vary according to the tissue to be created, there are general properties that are desirable, which include the following:

- Mechanical properties that match the biological application.
- Biodegradable with rate of degradation match the rate of native tissue regeneration.
- Does not raise an inflammatory or toxic response.
- Easily processable into the final product form.
- Acceptable shelf life.
- Easily sterilised.

Among all the polymers which are biocompatible, biodegradable, and approved by the Food and Drug Administration (FDA), poly lactic acid (PLA) is advantageous due to its controlled degradation behaviour, compatibility, and nonimmunogenicity (Rasal et al., 2010).

PLA is a chiral molecule and exists in mainly two enantiomeric forms: (i) the left-handed (L-lactic acid) and (ii) the right-handed (D, L-lactic acid) (Rasal et al., 2010). Mechanical properties, crystallinity and degradation of PLA can be controlled by the ratio and type of the enantiomers. The L-enantiomer provides PLA with higher mechanical strength and adding D-enantiomers to

poly(L-lactic acid) reduces its melting temperature and crystallinity (Gupta et al., 2007). The ratio and distribution of enantiomers can defind the mechanical and biological properties of PLA (Mehta et al., 2005). Four different morphological types of polymers with different properties can be prepared depending on the enantiomers; Poly D-lactic acid (PDLA), Poly(L-lactic acid) (PLLA), Poly(D,L-lactic acid) (PDLLA) and Meso-PLA.

2.3.2.3 Scaffold Topography

Cells in native tissues are typically orientated and spatially patterned. Scaffolds not only provide mechanical support but they can act as “intelligent surfaces” capable of providing chemical and topographical signals to guide cell adhesion, spreading, morphology, proliferation and, eventually, cell differentiation. Curtis and Varde reported that contact guidance is one of the basic methods by which cells can migrate from their source to their destination (Curtis and Varde, 1964).

Since then there has been increasing interest in the topography of the extracellular micro-environment and its essential role in cellular behaviour, from attachment and morphology to proliferation and differentiation through contact guidance (Curtis et al., 2006, Xie et al., 2010). Several techniques have been developed to modify scaffold topography and control cell orientation including: grooves, pits, tubes, micro/nano patterning (Photolithography, nanoimprint lithography, and dip-pen nanolithography), and aligned-fibres (Martinez et al., 2009, Hoffman-Kim et al., 2010, Nie and Kumacheva, 2008). A list of studies which addressed the effect of different

scaffold topography on cells morphology, orientation and phenotype is presented in Table 2-2.

Table 2-2: The effect of different scaffold topography on cell behaviour in tissue engineered constructs.

Pattern type	Material	Cell type	Effects on cells	Authors
Grooves	Silicon wafer	Gingival fibroblasts	Cytoskeleton oriented with grooves	(Meyle et al., 1993)
Grooves	Polystyrene	Osteoblast	Cells closely followed the surface on wider grooved scaffolds	(Matsuzaka et al., 2003)
Microgroove	Polyimide	Osteoblast	Cell membrane, and cell nucleus, were aligned with the microgrooves	(Charest et al., 2004)
Nanogrooves using laser interference lithography	Glass	PDLFs	Cells were highly elongated parallel to the groove long axis	(Hamilton et al., 2010)
Pits	Polycaprolactone	Fibroblast	Cells show reduced adhesion and α-actin cytoskeleton less developed	(Gallagher et al., 2003)
Aligned-fibres	Poly (L-lactic acid)	Neural stem cells (NSC)	NSC and its neurite elongated parallel to the direction of the fibres of aligned scaffolds.	(Yang et al., 2005)

Aligned electrospun fibres can provide topographic cues to different cells, resulting in an alignment of cells along the axes of the fibres (Chew et al., 2008, Yang et al., 2005). The ability to control cellular alignment on scaffolds can be an influential approach to recreate the micro and nano scale architecture of the lost tissues. This might be important for the

regeneration of a wide variety of human tissues with a highly orientated, patterned ECM, such as tendon and ligament tissue (Yin et al., 2010, Shang et al., 2010).

The alignment of ECM or scaffold fibres can significantly influence cell behaviour and matrix formation in both natural and engineered tissues. It was reported that human coronary artery, smooth muscle cells attached and migrated along the axis of aligned poly(l-lactid-co-ε-caprolactone) and expressed a spindle-shaped, contractile phenotype. Furthermore, the distribution and organisation of cytoskeletal proteins were parallel to the direction of the nanofibres (Xu et al., 2004). Aligned electrospun poly(ε-caprolactone) scaffolds have been used to provide contact guidance for human Schwann cells. After 7 days of culture, cell cytoskeleton and nuclei were observed to aligned and elongated along the long axis of the fibres (Chew et al., 2008). It has been observed that embryonic stem cells seeded on aligned poly(ε-caprolactone) electrospun scaffold differentiated into neural lineages which suggested that the alignment of the fibres controlled the direction of neurite outgrowth from the seeded cells (Xie et al., 2009).

The cell alignment following the alignment of the fibres might be valuable for tissue repair by restoring the native architecture of the lost tissue. In periodontal ligament where collagen fibres are highly oriented, scaffolds that maintain this architecture may be essential. To date, few studies have evaluated the effect of fibre-alignment on periodontal ligament fibroblast behaviour. Shang and co-workers reported that rat periodontal ligament fibroblasts (RPDLFs) seeded on aligned-PLGA scaffolds were elongated

along the long axis of the fibres after 3 days in culture. RPDLFs on aligned scaffolds showed a higher rate of proliferation and migration compared to the controls. They concluded that aligned scaffolds can promote organised regeneration of periodontal tissue. However, no attempt was made to investigate the impact of fibre alignment on periodontal ligament fibroblast gene expression and matrix production (Shang et al., 2010). Table 2-3 lists some of the studies that investigated the effect of aligned electrospun fibres on the cellular behaviours of different cell types.

Table 2-3: The effects of electrospun aligned-fibres on different cell types in tissue engineered constructs.

Material	Cell type	Culture time	Effects on cells	Reference
PCL Collagen type I	Human umbilical vein endothelial cells (HUVEC)	3 days	Cells were parallel to the direction of fibre alignment. Under fluid flow, ECs on highly aligned scaffolds had greater resistance to detachment compared to cells cultured on random scaffolds	(Whited and Rylander, 2013)
Polystyrene	Mouse myoblasts C2C12	12 h	Cells were elongated along the fibre axes and migrated faster on aligned scaffolds	(Sheets et al., 2013)
Silk fibroin	mesenchymal stem cells (MSCs)	14 days	Aligned scaffolds increase the expression of tenogenic markers in MSCs and the production of tendon/ligament-related proteins. Mechanical loading of MSCs within a 3D aligned scaffolds encourage tenogenic differentiation and tissue maturation *in vitro*.	(Teh et al., 2013)
MeHA PEO	Human umbilical vein endothelial cells (HUVEC)	12-24 h	Cells migrate along the orientation of the fibres irrespective to the chemical gradient. This suggests that topographical cues may be more influential than chemical cues in directing cell motility.	(Sundararaghavan et al., 2012)
Tussah silk fibroin (TSF)	human embryonic stem cells (hESCs)	7 days	Aligned TSF-scaffold significantly promotes the neuronal differentiation and neurite outgrowth of hESC-derived neurons compared with random TSF-scaffold.	(Wang et al., 2012)
Human Elastin	Human coronary artery smooth muscle cells	7 days	SMCs became elongated in parallel to the fibres orientation and expressed native α-smooth muscle actin	(Nivison-Smith and Weiss, 2012)

Material	Cell type	Culture time	Effects on cells	Reference
	(SMCs)			
PDC	Porcine articular chondrocytes	7 days	On aligned-fibres the chondrocytes exhibited a more spindle-shaped morphology Chondrocytes produced collagen type II in both scaffolds	(Schneider et al., 2012)
PLLA	Bone marrow stromal	21 days	Cells aligned with the direction of fibres, alignment had no effect on the cell proliferation (DNA content), mineralisation was higher on aligned-fibres, no difference between the expression levels of the osteogenic marker	(Ma et al., 2011)
PLGA	Tendon fibroblasts	7 days	Cells and actin filaments were aligned along the direction of fibres alignment, collagen type I produced in comparable amount in both random and aligned scaffolds, collagen type I was organised along the direction of fibre alignment.	(Xie et al., 2010)
PLGA	Rat periodontal ligament fibroblasts	7 days	Cells were elongated along the fibre, metabolic activity of the cells on aligned-fibres was higher , cells proliferated and migrated more in aligned scaffolds	(Shang et al., 2010)
PHBV	Human osteoblast-like Cells	14 days	Cells spread randomly on random fibres and elongated along the aligned-fibres, cells proliferation on random and aligned scaffolds was comparable.	(Tong et al., 2010)
Collage chitosan (TPU)	Endothelial Cells and Schwann cells	7 days	Cells were viable and scaffolds were biocompatibility with no difference between the two type of scaffolds, cells exhibited spindle shaped morphology on aligned-fibres (aligned-fibres can regulate cell morphology)	(Huang et al., 2010)

Material	Cell type	Culture time	Effects on cells	Reference
Knitted Suture material coated with [P(LLA-CL)]	Bone marrow mesenchymal stem cells	14 days	Aligned-fibres promoted higher cell activity , cells adopted a spindle-like morphology and were orientated along the fibres, cells on aligned scaffold produced a higher level of collagen type I and III	(Vaquette et al., 2010)
Methacrylic terpolymer	Human umbilical vein endothelial cells	7 days	cells were elongated in the direction of fibres orientation, cells seeded on to random scaffold display an increased rate of proliferation compared to aligned	(Heath et al., 2010)
SIBS	PC12 (cell line from rat adrenal medulla)	8 days	Neurite were extended parallel along the alignment of the fibres	(Liu et al., 2010)
PLGA	C2C12 murine myoblasts	14 days	Cells appear to align along the direction fibres with an elongated morphology, myoblasts on aligned-fibres have organise actin parallel to the fibres, cells differentiated more on aligned-fibres compared to random aligned or glass	(Aviss et al., 2010)
PU PLLA	L929 mouse fibroblast cell line	12 days	No difference between aligned and random in term of cells activity and attachment, cells on aligned scaffolds appeared to orientate along the fibres.	(Truong et al., 2010)
PLLA	Human tendon stem/progenitor cells	*In vivo*: 1-6 weeks	Cells and their nuclei aligned and elongated parallel to the fibres, alignment had no effects on cells attachment and proliferation, cell orientation induced by alignment of the scaffold can influence cell differentiation. *In vivo* cells and collagen fibres were organised in alignment with the fibres directions, extracellular matrix was denser in aligned scaffolds	(Yin et al., 2010)

Material	Cell type	Culture time	Effects on cells	Reference
PLLA	E9 chick dorsal root ganglia	5 days	Neurites were longer on large and intermediate diameter fibres, cells migrated more in scaffolds with larger diameter fibres,	(Wang et al., 2010)
PCL	Embryonic stem cells	14 days	Although fibre alignment discourages the differentiation of cells into astrocytes (desirable), cell differentiation was alignment-independent with no difference observed between cells cultured on random or aligned scaffolds. Aligned-fibres can enhance the rate of neurite extension as well as their direction.	(Xie et al., 2009)
PMMA	Adult human dermal fibroblasts	9 days	Cell proliferated in both electrospun scaffolds despite the alignment; cell migration was higher in the aligned-fibres.	(Liu et al., 2009)
PCL	Human Schwann cells	7 days	Cytoskeleton and nuclei aligned and elongated along the fibre axes, there was no difference in gene expression in cells seeded into the two type of scaffolds, however myelin protein zero (P0) was observed only in cells seeded on aligned-fibres	(Chew et al., 2008)
PCL collagen	Human skeletal muscle cells	7 days	Cells attachment and proliferation was independent of the alignment of fibres, cells, myotubes and actin filaments were consistently aligned along the fibres. Cell differentiation was independent of fibre alignment. Myotubes were significantly longer in aligned scaffolds.	(Choi et al., 2008)
PU	Mouse skeletal myoblasts (C2C12 cell line)	14 days	Actin filaments in the attached cells were highly aligned and elongated along the fibres in aligned-fibre scaffolds. Myoblasts differentiated on aligned-fibres when subjected to electromechanical stimuli	(Liao et al., 2008)

Material	Cell type	Culture time	Effects on cells	Reference
PCLEEP	Human glial Cell derived neurotrophic factor (GDNF)	*In vivo*: 3 months	Electrophysiological recovery was higher in rats implanted with the electrospun fibres compared to the control.	(Chew et al., 2007)
PLLA	Neural stem cells	2 days	Cells and neurites were elongated parallel along the fibres direction, cell differentiation was not affected by fibre alignment. The length of neurite outgrowth was dependent on fibre diameter rather than fibre alignment.	(Yang et al., 2005)
[P(LLA-CL)]	Coronary artery smooth muscle cells	7 days	Cells, actin and myosin filaments were aligned along the fibres.	(Xu et al., 2004)

Methacrylated HA (MeHA), polyethylene oxide (PEO), Copoly(ether)esterurethane (PDC), Poly(L-lactic acid) (PLLA), Poly(e-caprolactone) (PCL), Polyurethane(PU), Poly(ester urethane)urea elastomer (PEUUR),Poly(methyl methacrylate) (PMMA), Copolymer of caprolactone and ethyl ethylene phosphate (PCLEEP), Poly(l-lactic-co-e-caprolactone) [P(LLA-CL)], Poly(lactic acid-co-glycolic acid) (PLGA), Polypyrrole(PPY)/poly(styrene-β-isobutylene-β-styrene) (SIBS), Poly(hydroxybutyrate-co-hydroxyvalerate) (PHBV)

2.3.2.4 Electrospinning

electrospinning has been used to fabricate fibrous scaffolds from either natural or synthetic polymers for using in tissue engineering applications. Scaffolds fabricated by electrospinning have nano- and micro-scale fibres with micro interconnected pores, resembling the extracellular matrix (ECM) of tissue (Li et al., 2007). The three dimensional nature of the electrospun scaffold allows cells to easily infiltrate the matrix and proliferate.

Recently, the electrospinning process has gained more attention due possibly to the growing interest in nanotechnology. Various polymers, scaffolds and carriers with diameters down to microns or nanometres can be easily fabricated using electrospinning (Yang et al., 2005, Xie et al., 2009, Ramakrishna et al., 2011). The electrospinning process involves subjecting a polymer solution fed through a needle to an electric field generated by high voltage. When the generated electric field exceeds the surface tension of the polymer, a polymer jet occurs. This polymer jet is targeted towards an electrically grounded collector and fibres are deposited on the collector in the form of a nonwoven fabric. Fibre diameter and porosity of the scaffold can be controlled by adjusting either the polymer concentration or the operating parameters such as the needle size, the electrical potential, the collector needle distance or the speed of the rotating mandrel in case of aligned-fibres (McClure et al., 2009, Tong et al., 2010). This highlights the role of electrospinning as a promising technique for scaffold fabrication in tissue engineering.

As compared to other techniques capable of producing nano and micro scale features such as photolithography and laser printing, the electrospinning technique is valuable for many reasons. First, electrospun nano-fibres produced by electrospinning are more physiologically relevant as they can mimic the 3D architecture of the extracellular matrix of native tissue. Secondly, electrospinning is simpler, faster and less costly for generating patterned nano-scale features such as the aligned scaffolds that can act as physical cues and guide cell growth.

2.3.2.5 Decellularisation Process

Natural, decellularised tissues are increasingly used in tissue engineering and regenerative medicine as scaffolds. These decellularised, tissue-based scaffolds have the advantage of preserving the 3D structure, surface topology, and composition of the ECM of the native tissue. Also, the retained ECM contains 'biological cues' that influence cell migration, proliferation, and differentiation (Vorotnikova et al., 2010).

Decellularised ECM scaffolds from a variety of tissues, including heart (Aubin et al., 2013), heart valves (Dijkman et al., 2012, Weber et al., 2013), lung (Gilpin et al., 2013), nerve (Szynkaruk et al., 2012), cartilage (Schwarz et al., 2012) and ligaments (Yoshida et al., 2012) have been prepared and used in tissue engineering and regenerative medicine. A wide range of these decellularised ECM tissues are FDA approved and commercially available for clinical use (refer to Table 2-4).

The aim of a decellularisation procedure is to remove all of the cellular components from the extracellular matrix while preserving its biological integrity and mechanical properties. Preservation of the native structure and composition of ECM during the process of decellularisation is absolutely essential. The decellularisation treatments should efficiently remove/diminish antigenicity and create a biocompatible graft for *in vivo* application. Several methods of decellularisation have been used including a combination of physical, enzymatic and chemical treatments (Rieder et al., 2004, Yoshida et al., 2012).

Physical treatments for decellularisation of tissues involve using agitation, sonication or freeze/thawing. Chemical treatments depend mainly on utilising acids, detergents, chelating agents [e.g., ethylenediaminetetraaceticacid (EDTA)], hypotonic solutions or hypertonic solutions to disrupt cell membranes. Enzymatic treatments include the use of protease or nuclease to cleave the peptide or nucleotide bonds. These methods can efficiently remove cellular components such as nuclei but may adversely affect the ECM composition and mechanical properties. Therefore, these methods should be appropriately combined to exploit the decellularisation efficacy and at the same time reduce any adverse effect on tissue ECM composition, biological activity and biomechanical properties. Also, an appropriate decellularisation method should be optimised for each specific tissue and organ to remove cellular content without compromising biological integrity of the tissue.

Triton X-100, sodium dodecyl sulfate (SDS) and sodium deoxycholate are the most common detergents used in the decellularisation process either alone or in combination. Triton X-100 is a non-ionic detergent, which hinders the lipid-lipid and lipid-protein interaction in tissues and can be used effectively to remove cell residues from 'thick' tissues. Sodium dodecyl sulfate (SDS) is an ionic detergent that destroys the cell membrane and appears more effective than Triton X-100 for removing nuclei material from dense tissues while preserving ECM integrity and mechanical properties. It has been reported that 0.1% SDS was effectively used to removed tendon cells from tendon fascicles with no alterations in ECM (Ingram et al., 2007, Pridgen et al., 2011).

During the decellularisation process, complete removal of the cellular content is not always possible. For this reason, it is essential to assess the cellular content left after decellularisation and quantitatively assay cell components such as DNA or membrane associated molecules such as phospholipids to avoid immunological adverse effect *in vivo*. The threshold concentration of residual cellular content that can elicit an *in vivo* negative response has not been investigated in detail and it may vary depending upon the ECM source and host immune function. However, it has been suggested that a decellularised tissue should contain no more than 50 ng DNA/mg of tissue dry weight and should show no visible nuclear material in tissue sections stained with a nuclear staining agent such as Hoechst or H&E (Crapo et al., 2011).

One of the earliest uses of a decellularised matrix as a graft material is that of decellularised bone, either allografts or xenografts, in orthopaedic or maxillofacial and oral surgeries. This clinical use again supports the concept that decellularised tissue grafts can be successfully used in regenerative medicine.

Avance® Nerve Graft is a decellularised ECM processed from human peripheral nerve tissue. Avance® Nerve Graft is prepared through a combination of chemical detergent, enzyme treatment and gamma irradiation. Over 5,000 Avance® Nerve Grafts have been used medically since 2007 after FDA approval for clinical use. In the largest multicenter report, 76 nerves in 59 patients were implanted using Avance® Nerve Graft and about 87% of cases showed significant recovery (Brooks et al., 2012).

It was reported that bone-patella-tendon-bone ligaments from rabbits were successfully decellularised using tri(n-butyl)phosphate (TBP) or SDS and reseeded with fibroblasts (Cartmell and Dunn, 2004). Also, it was observed that tenocyte repopulation of decellularised tendon, prepared using 0.1% SDS, was improved by using ultrasound before seeding (Ingram et al., 2007). A study which compared the effectiveness of three different extraction methods, using a combination of the surfactants sodium lauryl sulfate (SLS), Triton X-100, and/or tributyl phosphate (TnBP); reported that all three decellularisation treatments maintained adequate mechanical and biochemical properties of the decellularised porcine bone-anterior cruciate ligament- bone graft. However, a combination of Triton X-100 with SDS was

observed to be more effective at eliminating cell nuclei from the anterior cruciate ligament (ACL) (Woods and Gratzer, 2005).

Porcine ACLs were successfully decellularised using 0.25% Triton X-100, 0.1% SDS and 0.1% trypsin (Vavken et al., 2009). All the decellularisation protocols used, reduced the DNA material and maintained the collagen and the total protein content. The decellularised porcine ACL tissues were effectively reseeded with human ACL fibroblasts which showed increased procollagen expression with time in culture. (Vavken et al., 2009).

Acellular dermal matrix (ADM) is a decellularised human skin which is widely used in different clinical application. Currently, several ADMs are available commercially for use in clinical application, including FlexHD®, AlloDerm®, Neoform™, DermaMatrix™, Permacol™ and Strattice®. These decellularised ECMs were used in the treatment of burns (Fang et al., 2013), alveolar ridge deformities (Jayavel et al., 2011), teeth root coverage (Thombre et al., 2012) and breast reconstruction after breast cancer (Ibrahim et al., 2013). In periodontology, acellular dermal matrix tissue has been confirmed to be equal to palatal connective tissue graft (gold standard) for root coverage procedures in randomised, controlled clinical studies (Carnio and Fuganti, 2013, Ayub et al., 2012).

In a recent report, porcine-derived temporomandibular joint (TMJ) discs were successfully decellularised using an SDS-based decellularisation method. The SDS-treated discs retained the general morphology of the native discs and retained the native collagen fibre organisation. The result

supports the potential of decellularised porcine TMJ for the engineering and reconstruction of damaged or diseased TMJ discs (Lumpkins et al., 2008).

In conclusion, all these studies have shown that decellularised tendons/ligaments can successfully provide a natural biochemical and biomechanical template for tendon/ligament regeneration and repair. To my knowledge, no attempt has been made to use decellularised ligaments as scaffolds for tissue engineered periodontal ligaments either for future clinical application or to develop an *in vitro* model to study regeneration and repair processes.

Table 2-4: Examples of commercially available clinical products composed of a decellularised extracellular matrix.

Products	Tissue Source	Application
AlloDerm®	Human dermis	Soft tissue
AlloPatch HD™	Human dermis	Tendon
FlexHD®	Human dermis	Breast
Zimmer® Collagen Repair Patch	Porcine dermis	Soft tissue
IOPatch™	Human pericardium	Ophthalmology
Prima™ Plus	Porcine heart valve	Valve replacement

2.3.3 Role of Mechanical Loading in Ligament and Tendon Tissues

The periodontal ligament acts as a cushion to withstand and respond to forces which result from mastication, parafunctional habits and orthodontic treatment. Mechanical loading plays an important role in periodontal ligament homeostasis and repair. Although much is known about the mechanical properties of teeth and alveolar bone, the exact mechanism through which the periodontal ligament responds to mechanical loading is not fully understood. *In vivo*, the periodontal ligament is subjected to tension forces on one side of the tooth while being simultaneously subjected to compressive forces on the other side of the tooth. Therefore, the mechanism through which the periodontal ligament perceives mechanical loading is very complex.

Mechanical loading not only plays a role in maintaining the structure of the ECM of native tissues, it also can modulate the ECM structure, composition, and mechanical properties of tissues created by tissue engineering (tissue engineered constructs) *in vitro*. Mechanical loading has been recognised as a critical component in tissue engineering especially when engineering load-bearing tissues such as periodontal ligaments and tendon (Jones et al., 2013, Scott et al., 2011). Appropriate biomechanical cues are essential for ECM organisation and alignment in engineered tissues *in vitro*. Studies have shown that mechanical loading can influence cell proliferation, differentiation, gene expression and protein synthesis (Jacobs et al., 2013, Liao et al., 2008, Liu et al., 2012, Tulloch et al., 2011).

Tendon cells seeded in a type I collagen matrix were subjected to uniaxial stretching (1% strain for 1 h at 1 Hz for 8 days), using the commercial Flexcell® strain unit. Genes for collagen type I, III, and XII as well as aggrecan and fibronectin were up-regulated in strained constructs. These results showed that tendon cells under mechanical loading assumed a phenotype that is similar to that of a native tendon (Garvin et al., 2003).

Three dimensional scaffolds seeded with patella tendon fibroblasts were loaded with tensile strain, rotational strain or a combined of rotational and tensile strain (Sawaguchi et al., 2010). At 21 days, the combined strain group showed a higher DNA content than that of the stretch or rotational group. Collagen type I and III mRNA expression was significantly higher in the combined-strain group than that in the stretched and rotational groups (Sawaguchi et al., 2010).

Therefore, mechanical loading is fundamental in developing tissue engineered ligaments to mimic the biomechanical properties of native ligaments.

Effect of mechanical compression on PDLFs *in vitro*

It is generally known that bone resorption occurs at sites of compression and bone formation in sites under tension. During compression, periodontal ligament cells release prostaglandin E2 and adenosine triphosphate (ATP) which invoke the expression of Receptor Activator of Nuclear Factor-kB Ligand (RANKL) which in turn stimulates the formation of osteoclasts which then leads to bone resorption (KANZAKI et al., 2002, Luckprom et al.,

2010). HPDLFs, grown as monolayers, were subjected to either continuous or intermittent compressive force for variable time periods (refer to Table 2-5) and showed increased RANKL and IL6 mRNA expression, with an intermittent force having a greater effect than a continuous force (He et al., 2004). Nakao et al. demonstrated that an intermittent force could induce the expression of RANKL via interleukin 1 (IL1) expression in HPDLFs under compression forces (Nakao et al., 2007).

Yamamoto et al., cultured human periodontal ligament cells in a 2D monolayer culture system and loaded the cultures using a hydrostatic pressure apparatus with compression regime of 1 MPa for 10 min, 1 MPa for 60 min or 6 MPa for 60 min. Interleukin 6 (IL6) and osteoprotogerin (OPG) mRNA expression was observed after exposure to as little as 1 MPa of hydrostatic pressure for 10 min. The expression of interleukin 8 (IL8), TNF-a, and RANKL mRNAs was specifically induced following exposure to 1 MPa of hydrostatic pressure for 60 min. After 6 MPa of loading for 60 min, increased expression of IL6, IL8, RANKL and OPG mRNAs was observed. The increase in IL6 and TNF$-\alpha$ expression might contribute to the bone resorption observed in PDL subjected to compressive forces. Also, no difference was observed in cellular activity or morphology between loaded and control groups (Yamamoto et al., 2006).

Effect of mechanical strain (stretching) on PDLFs *in vitro*

Strain has been reported to influence PDLF proliferation rate. Periodontal ligament fibroblasts seeded in a 3D collagen gel and subjected to 8% mechanical stretching showed no increase in cell number between day 1 and 3. At day 5, the PDLF cell number was higher in the stretched constructs compared to the control non-stretched constructs, this increase was unaffected by Emdogain (EMD) addition (Oortgiesen et al., 2012). Yu and collaborators showed no increase in cell numbers of PDLFs subjected to uniaxial cyclic strain of 8% at day 2. However cell number increased in the stretched group at day 3 compared to the non-loaded group (Yu et al., 2012). It has been demonstrated that mechanical loading can slow down proliferation and lead to cell cycle arrest of PDLFs subjected to cyclic strain for 2 h. Also, early apoptosis of HPDLFs in response to uniaxial strain has been reported. HPDLF monolayers subjected to 10 and 20% strain for 6 and 12 h showed a load-dependent induction of early apoptosis within 6 h which decreased at 12 h (Zhong et al., 2008). These early cell responses of PDLFs to mechanical strain of cell cycle arrest and apoptosis, can be viewed as an adaptation and protective mechanism where proliferation ceases and the cells undergo adaptation to the mechanical load and restore their mechano-sensitive properties before resuming cell proliferation.

Mechanical strain not only influences PDLF proliferation and activity but also can affect the cell morphology. It has been observed that PDLFs became oriented perpendicular to the strain direction when they were cultured as a monolayer (Yu et al., 2012, Zhong et al., 2008). Tendon cells cultured in 3D gels of collagen type I and subjected to strain using a Flexcell® strain unit showed that in the mechanically loaded constructs the tendon cells aligned along the long axis of force direction with more elongated nuclei and cytoplasmic extensions compared to non-loaded constructs (Garvin et al., 2003). However in contrast, Oortgiesen et al., reported that PDLFs, cultured in 3D collagen gels and strained using a custom made loading unit, aligned perpendicular to the force direction (Oortgiesen et al., 2012). This difference in the results may be due to the nature of mechanical stress, the type of cells used or the difference in the loading system.

A number of studies have found that PDLFs showed variable responses to different levels of mechanical loading (Liu et al., 2012, Monnouchi et al., 2011, He et al., 2004). PDLFs subjected to 10% cyclic equi-biaxial compression for 24 h showed down regulation of collagen type I mRNA expression and a 50% reduction in total protein levels compared to non-loaded control PDLFs (He et al., 2004). However, 10% stretching increased COL1A1 expression and total protein levels. This might suggest that PDLFs can perceive different types of mechanical loading and respond in different ways based on the loading nature, duration of loading and the loading system used.

Jacobs et al. reported that PDLFs strained for 12 h with 1, 5 and 10% strains showed a significant, 8-fold up-regulation of cyclin D1 mRNA expression. Cyclin D1 is a protein which plays a central role in the regulation of cell proliferation. Both alkaline phosphatase (ALPL) and osteoprotegerin (OPG) gene expression increased about three fold while RANKL expression was down-regulated, which may indicate new bone formation. Also, ALPL activity and OPG synthesis were increased in a strain-dependent manner highlighting the ability of PDLFs to differentiate to bone forming cells under loading (Jacobs et al., 2013).

Liu et al. described an increased gene expression of collagen type I when PDLFs underwent a 12% uniaxial cyclic strain for 24 h. However, 5% and 10% static mechanical strain for 12 h did not stimulate COL1A1 expression in the PDLFs (Jacobs et al. 2013). The discrepancies between these results could be due to the heterogeneous nature of PDLFs and cell subtypes that react differently or through the investigators using different loading regimens, i.e. static vs. cyclical conditions (Jacobs et al., 2013, Liu et al., 2012).

Microarray data showed significant up-regulation of 21 osteogenic-related genes in PDLFs subjected to 12% strain for 24 h using a Flexcell® strain unit. The up-regulated genes included 10 extracellular matrix genes, 10 growth factors genes and one cell adhesion gene (Liu et al., 2012). Most mechanical loading research has been focused on loading PDLF cells in a 2D model system, i.e. cells in monolayer culture. However, native ligaments composed of PDLF cells are surrounded by a 3D extracellular matrix composed mainly of collagen fibres. One of the few studies which addressed the effect of mechanical loading PDLFs in a 3D model was carried out by Oortgiesen et al., using a 3D collagen gel seeded with PDLFs. The cell-collagen gel was stretched using an 8% uniaxial cyclic strain and frequency of 1Hz for 3 days. At day 3, they reported up-regulation of bone sialoprotein (BSP) and collagen type I and ECM synthesis-related genes, and down regulation of RUNX2, early osteoblast differentiation gene. This may suggest that PDLFs under cyclic strain within the physiological loading limit, retained their ligamentous properties (Oortgiesen et al., 2012).

In conclusion, mechanical strain can modulate the periodontal ligament fibroblast response depending on the type of loading, frequency and magnitude of mechanical stress. However, there have only been a few studies on the impact of mechanical strain on tissue engineered ligament or periodontal ligament fibroblasts cultured in 3D systems. Moreover, these have produced inconsistent results.

Table 2-5: Effect of mechanical loading on PDLFs and other cell types.

Cell type	Culture system	Loading system	Results	Conclusion	Authors
			Effect of Strain Loading on PDLFs		
Commercial HPDLFs	Monolayer	Flexcell® strain Unit 1%, 5% and 10% static strain for 12 h	Cellular activity and apoptosis were not affected by strain. PDLFs showed a strain dependent expression of cyclin D1, ALPL and osteoprotegerin at 5% strain. COL1A1 expression was not affected by strain.	PDLF osteogenic differentiation correlated to increasing strain. Also, 5% strain suggested as the best conditions for periodontal remodelling bone formation at the tension site.	(Jacobs et al., 2013)
RPDLFs	Collagen gel 3D system	Custom made loading system 8% unilateral cyclic stretch for 1, 3, or 5 days	Cells oriented perpendicular to the loading direction. Cell number increased with stretching. COL1A1 and Sialoprotein were up-regulated with loading and RUNX2 was downregulated.	Strain loading plays a role in the up-regulation of ECM formation related genes, COL1A1 and sialoprotein, and down-regulation of RUNX2. This might suggest that PDLF under loading retain their ligament properties.	(Oortgiesen et al., 2012)
HPDLFs	Monolayer	Flexcell® strain Unit FX 3000 12% uniaxial for 24h.	Strained group showed a different gene expression in the microarray gene chip. Increased expression of epidermal growth factor receptor (EGFR) gene, but no change expression of some osteoblast	12% cyclic stretch inhibits the differentiation of HPDLFs to osteoblast-like cells. HPDLFs under mechanical strain exhibited some osteogenic features, yet	(Liu et al., 2012)

			marker genes, such as ALPL, BGLAP and BMP.	retained their ligamentous nature.	
HPDLFs	Monolayer	Grooved plate 8% unilateral cyclic stretch for 2 and 8 days	Cells were oriented along the groove direction. When loading applied cells oriented perpendicular to the loading direction. No difference in the cell number except at day 3 for the grooved loaded group. Scleraxis and elastin were highly expressed in the stretched group at day 8. RUNX2 and BGLAP were expressed higher in the grooved loaded group as early as day 2.	A synergistic effect was observed on the expression of RUNX2 at Day 8 when dual stimulation was used (loading and grooved plate); while for the ligament related genes (scleraxis and elastin), only the mechanical loading proved to be a positive critical factor.	(Yu et al., 2012)
HPDLFs	Monolayer	Custom made force loading plates	Cyclic tensile stress induced decreased ability of proliferation and cell arrest Flow cytometry of cells showed that cells in G1 and G2 phase increased, whilst S phase cells decreased after cyclic tensile stress loading for 2 h.	Cell cycle arrest and the slowdown proliferation can benefit PDLCs to have more time to respond to the loading and decide either to proliferate or differentiate	(Wang et al., 2011)
HPDLFs	Monolayer	Flexcell® strain unit Using 1.5% elongation for 0-12 h	Strain stimulated COL1A1 and MMP1 mRNA expression. Strain activated Mitogen-Activated Protein Kinases (MAPKs) including extracellular signal-regulated kinase (ERK), c-Jun NH_2-terminal kinase (JNK).	Increased expression of COL1A1 and MMP-1 in the strained group was controlled by the ERK/JNK-AP-1 and ERK-NF-κB signalling pathways.	(Kook et al., 2011)

HPDLFs	Monolayer	STREX Mechanical Cell Strain Manual Stretcher. 0, 8, or 12% elongation for 1 h.	RANKL mRNA expression was down-regulated by 8% stretch and up-regulated by 12% stretch loading. OPG mRNA expression was up-regulated by both 8% and 12% stretch. TGF-β1, ALPL and angiotensinogen (Ang) mRNA were up-regulated by exposure to 8% stretch.	8% elongation may exert inhibitory effects on osteoclastogenesis in HPLF. Data suggest that Ang II is involved in the cellular signalling of stretched PDL tissues.	(Monnouchi et al., 2011)
HPDLFs	Monolayer	STREX Mechanical Cell Strain Manual Stretcher. (stretch ratio: 105%)	COL1A1 mRNA and protein expression decreased until day 3, and then slowly increased until day 7 after loading. Osteogenic differentiation of HPDLFs showed slightly up-regulation of COL1A1 during osteogenesis, in time-dependent manners.	Results indicated that the expression patterns induced by loading were different from those induced by osteogenic stimulation in PDL cell.	(Nemoto et al., 2010)
HPDLFs	Collagen gel 3D system	Custom made loading system. Intermittent axial displacement of 0–20 mm, 0–100 mm, or 0–200 mm for 2, 3, 4 and 24 h.	COL1A1 gene expression was not affected by 20 mm or 100 mm displacements but 200 mm increase of COL1A1 expression Expression of COX 1, RUNX2 and OPN and BMP1, were not affected by all loading regime. Loading had no measurable effect on synthesis of ECM proteins.	Only the highest displacement (200 mm) resulted in an increased COL1A1 gene expression which may suggests that load applied to the 3D ligament may not have been preserved by fibroblast in the collagen as in the periodontal ligament *in vivo.* The engineered ligament showed response to loading as little as 5% stretching	(Berendsen et al., 2009)

HPDLFs	Collagen gel 3D system.	Static tensional force via elevating the flexible bottom of the plate under the collagen gel	COL1A1, COL1A2, COL4A2, and COL5A3 expression increased after 12 h loading ALPL expression increased after 2 h loading in Microarrays data. However, qRT-PCR revealed its expression decreased after 2 h then increased after 12 h Protein level of vascular endothelial growth factor (VEGF) also increased after 72 h loading.	Many genes that up-regulated by static loading are related to osteogenic processes such as matrix synthesis and angiogenesis. Also, increased expression of VEGF mRNA and protein in PDLFs could explain the new bone formation on the tension side	(Ku et al., 2009)
HPDLFs	Monolayer	Custom made system 1,10 and 20% stretching strain for 30 min, 1, 6 and 12 h.	Cells aligned and elongated perpendicular to the stretching force and alignment increased with increasing loading. Time and force dependent induction of early apoptosis of human PDL cells in response to stretching strain within 6 h, and then decreased at 12 h	In cells stretched for 12 h, the rate of apoptosis of each strain group decreased markedly which might suggest that early apoptotic cells came into late apoptosis stage or cells restore their mechano-sensitivity properties.	(Zhong et al., 2008)
HPDLFs	Monolayer	Flexcell® strain unit 12% cyclic stretching for 6 and 24 h	IL1A, IL1F7, IL6 and IL7 mRNA were down-regulated by strain IL8, IL11 and IL12A mRNA were up-regulated. TNF and RANKL were not expressed in strained cells.	Cytokines play an important role in cell-to-cell signalling in periodontal ligament under mechanical loading. The cytokine expressed in response to strain were pleiotropic cytokines, such as IL1A, IL6 and have multiple biological activities.	(Pinkerton et al., 2008)

HPDLFs	Monolayer	Custom made loading system Cycle strain for 0, 2, 4, 6,12 and 24 h.	Loaded PDLFs for 24 h showed up-regulation of ALPL mRNA and down-regulation of OPG mRNA which then levelled off at the end of a 24 h. BGLAP mRNA was expressed at the late phase of the 24 h loading. ALPL protein was increased at the beginning of loading and at 24 h loading.	Mechanical stress triggers differentiation of PDLFs with high differentiation potential to express osteoblastic characteristics as well as osteoclastic activity.	(Yang et al., 2006)
HPDLFs	Monolayer	Flexcell® strain unit 15%Cyclical tensile force for 0.5, 1.5, 6, 24, 48 and 72 h.	Tensile force significantly up-regulated OPG production. This increase was inhibited dose dependently by anti-TGF β1 antibodies. Cyclical tensile force up-regulated TGF-β1 mRNA expression in PDL cells. Anti-TGF-beta antibodies inhibited the up-regulation of TGF-β1 mRNA in PDL cells stimulated by cyclical tensile force	The application of tensile force up-regulated OPG expression in PDLFs thorough the stimulation of TGFβ1. Therefore, tensile loading inhibited the osteoclastogenesis of PDLFs and maintain alveolar bone homeostasis.	(Kanzaki et al., 2006)
HPDLFs	Monolayer	10% cyclic equibiaxial tensional and compressive forces.	Compression force group showed decreased in collagen type I and fibronectin protein, Col1A1 mRNA, and increases in total protein, MMP-2 protein, and MMP-2 mRNA. Tensional force group showed increased total protein, type I collagen, Col1A1 mRNA, as well as MMP-2 and TIMP-2 mRNA.	FPDLFs can perceive two different forms of mechanical stimuli and respond in a differential manner.	(He et al., 2004)

Bovine PDLFs	Monolayer	Flexcell® strain unit 0.2, 1, 2, 3, 10, 18% strain loading.	Low magnitude strain (1, 2 and 3%) induced the increase of collagen type I and decorin mRNA expression without changing ALPL activity. Strain of high magnitude (10 and 18%) induced the increase of collagen type I and decorin mRNA expression while decreasing ALPL activity.	Data suggest that different magnitudes of mechanical strain induce different responses from periodontal ligament cells.	(Ozaki et al., 2005)
HPDLFs	Monolayer	Flexcell® strain unit 15% strain for 0, 30, 90 min and 6 h.	BGLAP mRNA expression was undetectable c-*fos* mRNA expression was up-regulated, with a peak at 30 min, and then down regulated after 30 min. No change of ALPL or matrix proteins mRNA expression was detected.	It is controversy whether the cellular response resulted from the increase in c-*fos* mRNA induced by mechanical loading.	(Yamaguchi et al., 2002)
HPDLFs	Monolayer	Flexcell® strain unit 6, 10 and 15% strain for 4 and 44 h.	Loading effectively inhibited autocrine induction of IL1 mRNA within 4 h. The inhibition sustained during the ensuing 44 h.	Loading may drastically reduce the amplification of IL1 dependent immune responses.	(Long et al., 2001)
			Effect of Compressive Loading on PDLFs		
HPDLFs	Monolayer	Compressive force continuous or Intermittent (8	Under compression PDLFs expressed less OPG mRNA, in a force and time dependent manner The intermittent force induced greater RANKL mRNA expression than did the	Compression induced RANKL and IL6 mRNA in PDLFs, with intermittent force having a greater effect than continuous force. This suggests that weak	(Nakao et al., 2007)

		h/day) Control, 2, or 5 g/cm^2 for 2, 3 or 4 days.	continuous force at both 2 and 5 g/cm^2 The intermittent force induced higher expression of IL1 mRNA	intermittent compression force could induce the expression of RANKL via IL1 expression in PDLFs.	
HPDLFs	Monolayer	Hydrostatic pressure apparatus 1 MPa for 10 min 1 MPa for 60 min 6 MPa for 60 min.	IL6, and OPG mRNA were observed after the exposure to as minimal as 1 MPa loading for 10 min. The expression of IL8, TNF-a, and RANKL mRNA was specifically induced following exposure to 1 MPa loading for 60 min.	Under compressive force, PDLFs showed increased expression of RANKL mRNA in a force- and time dependent manner which may affect bone metabolism in terms of bone resorption.	(Yamamoto et al., 2006)
Effect of Mechanical Loading on Different Cell Types					
Tendon fascicles dissected from bovine foot		Custom made strain chamber cyclic tensile strain at 30% or 60% for 15 min, 30 min, 1, or 5 h.	Gene expression of 30% of strain at failure for 1 h significantly showed higher expression of COL1A1 and IL6.	IL6 may play a role in stimulating collagen synthesis suggesting a role of IL6 in tendon adaptation to exercise.	(Legerlotz et al., 2011)

Human dermal fibroblasts	Chitosan sponge scaffolds coated with type I collagen	Custom made bioreactor unit 14% uniaxial cyclic strain for 3 and 7 days.	Increased cellular proliferation Fibronectin expression increased with cyclic loading as well as the activity of metalloproteinase 2 (MMP2) cyclic strain increased the expression of vascular endothelial growth factor (VEGF) and IL6.	Uniaxial cyclic strain can enhance the wound healing potential	(Park et al., 2013)
Human tracheal fibroblast	3D porous elastomeric substrates	10% cyclic strain for 7 days.	Increases in collagen type I and fibronectin matrix accumulation in response to cyclic strain. Short term application of cyclic strain also stimulated a significant increase in a1 procollagen type I, TGF-β1, and elastine mRNA expression. Hitchcock cyclic strain bioreactor 10% strain, 8 h/day for 7 days.	Cyclic strain regimen stimulates fibroblast matrix gene expression and protein synthesis. Increased matrix accumulation, mainly collagen type I, may be mediated by strain-induced production of profibrogenic cytokines like TGFβ1	(Webb et al., 2006)

2.3.4 Effects of Growth Factors on PDLFs

Growth factors are a group of naturally occurring proteins or polypeptides capable of instructing specific cellular responses in the biological environment. The cellular effects of growth factors are known to be complex, they can be chemotactic factors (direct cell migration), morphogenetic factors (induce cellular differentiation), mitogenic factors (stimulate cell division and proliferation), apoptotic factors (initiate programmed cell death), metabolic factors (modulate cellular metabolic activity) (Lee et al., 2010).

There is a great interest in the potential therapeutic application of growth factors in periodontal regeneration and tissue engineering (Somerman, 2011, Chen et al., 2009). The growth factors that have been most investigated in periodontal regeneration include bone morphogenetic proteins (BMPs) (Ripamonti and Renton, 2006, Chen et al., 2007), platelet-derived growth factors (PDGFs) (Giannobile et al., 1996, Cooke et al., 2006), basic fibroblast growth factor (b-FGF) (Sato et al., 2004, Rossa Jr et al., 2000), transforming growth factor beta 1 (TGF-β1) (Tatakis et al., 2000), insulin-like growth factor 1 (IGF-1) (Sant'Ana et al., 2007) and enamel matrix derivative (EMD) (Esposito et al., 2010). These growth factors have significant effects on proliferation, alkaline phosphatase activity, mineralised nodule formation, and extra cellular matrix synthesis by HPDLFs (Fujii et al., 2010, Kono et al., 2013).

Enamel matrix derivatives composed of proteins derived from Hertwig's root sheaths. Emdogain® (EMD) is a commercial extract of porcine enamel matrix and contains amelogenins of various molecular weights. Amelogenins are involved in the formation of enamel and periodontal attachment during tooth development. Although EMD is not a growth factor, it behaves like one (Esposito et al., 2010). EMD-induced cellular proliferation is mediated through the amelogenin it contains, while the differentiation of PDLFs to bone-forming cells is largely due to BMP signalling. EMD is believed to contain bone morphogenetic proteins (BMPs), mainly BMP2 and BMP7 which might contribute to its osteoinductive activity (Kémoun et al., 2011).

In vitro studies have shown that EMD enhanced PDLF proliferation in a time-dependent manner (Palioto et al., 2004). Also, EMD promoted protein and collagen production, differentiation and osteoprotegerin production of PDLFs (Palioto et al., 2004, Rodrigues et al., 2007, Palioto et al., 2011). Stimulation of PDLFs with EMD *in vitro* was found to stimulate IGF-I and TGF-β1 gene and protein expression (Rodrigues et al., 2007). Some studies reported that EMD showed no effect on the osteoblastic phenotype expression of PDLFs *in vitro* (Okubo et al., 2003, Tanimoto et al., 2012). However, Amin et al., reported that PDLFs cultured in basic culture media showed up-regulation of early osteogenic genes including RUNX2, ALPL and OP mRNA. When HPDLFs were cultured in osteogenic media and stimulated with EMD for 7 days, early osteogenic genes were up-regulated 1.5 to 2.5 fold compared to non-stimulated cells (Amin et al., 2012).

Differences between the results observed in *in vitro* studies could be due to the heterogeneity of the PDLFs or differences in the culture conditions and EMD dilution methods and concentrations.

EMD used in combination with IGF-I enhanced PDLF proliferation but had no additional effects in the adhesion, migration, expression or production of collagen type I than those obtained when EMD was used alone (Palioto et al., 2004). It has been reported that combination of EMD and PDGF *in vitro* resulted in greater PDLF proliferation and wound-filling than when either of them was used alone (Chong et al., 2006). The combination of EMD with TGF-β1 did not positively alter PDLF behaviour; this combination showed that the influence of EMD was greater than that of TGF-β1 (Rodrigues et al., 2007).

In controlled clinical trials, intra-bony defects treated with EMD showed significantly higher attachment gain and more bone-fill than control sites treated with open flap debridement only (Tonetti et al., 2002, Tonetti et al., 2004, Cortellini and Tonetti, 2007). In wide defects, EMD can support repair of flap and periodontal defects which normally would fill with soft tissue rather than undergoing PDL regeneration. Therefore, EMD has been combined with membranes or bone substitutes to maintain the space for regeneration (Siciliano et al., 2011, Kasaj et al., 2012).

Transforming growth factor beta 1 (TGF-β1) is a multifunctional cytokine that regulates a range of cellular activities including cellular proliferation, differentiation and ECM synthesis (Shi and Massagué, 2003). Also, TGF-β1 is known to be an essential regulator of the COL1A1 gene during the healing process in tendons (Klein et al., 2002). Many studies have shown that stimulating PDLFs with TGF-β1 *in vitro* induced cellular proliferation and increased expression of ECM components (Okubo et al., 2003, Fujita et al., 2004, Fujii et al., 2010). However, the effects of TGF-β1 on differentiation and matrix synthesis of PDLFs during periodontal regeneration are not fully understood.

TGF-β1 is assumed to have dual effects on PDLF proliferation, being either inhibitory or stimulatory depending on the differentiation stage of the cells (Okubo et al., 2003, Sant'Ana et al., 2007, Fujii et al., 2010). Transforming growth factor beta 1 is reported to contribute to fibroblastic differentiation of PDL cells by up-regulating COL1A1 and FBNI gene expression. TGF-β1 was shown to have less effect on the expression of these molecules in mature PDLF cultures and cell lines (Fujii et al., 2010).

It has been reported that exogenous TGF-β1 induces the gene expression of α-smooth muscle actin (α-SMA) and collagen type I mRNA in dermal fibroblasts, tenocytes, myofibroblasts and periodontal ligament fibroblasts (Ghosh et al., 2000, Kissin et al., 2002, Ono et al., 2007, Kono et al., 2013). Also, PDLFs stimulated with TGF-β1 showed significant increases in periostin mRNA levels in comparison to untreated control groups (Wen et

al., 2010). Kono et al., suggested usage of a bFGF/TGF-β1 combination for an effective regeneration of a functional periodontal ligament. Basic FGF stimulated cellular proliferation of periodontal ligament fibroblasts, while exposure of the cells to TGF-β1 for 2 days increased COL1A1 mRNA expression as compared with group stimulated with FGF alone or the control un-stimulated group (Kono et al., 2013). On the other hand, the combination of EMD and TGF-β1 did not induce any effect compared to when the two factors were used individually (Rodrigues et al., 2007). Using PDGF, TGF-β1 and IGF, alone or in combination, stimulated a mitogenic response in PDLFs and enhanced their adhesion to the root surface of teeth *in vitro*; observations which highlight the role of growth factors in periodontal ligament regeneration (Sant'Ana et al., 2007).

Stimulation of PDLFs with exogenous TGF-β1 for 24 h *in vitro* had no effect on the expression of the TGF-β1 gene (Fujii et al., 2010). Hence, the expression of endogenous TGF-β1 in the periodontal ligament might be regulated by other factors. It has been reported that PDLFs release high levels of TGF-β1 in the presence of EMD (Van der Pauw et al., 2000, Suzuki et al., 2005).

Also, PDLFs exposed to EMD showed higher expression of TGF-β1 and IGF-I at both gene and protein levels (Rodrigues et al., 2007). These data suggest that the effect of EMD in periodontal regeneration might be partially mediated by the endogenous TGF-β1 and IGF-I produce by the EMD stimulation (Okubo et al., 2003, Parkar and Tonetti, 2004, Suzuki et al., 2005, Fujii et al., 2010). However, the underlying molecules and mechanisms through which EMD induces endogenous TGF-β1 are still not completely understood.

In summary, growth factors have been used in animal studies and in human clinical applications for periodontal regeneration. However, the results were not consistent. While the *in vitro* effects of growth factors on PDLFs cultured as monolayers are well established, less is known about the mode in which growth factors affect *in vitro* 3D engineered periodontal ligaments.

3. AIM AND OBJECTIVES

Periodontal ligament regeneration remains one of the most significant challenges in dentistry, and new therapeutic approaches are needed if a solution is to be found. The cell alignment following the alignment of the fibres might be valuable for tissue regeneration by restoring the native architecture of the lost tissue. In periodontal ligament, where collagen fibres are highly oriented, scaffolds that maintain this architecture may be essential.

Hypothesis:

Aligned fiber scaffolds can maintain the fibroblastic phenotype which enhance the development of *in vitro* tissue engineered constructs better than random fiber scaffolds.

The aim and objectives:

The aim of this study was to investigate the effect of fibre-alignment of scaffolds on periodontal ligament fibroblast (PDLF) phenotype and behaviour. Also, the response of the PDLFs seeded on theses scaffolds to the application of mechanical strain and growth factors has been investigated.

The specific objectives were:

1. To fabricate synthetic scaffolds of poly(L-lactic acid) (PLLA) composed of either random or aligned-fibres using electrospinning.

2. To prepare aligned and random scaffolds based on decellularised bovine ligament and skin which have naturally aligned and random collagen fibres respectively.

3. To identify a suitable cell source for the development of an *in vitro* model for periodontal ligament tissue engineering.

4. To combine the research into scaffolds and cell sources to develop a tissue engineering approach to preparation of constructs that could be used to investigate the effect of fibre-alignment on the biological response of PDLFs.

5. To evaluate the effect of mechanical strain on gene expression of 3D tissue engineered periodontal ligament constructs or PDLFs embedded in collagen gels.

6. To evaluate the effect of fibre-alignment on the gene expression of tissue engineered ligament constructs in response to the application of static mechanical strain.

7. To investigate the effect of EMD and TGF-β1, on cell phenotype and differentiation of the tissue engineered ligament constructs.

On completion of this study, the potential for the development of a new therapeutic approach to periodontal ligament regeneration based on tissue engineering will be much clearer. Moreover, the relative importance of scaffold topography, mechanical strain and biological signals will be demonstrated. This work will therefore generate data that will add to the body of existing knowledge in periodontal tissue engineering. It will provide better insight towards the development of *in vitro* model that can be used to understand better the regeneration and repair in periodontal ligament.

4. MATERIALS AND METHODS

4.1 Materials

4.1.1 Scaffold Fabrication and Preparation

4.1.1.1 PLLA Electrospun Scaffolds

- Poly(L-lactic acid) (PLLA) cat. No. 81273 (Sigma-Aldrich, Poole, UK)
- Dichloromethane (DCM) (Fisher Scientific Loughborough, UK)
- 1 ml syringe (TERUMO, Belgium)
- Magnetic Stirrer (Stuart, Scientific lab., UK)
- 20 G metal needles (I&J Fisher Inc., USA)
- A high-voltage supply (ALPHA IV brandenburg model 4807, 30 kV)
- High speed dremel (Dremel 400, Digital)
- Syringe Pump (KD Scientific)
- Isopropyl alcohol for scaffolds disinfection (Fisher Scientific Loughborough, UK)

4.1.1.2 Decellularisation Process

- Skin and ligaments from bovine ankles
- Incubator [Galaxy R Plus CO_2 incubator, 37^{o}C with an atmosphere of 5% CO2, 95% humidity (Scientific Laboratory Supplies, Nottingham)]
- Ca2+ /Mg2+ free phosphate buffer saline (PBS) (Sigma-Aldrich, Poole, UK)
- Magnesium chloride (Sigma-Aldrich, Poole, UK)
- Sodium deoxycholate (Sigma-Aldrich, Poole, UK)
- Triton™ X-100 (Sigma-Aldrich, Poole, UK)
- Ribonuclease A from bovine pancreas (Sigma-Aldrich, Poole, UK)
- Deoxyribonuclease I from bovine pancreas (Sigma-Aldrich, Poole, UK)
- Microtome (Leica-Reicher)
- Optimal cutting temperature (OCT) tissue mounting medium, (VMR International, UK)
- Lab Rotator (Thermo, Hertfordshire, UK)
- Peracetic acid solution (Sigma-Aldrich, Poole, UK)
- Freeze drier (VisTis, Benchtop SLC, US)

4.1.2 Cell Sources and Cell Culture

4.1.2.1 Basic Cell Culture Materials

- Class II laminar flow cabinet (Walker Safety Cabinets Ltd, Glossop, UK)
- 25, 80 and 175 cm^2 Flasks (Nunclone, Fisher Scientific UK, Loughborough, UK)
- Centrifuge tubes (Greiner Bio-one, Germany)
- Centrifuge (Sanyo, Harrier 18/80)
- Pipettes (Costar, USA), Pipette tip (Starlab, UK)
- Plastic containers (Sarsted, Germany)
- 70% vol/vol industrial methylated spirit (IMS) (Fisher Scientific, Loughborough, UK)
- Stainless steel rings (6 mm inner width, 250 µl volume) (Medical Workshop, University of Sheffield)
- Dulbecco's Modified Eagle's Medium (DMEM) with high glucose formula containing 200 mM L-Alanyl-L-Glutamine (Sigma-Aldrich, Poole, UK)
- 10,000 units/ml penicillin (Sigma-Aldrich, Poole, UK)
- 10,000 µg/ml streptomycin (Sigma-Aldrich, Poole, UK)
- Foetal calf serum (FCS) (Biosera, Ringmer, UK)
- Trypsin-EDTA solution: 0.05% wt/vol porcine trypsin and 0.02% wt/vol tetra sodium EDTA in Hanks balanced salt solution containing phenol red (Sigma-Aldrich, Poole, UK)

- Ca2+/Mg2+ free phosphate buffer saline (PBS) (Sigma-Aldrich, Poole, UK)
- β-glycerophosphate disodium salt hydrate was dissolved in basic medium to give a 10 mM solution and filter-sterilised (Sigma-Aldrich, Poole, UK)
- Dexamethasone: Stock solutions of 1mM dexamethasone were prepared in dimethyl sulphoxide and stored in aliquots at -20^{0}C. Further dilutions were prepared in medium to a final concentration of 10^{-7} M (Sigma-Aldrich, Poole, UK)
- L-Ascorbic acid 2-phosphate was dissolved in basic medium to give a 50 mg/ml solution which was filter-sterilised. This solution was added to culture medium to give a final ascorbic acid concentration of 50 µg/ml (Sigma-Aldrich, Poole, UK)
- Incubator [Galaxy R Plus CO_2 incubator, 37^{o}C with an atmosphere of 5% CO_2, 95% air, 95% humidity (Scientific Laboratory Supplies, Nottingham)]

4.1.2.2 Isolation of Rat and Porcine Periodontal Ligament Cells

- Wistar rats, 4-5 weeks old were obtained from the Field Laboratory (University of Sheffield). Periodontal ligament tissue was obtained within 1h of euthanasia.
- Porcine heads were obtained from the local abattoir within 1-2 h of slaughter.

- Dissection tray containing scalpels, blades, forceps and tooth extraction and bone removal instruments
- 70% vol/vol industrial methylated spirit (IMS) (Fisher Scientific, Loughborough, UK)
- Cell strainers with 70 µm pore size (BD Biosciences, Erembodegem, Belgium)
- Sterile syringe filters with 0.2 µm pore size (Starsted, Germany)
- Bacterial collagenase from Clostridium histolyticum type 1, used at concentration of 2mg/ml in PDLF basic medium without bFGF (Sigma-Aldrich, Poole, UK)
- Ca^{2+}/Mg^{2+} free phosphate buffer saline (Sigma-Aldrich, Poole, UK)
- Basic fibroblast growth factor (bFGF), 10 µg/ml basic fibroblast growth factors (bFGF) in PBS containing 1mg/ml bovine serum albumin stored in aliquots at -20^0C (PrepoTech, London, UK)
- ***Porcine and rat PDLF basic culture medium***: Dulbecco's Modified Eagle's Medium (DMEM) with high glucose formula containing 2 mM L-Alanyl-L-Glutamine, 100 units/ml penicillin, 100 µg/ml streptomycin, 10% foetal calf serum (FCS) and 10 ng/ml of bFGF

4.1.2.3 Human Periodontal Ligament Fibroblasts Expansion

- Basic cell culture materials (section 4.1.2.1)
- Commercially available human primary periodontal ligament fibroblasts (ScienCell, USA; Cat No. 2630)

- ***PDLFs basic culture medium:*** Dulbecco's Modified Eagle's Medium (DMEM) with high glucose formula containing 2 mM L-Alanyl-L-Glutamine, 100 units/ml penicillin, 100 μg/ml streptomycin, 10% foetal calf serum (FCS)

4.1.2.4 PDLFs Characterisation in Monolayer

- Basic cell culture materials (section 4.1.2.1)
- 4% paraformaldehyde in PBS, pH= 7.4 (Sigma-Aldrich, Poole, UK)
- Sigmafast™ BCIP®/NBT (5-bromo-4-chloro-3-indolyl phosphate/nitro blue tetrazolium) (Sigma-Aldrich, Poole, UK)
- ***Mineralisation culture medium***: PDLF basic medium (section 4.1.2.3) containing L-Ascorbic acid 2-phosphate (50 μg/ml), Dexamethasone (10^{-7} M) and β-glycerophosphate (10 mM) (Sigma-Aldrich)
- 2% Alizarin Red S wt/vol solution in distilled water (Sigma-Aldrich, Poole, UK)
- Spot software (Diagnostic Instruments, Sterling Heights, MI, USA)

4.1.2.5 Seeding HPDLFs on Scaffolds

- Basic cell culture materials (section 3.1.2.1)
- Stainless steel rings (6 mm inner width, 250 μl volume) (Medical Workshop, University of Sheffield)
- 6, 12, 24, 96-well culture plates (Greiner Bio-One, Germany)
- L-Ascorbic acid 2-phosphate (Sigma-Aldrich, Poole, UK).

- ***Tissue engineering medium***: PDLF basic medium (section 4.1.2.3) containing L-Ascorbic acid 2-phosphate (50 µg/ml)

4.1.3 Variable Laboratory Techniques

4.1.3.1 Scanning Electron Microscopy (SEM)

- 0.1 M Cacodylate buffer, PH=7.4 (Agar Scientific Limited, Essex, UK)
- 2% (vol/vol) aqueous osmium tetroxide (Agar Scientific Limited, Essex, UK)
- 3% (vol/vol) gluteraldehyde (Agar Scientific Limited, Essex, UK)
- Adhesive carbon tabs and aluminium stubs (Agar Scientific Limited, Essex, UK)
- Ethanol (75%, 95%, 100% vol/vol and 100% vol/vol dried over anhydrous copper sulfate) (Fisher Scientific, Loughborough, UK)
- Hexamethyldisilazane (50%, 100% vol/vol) (Fisher Scientific Loughborough, UK)
- Gold sputter (Edwards S150B, UK)
- Philips XL-20 scanning electron microscope

4.1.3.2 Fluorescence Staining

- Ca2+/Mg2+ free phosphate buffer saline (PBS) (Sigma-Aldrich, Poole, UK)
- 4% (vol/vol) paraformaldehyde, (Sigma-Aldrich, Poole, UK)

- 1% (vol/vol) Triton X-100, (Sigma-Aldrich)
- 1% (vol/vol) bovine serum albumin (BSA) solution, (Sigma-Aldrich, Poole, UK)
- TRITC-conjugated phalloidin, (Sigma-Aldrich, Poole, UK)
- Hoechst staining, (Bisbenzimide Hoechst 3342 Trihydrochloride, Sigma, UK)
- ProLong® Gold reagent, (Invitrogen, UK)

4.1.3.3 Histological Preparation

- Ca2+/Mg2+ free phosphate buffer saline (PBS) (Sigma-Aldrich, Poole, UK)
- 4% (vol/vol) paraformaldehyde in PBS, pH = 7.4 (Sigma-Aldrich, Poole, UK)
- Microtome (Leica-Reicher)
- Optimal cutting temperature (OCT) tissue mounting medium, (VMR International, UK)
- DPX mountant (BDH labs, UK)
- Hematoxylin and eosin staining using Shandon Linear Stainer (Shandon Scientific Limited, UK).
- Glass slides (Menzel-Glaser, Braunschweig, Germany)
- 4% (vol/vol) (3-aminopropyl)triethoxysilone (APES) (Sigma-Aldrich, Poole, UK)
- Light microscope (Nikon Labophot-2 AFX-DX) and Olympus (cellsD imaging software)

4.1.3.4 Cellular Activity Assay

- 96-well culture plates (Greiner Bio-One, Germany)
- Ca2+/Mg2+ free phosphate buffer saline (Sigma-Aldrich, Poole, UK)
- alamarBlue® assay (Invitrogen, UK)
- Fluorescent plate reader (Infinite® 200 PRO, Tecan, Reading, UK)

4.1.3.5 DNA Quantification Assay

- Ca2+/Mg2+ free phosphate buffer saline (Sigma-Aldrich, Poole, UK)
- Papain from papaya latex (Sigma-Aldrich, Poole, UK)
- 200 mM phosphate buffer solution (Sigma-Aldrich, Poole, UK)
- 1 mM ethylenediaminetetraacetic acid, EDTA, (Sigma-Aldrich, Poole, UK)
- N-Acetyl-L-cysteine (Sigma-Aldrich, Poole, UK)
- Heat block (Jencons-PLS, UK)
- DNA Quantitation Kit, Fluorescence Assay (Sigma-Aldrich, Poole, UK)
- 96-well culture plates (Greiner Bio-One, Germany)
- Fluorescent plate reader (Infinite® 200 PRO Tecan, Reading, UK)

4.1.3.6 Total Protein Assay

- Complete Protease Inhibitor Cocktail, EDTA free (Roche, Burgess Hill, UK)
- RIPA buffer (Sigma-Aldrich, UK)
- Colorimetric Bicinchoninic Acid (BCA) Protein Assay kit (Thermo, Hertfordshire, UK)
- 96-well culture plates (Greiner Bio-One, Germany)
- Plate reader (FLUOstar Galaxy, BMG Labtechnologies, Durham, UK)

4.1.3.7 Total RNA Extraction

- RNeasy Mini Kit (Quiagen kit, UK)
- 70% (vol/vol) ethanol (Sigma-Aldrich, Poole, UK)
- RNase/DNase-free water (Quiagen, UK)
- High speed centrifuge (GH-Merton, Promega, London)
- Needles and syringes (Sigma-Aldrich, Poole, UK)
- Nanodrop spectrophotometer (Thermo, Hertfordshire, UK)

4.1.3.8 Reverse Transcription

- High Capacity cDNA Reverse Transcription Kit (Applied biosystem, UK)
- RNase/DNase-free water (Quiagen, UK)

- MJ Thermocyler (Bio-Rad Laboratories Ltd, Life Science, Hemel Hempstead, UK)
- PCR tubes (Sigma-Aldrich, Poole, UK)

4.1.3.9 Quantitative Real Time Polymerise Chain Reaction (qRT-PCR)

- TaqMan® Gene Expression Master Mix (Applied Biosystems, Foster City, USA)
- Purified cDNA samples
- Taqman® gene primers, listed in Table 4-1 (Applied Biosystems, Foster City, USA)
- DNase/RNase-free water (Quiagen kit, UK)
- MicroAmp® Fast Optical 96-Well Reaction Plate (ABI)
- 7900HT Fast Real-Time PCR System (Applied Biosystems, UK)

Table 4-1: Details of Taqman® gene expression assays used in qRT- PCR.

Gene name	Abbreviation	Assay ID
Collagen type I alpha 1	COL1A1	Hs00164004_m1
Periostin	POSTN	Hs01566750_m1
Alkaline phosphatase	ALPL	Hs01029144_m1
Scleraxis homolog A	SCXA	Hs03054634_g1
Runt-related transcription factor 2	RUNX2	Hs00231692_m1
Bone gamma-carboxyglutamate protein	BGLAP	Hs01587814_g1
Interleukin-6	IL6	Hs01075666_m1
Human beta-2-microglobulin	β2M	NM_004048.2

4.1.3.10 Immunohistolocalisation

- 4% (vol/vol) paraformaldehyde in PBS, pH = 7.4 (Sigma-Aldrich, Poole, UK)
- Ca^{2+}/Mg^{2+} free phosphate buffer saline (Sigma-Aldrich, Poole, UK)
- 3% (vol/vol) hydrogen peroxide in 50% (vol/vol) methanol (Sigma-Aldrich, Poole, UK)
- Sodium deoxycholate (Sigma-Aldrich, Poole, UK)
- Primary antibody for collagen type I, periostin, RUNX2 and osteocalcin (see Table 4-3)
- Normal goat serum (NG) (Vector laboratories Ltd, Peterborough, UK)
- Normal rabbit serum (NRS) (Vector laboratories Ltd, Peterborough, UK)

- Vectastain® Elite ABC Kit, with biotinylated goat IgG (Vector Laboratories Ltd, Peterborough , UK)
- DAB Peroxidase Substrate Kit (Vector Laboratories Ltd, Peterborough, UK)

4.1.3.11 Western Blots

- Colorimetric Bicinchoninic Acid (BCA Assay (BCA™ protein assay kit, Thermoscientific)
- Reducing agent (NuPAGE 10X, Invitrogen)
- Readymade SDS-PAGE gels (NuPAGE-Tris Mini Gels Novex, Invitrogen)
- Mini-PROTEAN® Tetra Cell (Bio-RAD, USA)
- Sodium dodecyl sulfate (SDS) running buffer, (NuPAGE 10X, Invitrogen) (see Table 4-2)
- Prestained protein ladder (Novex® Sharp Pre-Stained Protein Standard, Invitrogen)
- Optitran Nitrocellulose transfer membranes (Blotting Membrane, BA-S 83, Whatman)
- 10% (vol/vol) methanol (Sigma-Aldrich, Poole, UK)
- 10% (vol/vol) NuPage transfer buffer 20X (Invitrogen)
- 3MM papers (Whatman, Sigma-Aldrich, Poole, UK)
- 5% (wt/vol) dried semi- skimmed milk (Table 4-2)
- Tris-buffered Saline (TBS) (Table 4-2)
- TBS containing 0.05% (vol/vol) Tween-20 (TBST) (Table 4-2)

- SuperSignal® West Pico Chemiluminescent substrate (Thermo Scientific)
- Saran wrap
- ECL film (Kodak)

Table 4-2: Range of buffers solutions used in Western blots.

Solution	Material	Measurement
SDS running buffer	TRIS Base Glycine SDS Distilled Water	6.04 g 28.8 g 2 g 1.8 L
TRIS Buffer Saline pH=7.4 (TBS)	TRIS Sodium chloride 1 M HCL Distilled Water	3.02 g 40 g 22 ml 1 L
1X TBST Tween-20 (TBST)	1X TBS Tween-20 Distilled Water	200 ml 1 ml 800 ml
Blocking solution	TBST Semi-skimmed milk powder	20 ml 1 g

4.1.4 Static and cyclic Mechanical Loading Application

- Custom-built loading chamber (Figure 4-6)
- Flexcell® Tissue Train® Culture System

  This culture system is composed of a Flexcell® FX-4000T™ with a Tissue Train® accessory package and Tissue Train® Culture plates (Dunn Labortechnik, Asbach, Germany)

- Rat tail type I collagen (First Link, Wolverhampton, UK)
- 10 M Sodium Hydroxide (Sigma-Aldrich, Poole, UK)
- Phenol red indicator (Sigma-Aldrich, Poole, UK)
- Dulbecco's Modified Eagle's Medium 10X, (Sigma-Aldrich, Poole, UK)
- RNA*later*® (Sigma-Aldrich, Poole, UK)

4.1.5 EMD and/or TGF-β1 Stimulated Tissue Engineered Periodontal Ligament Constructs

- Basic cell culture materials (section 4.1.2.1)
- ***Growth factor medium***: Dulbecco's Modified Eagle's Medium (DMEM) with high glucose formula containing 2 mM L-Alanyl-L-Glutamine, 100 units/ml penicillin, 100 μg/ml streptomycin, 0.2% Foetal calf serum (FCS) and L-Ascorbic acid 2-phosphate (50 μg/ml)
- A commercially available Emdogain® (EMD) preparation (30 mg/ml in a propyl glycol alginate carrier) was given courtesy of Straumann
- Transforming growth factor beta 1 (TGF-β1): A stock solution of 10μg/ml was prepared in PBS containing 1 mg/ml BSA as a carrier protein. The stock solution was stored in aliquots at -20^{0}C and diluted in culture medium to the final required concentration (PeproTech EC, London, UK).

4.2 Methods

4.2.1 Scaffold Fabrication

4.2.1.1 Electrospinning of Scaffolds

Random and aligned-fibre PLLA scaffolds were obtained by the electrospinning process. An 8% (wt/vol) poly(L-lactic acid) solution was prepared by dissolving 0.4 g of poly(L-lactic acid) in 4.6 g of dichloromethane (DCM). After stirring the mixture overnight, the polymer solution was placed in a 1 ml glass syringe fitted with a 20 G metal needle. The electrospinning equipment used in this study consisted of a syringe, pump, and metal needle (Figure 4-1). A grounded target (negative electrode) consisting of a speed-controlled rotating drum attached to a rotating dremel at 5000 rpm was used to collect the aligned-fibres, or a static plate for random fibres, under a high-voltage supply. The distance between the needle tip and the ground collector/rotating drum was 20 cm (Figure 4-2).

The experimental electrospinning parameters were adjusted until a good Taylor cone shape and a continuous thin polymer jet were obtained. The influence of the voltage and polymer flow rate was investigated and optimised. In this case, the polymer concentration and the distance between the needle tip and the ground collector were kept constant, while the electrical potential and the polymer flow rate varied (16 and 18 kV and 1- 4 ml/h respectively) based on the SEM analysis of the effect of the above parameters on the fibres produced.

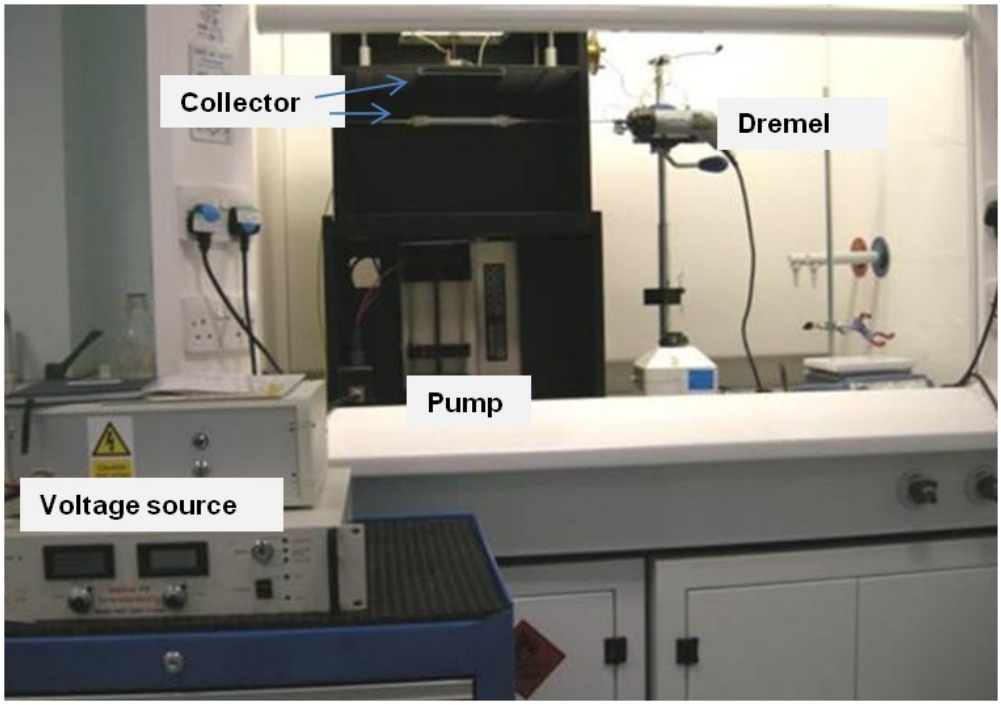

Figure 4-1: Photograph of the electrospinning equipment used.

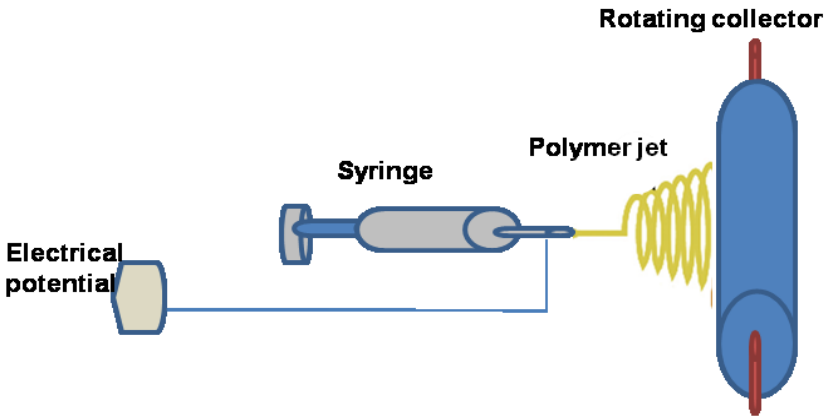

Figure 4-2: Schematic diagram of the experimental set-up used to collect aligned electrospun PLLA fibres. Rotating drum at high speed used to collect the polymer jet while applying high voltage.

4.2.1.2 Decellularisation Process

Bovine skin and ligaments were obtained from a local abattoir and excised of adherent tissues. Some tissue samples were retained at this stage for use as a control (native) while the remaining samples underwent a decellularisation procedure (decell-skin, decell-ligament). Rieder et al's decellularisation protocol was adopted (Rieder et al., 2004). Two commonly used detergents, namely Triton X-100 and sodium deoxycholate, were used. Samples for decellularisation were constantly agitated for 24 h at 37°C in PBS containing 0.25% Triton X-100 and 0.25% sodium deoxycholate. Samples were then washed for 72 h with PBS at 4°C. Following the wash cycle, the samples were treated with RNase A (100 µg/mL) and DNase I (150 IU/mL) with 50 mM $MgCl_2$ in PBS for 24 h at 37°C. After nuclease digestion, the samples were again washed with PBS for 24 h at 4°C. All steps were conducted with continuous shaking. The treated samples were then wrapped with parafilm and embedded in OCT and stored at -20^0C. Using a cryostat, 120 µm thickness frozen sections were cut from the OCT-embedded blocks. Decell-skin/ligaments were freeze-dried and stored at 4ºC until required (Figure 4-3). Before seeding, decell-skin and decell-ligament samples were sterilised using 0.1% peracetic acid in PBS for 30 min and then washed three times with PBS.

Figure 4-3: Samples of decell-skin, on the left, and decell-ligament on the right after the decellularisation process and slicing.

4.2.2 Scaffold Characterisation

4.2.2.1 PLLA Scaffolds

Scanning electron microscope examination

The poly(L-lactic acid) scaffolds were air-dried in a fume hood and then mounted onto aluminium stubs using carbon tabs. Scaffolds were gold-coated by an automatic sputter coater for 4 min to reach a conductive layer thickness of around 200 nm. SEM photographs were taken using a Philips XL-20 scanning electron microscope at 20 kV.

Measurement of fibre alignment and scaffold anisotropy

Fast Fourier Transformation (FFT) was used to characterise fibre alignment as a function of electrospinning conditions. Fast Fourier transformation is a non-invasive method that is used to precisely measure fibre alignment and overall scaffold anisotropy (Ayres et al., 2008). The FFT analysis was used to

evaluate fibre alignment based on the SEM images of the electrospun PLLA scaffolds. The FFT function converts information present in the original image from the 'real space' into the mathematically defined 'frequency space'. The resulting FFT output image contains grayscale pixels that are dispersed in a pattern that represents the degree of fibre alignment existing in the SEM image. SEM images were converted to 8-bit grayscale TIF files and were cropped to 250×250 pixels. The micrographs were then analysed with Image J software (National Institutes of Health, USA).

4.2.2.2 Decellularised Bovine Skin and Ligaments

The following methodologies were used to 1). evaluate the efficacy of the decellularisation process on the ligament and skin tissues and 2). investigate tissue integrity after the decellularisation process.

Histological evaluation

Samples of decellularised and non-decellularised skin and ligament were fixed in 10% formalin and incubated overnight at room temperature using gentle movement by a rotator. The samples were then washed three times in PBS, embedded in OCT and sectioned as 8 µm thickness specimens. The sections were mounted on glass slides coated with 4% APES and stained with H&E staining using a Shandon Linear Stainer. After staining, the slides were collected and mounted with DPX and covered with glass cover slips. The specimens were observed using a light microscope and photographs were taken using cell image software.

Scanning electron microscope examination

Decellularised and non-decellularised skin and ligament were prepared as described in section 4.1.1.2 and mounted onto aluminium stubs using carbon tabs. The specimens were then gold coated by an automatic sputter coater for 4 min to achieve a conductive layer thickness of around 200 nm. SEM photographs were taken using a Philips XL-20 scanning electron microscope at 20 kV.

Fluorescence staining of nuclei

To evaluate the efficiency of total nuclei removal from the decellularised skin and ligament, decellularised and non decellularised skin and ligaments were stained with Hoechst dye to detect nuclei. Skin and ligament samples were embedded in OCT and sectioned as 8 µm thickness specimens and the cells were permeabilised using 0.1 % Triton X-100 for 10 min at room temperature. After washing with PBS, the tissues were then incubated in 1 % bovine serum albumin (BSA) in PBS for 15 min at room temperature. The decellularised and control native skin and ligaments were then washed three times with PBS and incubated with Hoechst reagent diluted (1/100) in PBS for 10 min, at room temperature, away from direct light, to stain the nuclei, The slides were then rinsed three times with PBS and mounted with ProLong® Gold mounting medium and were covered with glass cover slips. The nuclei staining was visualised using a fluorescent microscope and images were captured using a Zeiss Axiovert 200.

DNA content

The DNA content remaining after the decellularisation process was measured using a DNA quantification assay (section 4.1.3.5). Decellularised and non-decellularised skin and ligament samples weight 50 mg were incubated with 200 µl papain in 200 mM phosphate buffer containing 1 mM EDTA, pH 6.8. The samples were incubated for 3 h at 60ºC to ensure total tissue dissociation. The samples were then diluted by adding 100 µl of the 10x fluorescent assay buffer. In 96 well plates, 200 µl of 0.1 µg/ml bisBenzimide solution (Hoechst 33258) was added to 50 µl of the samples. The fluorescence intensity was measured using a fluorescent plate reader at an excitation wavelength of 356 nm and emission wavelength of 470 nm. The DNA standard curve was plotted using measurements from six serial dilutions of calf thymus DNA (provided in the kit), ranging from 0 to 5 µg/ml. The fluorescence of the six standards was plotted against their known concentrations in order to construct a reference standard curve. To calculate the DNA concentration in the target samples, the fluorescence of each sample was compared to that of the known DNA and calculated using the standard curve.

4.2.3 PDLF Sources and Characterisation

4.2.3.1 PDLF Isolation and Culture

Isolation and culture of Porcine and Rat PDLFs

Rat and porcine heads were obtained as soon as possible after euthanasia of the animals. Healthy anterior porcine and rat incisors were extracted with minimum trauma (section 4.1.2.2). The periodontal ligaments were scraped from the middle third of the root surfaces with a periodontal curette as described previously (Somerman et al., 1990) (Figure 4-4). The periodontal tissue was then minced with a scalpel. For explant culture, small pieces of ligament tissue were transferred to 25 cm^2 adherent culture flasks and porcine or rat PDLF culture medium added accordingly. The flasks were then transferred to a humidified incubator at 37^0C with a 95% air and 5% CO_2 atmosphere. Media changes were carried out twice weekly.

For enzymic isolation of PDLFs, the minced periodontal tissue was digested with 2 mg/ml collagenase type I for 1 h at 37°C to digest the tissue and obtain a cell suspension (Shi et al., 2005). A suspension of single cells was obtained by passing the digested tissue through a 70 µm strainer. The cells were then pelleted by centrifugation (110 g for 10 min). The supernatants were removed and the pellets washed twice to remove any remaining collagenase activity. The final cell pellets were resuspended in the porcine or rat PDLFs culture medium depending on the tissue source and plated out in 25 cm^2 flasks (section 4.1.2.2). After 24 h, non-adherent cells were removed and fresh

medium was added. Cells were grown to sub-confluence at 37°C and an atmosphere of 95% air/ 5% CO_2 in a humidified incubator. Media changes were carried out twice weekly.

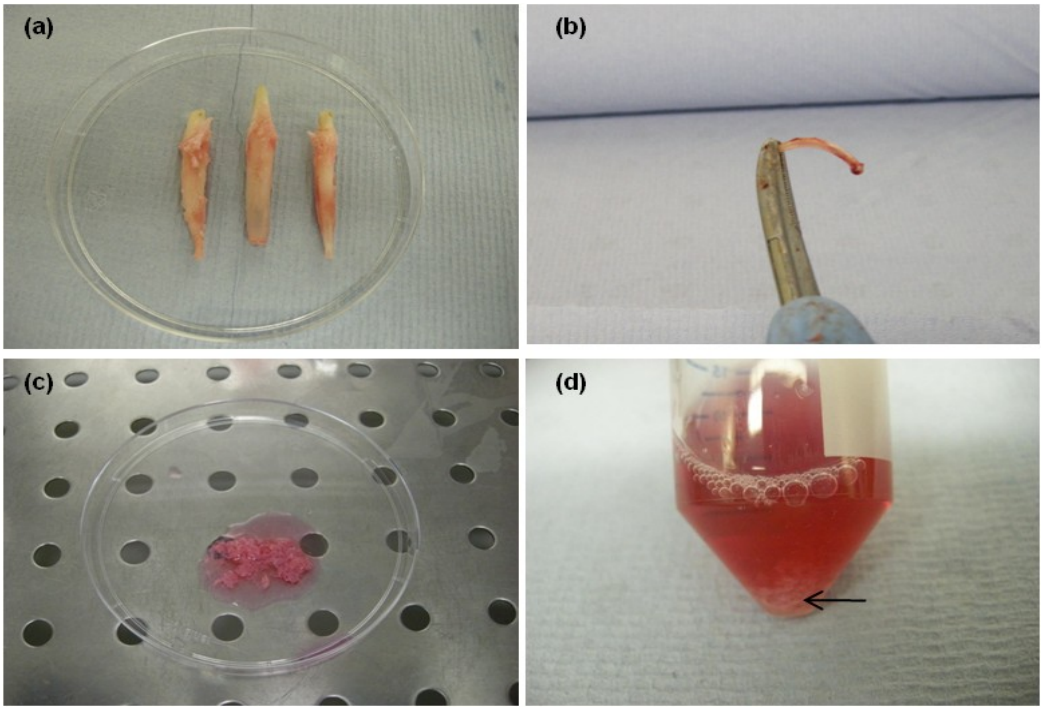

Figure 4-4: Photographs show (a) the extracted porcine anterior teeth after the periodontal ligament has been scraped off, (b) the extracted anterior rat tooth, (c) the periodontal ligament tissue harvested from porcine anterior teeth and (d) the tissue after digestion with collagenease for 1 h (the arrow indicates the tissue remnants after being digested).

Human periodontal ligament fibroblasts (HPDLFs)

Human PDLFs were delivered frozen in dry ice and were stored in liquid nitrogen until use. Each vial contained approximately ≈ 5 x 10^5 cells in 1 ml volume. The PDLFs were derived from pooled periodontal ligament tissue from several patients. When required, a vial of HPDLFs was transferred from liquid nitrogen and thawed in a water bath at 37°C. The vial was disinfected with 70% ethanol and the cell suspension transferred to a 15 ml tube containing HPDLFs basic medium (section 4.1.2.3). After centrifugation for 5 min at 110 g, the supernatant was discarded and the cell pellet resuspended in 15 ml of fresh PDLF basic medium and transferred to a 25 cm^2 flasks. The cells were incubated at 37ºC in a humidified atmosphere of 95% air and 5% CO2. The culture medium was changed every 3 days, until the cultures reached 80- 90% confluence.

Sub-culture (Passaging) of PDLF Cultures

When the PDLFs were 80-90% confluent, the cell layer was washed twice with PBS and detached from the culture plate by incubation with 0.25% trypsin/EDTA for 5 min at 37ºC. Cell detachment was monitored visually using an inverted light microscope. When the cells detached, the activity of the trypsin reaction was neutralised by addition of PDLF basic medium. The cell suspension was centrifuged at 110 g for 5 min. The supernatant containing the trypsin was removed and the cell pellet was resuspended in PDLF basic medium. Cells were counted using a haemocytometer and new T75 flasks were then seeded with 5 x I0^5 cells in 15 ml of PDLF basic medium. The

flasks were labelled and incubated at 37ºC in humidified atmosphere of 95% air and 5% CO_2. For PPDLFs and RPDLFs only early passages from 2-4 were used, while HPDLFs between passages 4 and 7 were used in most of the experiments. For experimental procedures, the cells were passaged, counted and seeded at appropriate cell densities and cultured under appropriate incubation conditions and media depending on the experimental design and purpose.

4.2.3.2 PDLF Characterisation in Monolayer

PDLFs show fibroblastic characteristics with some osteoblastic properties. The cells exhibit high levels of alkaline phosphatase, which relate to their ability to differentiate into osteoblasts or cementoblasts. To characterise PDLFs, the morphology and the ability of the cells to express ALPL and form mineralised tissue were examined. Human, rat and porcine PDLFs were seeded into 6-well culture plates at a density of $5x10^4$ cells/well. The HPDLFs were maintained in the basic medium (section 4.1.2.3), while the RPDLFs and PPDLFs were cultured in basic medium (section 4.1.2.2) containing 10 ng/ml bFGF until they reached 90% confluence.

PDLF Morphology

When confluent, the cell layers were washed twice with PBS and fixed with 4% paraformaldehyde for 10 min at 4ºC. PDLF morphology was examined under phase contrast using an inverted microscope and photographs were taken using Spot software.

Alkaline Phosphatase Localisation (ALPL)

The alkaline phosphatase was localised using SIGMA*FAST*™ BCIP®/NBT 2% (Sigmafast™ 5-bromo-4-chloro-3-indolyl phosphate/nitro blue tetrazolium tablets). One tablet of BCIP/NBT was dissolved in 10 ml distilled water. When confluent, PDLFs from different sources were fixed with 4% paraformaldehyde, washed twice with deionised water and 500 µl of SIGMA*FAST*™ BCIP®/NBT solution were added to each well and incubated for 10 min at room temperature. The cells then were rinsed with deionised water and observed using an inverted microscope. Photographs were taken using Spot software.

Mineralised Nodule Formation

To assess the ability of PDLFs to form mineralised nodules in 2D monolayer cell culture, 2% Alizarin Red S was used to stain any mineralised nodules. Human and rat PDLFs were cultured in 6-well plates at a cell density of $5x10^4$ cells/well in PDLF basic medium. When confluence was reached, the PDLFs were cultured in mineralisation medium for 40 days (section 4.1.2.4). The cultures were then washed twice with deionised water and were fixed using 70% ethanol for 5 min at 4ºC. The cells were washed with deionised water to remove any ethanol and then incubated with Alizarin Red S for 10 min at room temperature. The cells were then washed three times with deionised water to remove any excess staining. The mineralisation was observed using an inverted microscope and photographs were taken using Spot software.

4.2.4 3D Tissue Engineered Periodontal Ligament Constructs

4.2.4.1 Seeding HPDLFs onto Scaffolds

PLLA scaffolds and decell-skin/ ligament were cut to 10 mm^2 size to fit into a 12-well plate. The PLLA scaffolds were sterilised with 70% isopropanol for 15 min. Alternatively, decell-skin and decell-ligament scaffolds were sterilised using using 0.1% peracetic acid then rinsed with PBS (section 4.2.1.2). The PLLA scaffolds were preconditioned with fresh basic medium for 3 h at 37ºC to enhance their hydrophilic properties. Stainless steel rings of 0.6 mm inner diameter were used to maintain prolonged cell contact with the scaffolds (Figure 4-5). 200 µl of a PDLFs suspension (containing the number of cells required for the experiment) were dispensed in the ring. After overnight incubation, the rings were gently removed and tissue engineering medium was added (section 4.1.2.5), unless stated otherwise.

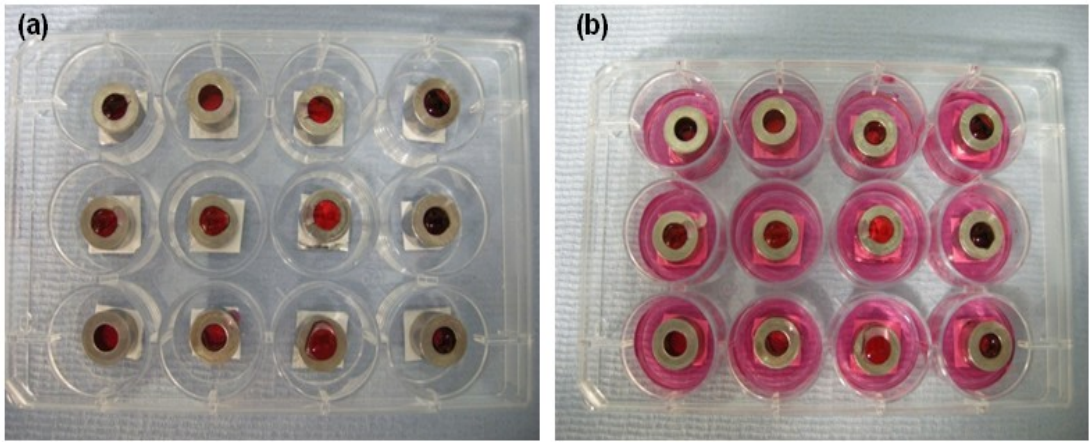

Figure 4-5: Photographs showing the technique used to seed HPDLFs onto PLLA and decellularised scaffolds (a) the steel rings were placed on the scaffolds and HPDLFs were seeded into the ring to ensure maximum time of cell/scaffold contact, (b) 500 µl of the medium was added to the outer area of each well and cells were incubated overnight for initial cell attachment.

4.2.4.2 SEM Imaging of HPDLF 3D-culture on Scaffold Materials

To evaluate the influence of scaffold fibre alignment on HPDLF morphology and orientation, PLLA and decellularised skin and ligaments were seeded with $1x10^5$ cells/scaffold and cultured, as described in section 4.2.4.1. At days 1 and 7, the constructs were rinsed in 0.1 M sodium cacodylate buffer and fixed with 3% glutaraldeyde in cacodylate buffer for 30 min. The samples were then treated with 2% osmium tetroxide for 2 h. After being rinsed with sodium cacodylate buffer, constructs were then dehydrated through a series of graded ethanol solutions: 75, 95 and 100% vol/vol, and 100% vol/vol dried over anhydrous copper sulfate for 15 min. The constructs then were dried to a critical point using 50/50 hexamethyldisilazane and ethanol followed by 100%

hexamethyldisilazane for 20 min. Samples were air-dried overnight in the fume hood before being mounted onto aluminium stubs using carbon tabs. Samples were gold-coated by automatic sputter coater for 4 min to reach a conductive layer thickness of around 200 nm. Scanning electron micrographs were taken using a Philips XL-20 scanning electron microscope at 20 kV.

4.2.4.3 Fluorescence Staining

HPDLFs were seeded onto PLLA scaffolds and decellularised skin and ligament at $1x10^5$ cells/scaffold, and cultured in HPDLF basic medium for 48 h (section 4.1.2.5). The scaffold/cell constructs were then washed twice with PBS and fixed in 4% paraformaldehyde at 4ºC for 15 min and washed three times in PBS. To ensure free access of the florescence stain, the cells were permeabilised using 0.1% Triton X-100 for 10 min at room temperature and washed three times with PBS. The constructs were then incubated for 15 min at room temperature in 1% bovine serum albumin (BSA) in PBS, to prevent nonspecific staining. The constructs were incubated, away from direct light, with phalloidin diluted 1/50 in PBS to stain actin filaments, for 10 min at room temperature. After rinsing once with PBS, the constructs were then incubated for 5 min with Hoechst reagent diluted 1/100 in PBS for to stain the nuclei. After rinsing three times with PBS, the constructs were gently transferred to glass slides, mounted with ProLong® Gold mounting medium and covered with glass cover slips. The stained constructs were visualised using a fluorescent microscope and images were captured using a Zeiss Axiovert 200.

4.2.4.4 Cellular Activity Assay

HPDLF cell activity was assessed using alamarBlue®. The active component of alamarBlue® is resazurin which is nontoxic, blue in colour and non-fluorescent. Viable cells reduce resazurin to the fluorescent resorufin, which can be detected by measuring fluorescence at 595 nm. Although a linear relationship between fluorescence and cell number is established, the level of fluorescence can be affected by both alteration in cell number (proliferation) and/or cell activity (Nakayama et al., 1997).

HPDLFs were seeded on both PLLA scaffolds and decellularised skin and ligament at a cell density of $2x10^5$ cells/scaffold for 0, 7 and 20 days as described in section 4.2.4.1. At the required time points, the medium was removed and fresh PDLF basic medium containing 10% (vol/vol) alamarBlue® was added to each construct according to the manufacturer's instructions. After 4 h incubation at 37ºC, triplicate, 200 µl samples from each well were placed into individual wells of a 96-well plate and the fluorescence intensity was measured with a Tecan fluorescent plate reader using an excitation wavelength of 540 nm an emission wavelength of 570 nm (section 4.1.3.5). The fluorescence readings of cell-free samples (i.e. the negative control), were determined to detect any dye changes occurring in the absence of cells. These negative controls indicated no significant interaction between alamarBlue® and the scaffolds. Therefore, fluorescence was corrected using the value of 10% alamarBlue® solution in medium without cell-seeded scaffolds as a negative control.

4.2.4.5 DNA Quantification Assay

To assess the ability of HPDLFs to proliferate on the various scaffold materials, the DNA content of the cell/scaffold constructs was measured. PLLA and decellularised skin and ligament scaffolds were seeded with $2x10^5$ HPDLFs and cultured for 0, 7 and 20 days (section 4.2.4.1). At the required time points, the constructs were washed twice with PBS and each sample was incubated with 200 µl papain in 200 mM phosphate buffer pH 6.8 containing 1 mM EDTA. The samples were incubated for 3 h at 60ºC to ensure total dissociation of cells from scaffolds. The digested samples were diluted by adding 100 µl of the 10x fluorescent assay buffer and stored at 4ºC until required. Total DNA quantification was carried out using the DNA Quantitation Kit, fluorescence assay. In a 96-well plate, 200 µl of 0.1 µg/ml bisBenzimide Solution was added to 50 µl of DNA from the samples. The fluorescence intensity was measured using a Tecan fluorescent plate reader at an excitation wavelength of 356 nm and emission wavelength of 470 nm. The DNA standard curve was plotted using values from six serial dilutions of calf thymus ranging from 0 to 5 µg/ml. Using the Excel program (Microsoft), the fluorescence of the six standards was plotted against their known concentrations to create a standard curve. To calculate the DNA concentration in the target samples, their fluorescence was applied in the equation of the standard curve created.

4.2.4.6 Total Protein Assay

Total protein quantity was measured using the BCA protein assay to assess the effect of scaffold topography on HPDLF protein synthesis capability. HPDLFs were seeded on PLLA scaffolds, as described in section 4.2.4.1, at a density of $2x10^6$ cells/scaffold. At day 1, 14 and 20 the constructs were washed twice in PBS and placed individually in 50 µl lysis buffer made of complete protease inhibitor cocktail and RIPA buffer in ratio of 1:10 for 30 min at room temprature. To measure the purified protein concentration, the colorimetric Bicinchoninic Acid (BCA) Protein Assay kit was used (Smith et al., 1985). Working reagent was prepared by mixing reagent A with reagent B in 1:50 ratio. The samples were diluted in 1:10 ratio. Only 10 µl of the diluted samples were aliquoted in triplicate in a 96-well plate. 200 µl working reagent was added to each well and reaction was allowed to take place at 37°C for 30 min. The optical density of the samples was then measured at 570 nm using a Tecan plate reader. The absorbance of six serially diluted protein standards with known concentrations (0, 0.125, 0.25, 0.5, 1 and 2 mg/ml) was plotted to create a reference standard curve. To calculate the protein concentration in the samples, their absorbance was applied in the equation of the standard curve and the result was multiplied by the dilution factor.

4.2.4.7 Histological Evaluation

HPDLFs were seeded onto the PLLA scaffolds and the decellularised skin and ligament at a density of $2x10^6$ cells/scaffold and were cultured for 2 weeks as described in section 4.1.2.5. At day 14, the constructs were washed twice with PBS and fixed in 4% paraformaldehyde for 15 min at 4°C. The constructs were then embedded in OCT and 8 µm frozen sections were prepared using a cryostat. The tissue sections were mounted on glass slides coated with 4% APES. The tissue sections were then stained with Hematoxylin and Eosin (H&E). Hematoxylin and Eosin is one of the most widely used staining techniques in which nuclei of cells are basophilic and stained blue by the hematoxylin stain, whilst the cytoplasm is stained pink by the eosin dye.

4.2.4.8 Immunolocalisation of PDLF Proteins

Random and aligned-fibre PLLA scaffolds were seeded with HPDLFs at a density of $2x10^6$ cells/scaffold and were maintained at 37°C and 5% CO_2 in a humidified incubator for 4 weeks and the tissue engineering medium was changed twice a week (section 4.1.2.5). At day 30, the constructs were washed twice with PBS then embedded in OCT. and kept at -80°C for sectioning. OCT-embedded frozen blocks were cryosectioned at 8 µm thickness and the sections mounted on glass slides coated with 4% APES. Mounted specimens were fixed in 4% paraformaldehyde for 15 min at 4°C. Sections for immunohistochemical analysis were washed with distilled water and immersed in 3% hydrogen peroxide in PBS for 5 min to inhibit

endogenous peroxidase activity. The specimens were incubated for 30 min with normal serum as a blocking agent to reduce non-specific binding. The sections were then incubated with the primary antibody at 4°C overnight. After washing in TBS, The sections were subsequently incubated for 1 h at room temperature with the appropriate secondary antibody (antibodies and their sources are listed in Table 4-3. The biotinylated secondary antibody was prepared from VECTASTAIN® ELITE ABC Kit as specified by the manufacturer and the antibody-antigen reaction was developed with the Peroxidase Substrate Kit (DAB) to visualise the bound antibody. After immunolocalisation was completed, the nuclei were counterstained with haematoxylin. For negative controls (non-specific binding), the sections were incubated with normal serum instead of the primary antibody. All reactions were carried out in a humidified chamber at room temperature and the slides were washed between reactions with PBS for 5 min. The slides were examined under a light microscope and images were captured using cell image software (section 4.1.3.3).

4.2.4.9 Osteogenic Differentiation

HPDLFs were cultured on the scaffold materials in osteogenic medium. These experiments were to investigate if 3D cultures of HDPLFs retained the ability to differentiate to osteoblast-like cells and form mineralised nodules. Random and aligned-fibre PLLA scaffolds were seeded at a density of $1x10^6$ cells/scaffold as described previously (4.2.4.1). After overnight incubation in basic medium, the HPDLFS were cultured in mineralisation medium for 40

days (section 4.1.2.4). The mineralisation medium was replaced every 2 days with freshly prepared media. On day 40, the random and aligned-fibre constructs were washed twice with deionised water and fixed using 70% ethanol for 5 min at 4ºC. The constructs were then washed twice with deionised water to remove any ethanol and incubated with Alizarin Red S for 10 min at room temperature. The constructs were washed three times with deionised water to remove any excess staining and mineralisation was observed using an inverted microscope. Photographs were taken using Spot imaging software.

Table 4-3: Antibodies used in immunolocalisation experiments.

Primary antibody	Concentration	Dilution	Secondary antibody
Collagen type I Goat monoclonal to collagen I (Southern Bioscience)	4 µg/ml	1:100	Anti-goat (Vectastain®Elite®ABC kit-PK-6100 series)
Periostin Rabbit polyclonal to periostin (ab14041, ABCAM	1 µg/ml	1:1000	Anti-rabbit (Vectastain®Elite®ABC kit-PK-6100 series)
RUNX2 Rabbit polyclonal to RUNX2 (ab23981, ABCAM)	2 µg/ml	1:250	Anti-rabbit kit (Vectastain® Elite® ABC kit-PK-6100 series)
Osteocalcin Mouse monoclonal to osteocalcin (ab13418, ABCAM)	10 µg/ml	1:100	Anti-mouse kit (Vectastain® Elite® ABC kit-PK-6100 series)

4.2.4.10 Quantification of Gene Expression Using Quantitative Real Time Polymerase Chain Reaction (qRT-PCR)

Poly(L-lactic acid) scaffolds and decellularised skin and ligament were seeded with HPDLFs at a density of $2x10^6$ cells/scaffold and cultured for 0, 7, 14 and 20 days. At the required time points, the constructs were washed with PBS and immediately stored at -80^oC.

mRNA Extraction

Total cellular RNA was extracted using the spin column technology, RNeasy Mini Kit, according to the protocol provided by the manufacturer (section 4.1.3.7).

The constructs were washed twice with PBS for complete removal of medium which might inhibit cell lysis, dilute the lysate and reduce the mRNA yield. The cells were disrupted by adding 500 µl of RLT lysis buffer to the constructs and incubating at room temperature for 15 min. Complete lysis of cells and homogenisation was then achieved by using a syringe and needle. The lysates were passed at least 5 to 10 times through a 20 G needle attached to a sterile plastic syringe until a homogeneous lysate was achieved. 400 µl of 70% ethanol was added to the homogenised lysate, and the samples mixed well by pipetting them up and down. Up to 700 µl of each lysate was transferred to individual RNeasy spin columns placed in 1.5 ml collection tubes. The lids were closed gently, and columns centrifuged for 15 s at 8000 g after which the flow-through was discarded. 700 µl Buffer RW1 was added to the RNeasy spin columns and the columns re-centrifuged for 15 s at

8000 g, the flow-through was again discarded. 500 µl of RPE washing buffer diluted with 4 volumes of ethanol was added to the RNeasy spin column and the columns re-centrifuged for 15 s at 8000 g. For total removal of ethanol from the spin column membranes, a second wash with 500 µl RPE buffer was performed and the columns centrifuged for 2 min at 8000 g. After centrifugation, the RNeasy spin columns were carefully removed from the collection tubes, avoiding any contamination with the flow-through. The RNeasy spin columns were placed in new 1.5 ml collection tubes and 30 to 50 µl RNase free water/column was added directly to the spin column membrane and the spin columns centrifuged for 1 min at 8000 g to elute the mRNA.

mRNA quantification

The concentration and purity of the mRNA was measured using a nanodrop Spectrophotometer (section 4.1.3.7). The mRNA quantities were recorded and the 260/280 ratios, which are an indication of the mRNA purity. All 260/280 ratios were found to be between 1.8 and 2, indicating satisfactory mRNA purity. The mRNA samples were labeled and stored at -80ºC until required.

Reverse transcription of mRNA

Reverse transcription was carried out using the High Capacity cDNA Reverse Transcription kit to prepare cDNA from the mRNA (section 4.1.3.8). For each sample, 10 µl of RT master mix were added to 1 µg of mRNA in a total volume of 20 µl (Table 4-4). Then the reaction mix was loaded into a thermal

cycler (ABI) programmed with the parameters detailed in Table 4-5. The cDNA obtained was either used directly for qRT-PCR or stored at -20°C until required.

Table 4-4: Components used for making 10 µl of cDNA synthesis.

Component	Volume (µl) / Reaction
25X dNTPs	0.8
10X Reverse Transcription Buffer	2
MultiScribe™ Reverse Transcriptase, 50 U/µL	1
10X random primers	2
Nuclease-free H2O	4.2
Total volume	10

Table 4-5: The thermal cycles of reverse transcriptase

	Step 1	Step 2	Step 3	Step 4
Temperature	25°C	37°C	85°C	4°C
Time	10 min	120 min	5 min	∞

Quantitative real time Polymerase chain reaction (qRT-PCR)

A Real-Time PCR System was used for quantitative detection of the previously prepared cDNA. TaqMan probes for COL1A1, SCXA, RUNX2, BGLAP, ALPL, POSTN, IL6 genes were used (section 4.1.3.9). In a 96-well reaction PCR plate, the reaction mix was combined with the cDNA. The components of the reaction mixture are listed in Table 4-6. The plate was

sealed and inserted into the Fast Real-Time PCR System. The thermal cycling program was set as in Table 4-7. The initial analysis was carried out by RQ Manager Software to normalise and express the detection values of target gene in relation to β2M values using the comparative C_t ($\Delta\Delta C_t$) relative quantitation method.

It was important to determine that the β2M, the internal control gene, showed constant expression and was not changed by experimental conditions such as uniaxial strain. Therefore, β2M expression in loaded and non-loaded constructs was determined. The results showed no change in the β2M levels and no statistical difference was observed between loaded and non-loaded constructs, indicating that β2M expression was not affected by mechanical loading.

Table 4-6: Components used in preparing 10 µl of TaqMan® qRT-PCR mix.

Component	Volume (µl) / Reaction
25X dNTPs	0.8
10X Reverse Transcription Buffer	2
MultiScribe™ Reverse Transcriptase, 50 U/µL	1
10X random primers	2
Nuclease-free H2O	4.2
Total volume	10

Table 4-7: Thermal cycles used in qRT-PCR protocol.

Cycle	Temperature	Time	No. of cycles
Hold	50°C	2 min	1
Melting and enzyme activation	95°C	10 min	1
Denaturation	95°C	15 sec	40
Annealing and extension	60°C	60 sec	40
Store	4°C	∞	

4.2.5 The Effect of Mechanical loading on HPDLFs Gene Expression

Mechanical loading has been recognised as a critical factor in tissue engineering, especially when engineering load-bearing tissues such as ligaments and tendons. Mechanical loading of ligaments, either static or cyclic, can influence cell proliferation, differentiation, gene expression and protein synthesis in the tissue. In the following experiments, HPDLFs were subjected to static or cyclic strain.

4.2.5.1 The Effect of Uniaxial Static Strain and Fibre-alignment on Tissue Engineered Periodontal Ligament constructs

Poly(L-lactic acid) scaffolds and decellularised tissue were cut to 6 mm width and 2.5 cm in length to fit the dimensions of the loading chambers. Scaffolds were seeded with HPDLFs at a density of $2x10^6$ cells/scaffold as described in section 4.2.4.1. The constructs were cultured in tissue engineering medium for 14 days before being mechanically loaded (section 4.1.2.5).

Each tissue engineered constructs were rolled and secured in individual custom-made stainless steel loading chambers with a grip to grip distance of 10 mm (Figure 4-6). The chambers were filled with serum-free basic medium and sealed with a Plexiglas cylinder. The engineered ligaments were then subjected to static strain of 0, 9, 14 and 20% for a short loading period of 3 h at 37ºC in a humidified atmosphere of 95% air and 5% CO_2. After 3 h, the constructs were washed three times with PBS and stored in RNA*later*® for mRNA extraction later.

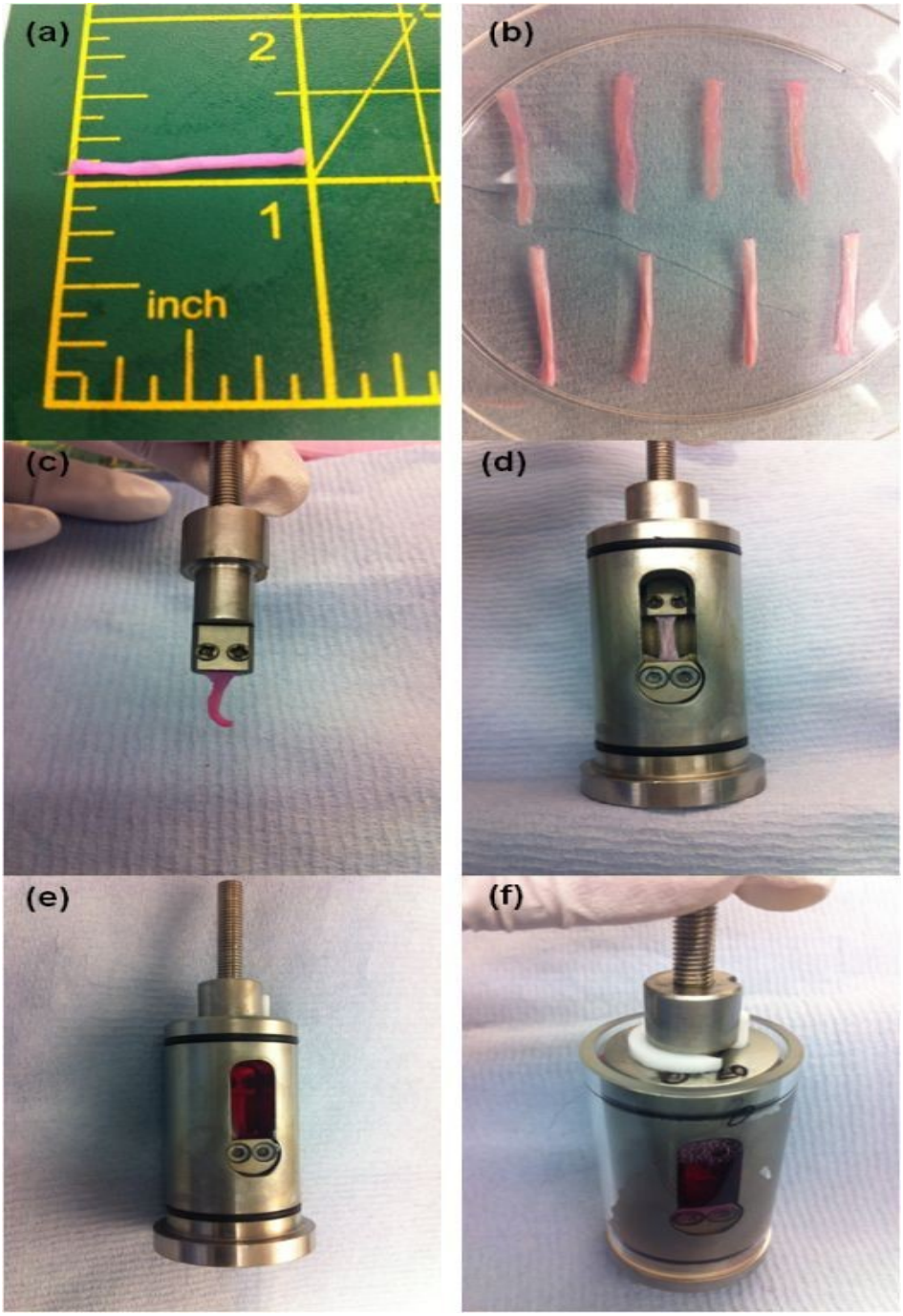

Figure 4-6: Tissue engineered periodontal ligament constructs of 2.5 cm in length (a) were rolled up to form a thin tissue strip (b), and the tissues fixed securely between the upper and lower grips of the loading chamber (c, d). The chamber was then filled with serum-free medium (e) and a uniaxial strain was applied using plastic inserts (f).

4.2.5.2 The Effect of Uniaxial Cyclic Strain on HPDLFs in a 3D Collagen Gel System

Collagen Gel 3D periodontal constructs

Cell density and collagen gel contraction

To determine the cell density of HPDLFs required for embedding in collagen gels without causing gel contraction, three different cell densities were assessed based on a previous study which used tenocytes (Jones et al., 2013). Rat tail type I collagen (2.2 mg/ml) was mixed with 10X DMEM at a ratio of 9:1 and the pH was adjusted to approximately 7 by the addition of 10 M Sodium Hydroxide (NaOH), using Phenol red indicator (Orange/red colour indicates a pH of approximately 7) to assess the pH. A defined number of cells were added to achieve final densities of 1×10^6, 1.5×10^6, 2×10^6 and 3×10^6 cells per ml of collagen solution. 200 µl of the cell-gel suspension were placed in individual wells of 24-well plate and after complete setting of the gels (15 min), 500 µl of serum free media was placed in the wells and culture plates were incubated at 37°C in a humidified atmosphere of 95% air and 5% CO_2. After 24 h, the gels were released using a 20 µl pipette tip. Any gel contraction was observed visually at 24, 48, 72 and 96 h post-release.

Loading the 3D cell-gel constructs

Human periodontal ligament fibroblasts were trypsinised and suspended at $3x10^6$ cells/ml, (double the final required cell density), in serum-free medium. Rat tail type I collagen was prepared as described above. The neutralised collagen solution and the HPDLF suspension were mixed 1:1 (1 mg/ ml collagen and $1.5x10^6$ cells/ml, final concentrations). 200 µl of the gel was pipetted into flexible-bottomed collagen type I coated Flexcell® tissue train plates (Figure 4-7). During this time the plates were under a continuous vacuum (which produced a 20% elongation of the rubber membrane) over a trough loader and base plate (Figure 4-8). The vacuum was controlled by the Flexcell® FX-4000™Tension System consisting of a computer running FX-4000™ software, a vacuum controller and a vacuum pump. 3D cell-gel constructs were allowed to set for 1 h under a constant vacuum and then 3 ml PDLF basic medium was added. After 72 h, the medium was replaced with fresh serum-free medium before applying the strain. Tissue train plates were transferred onto arctangle loading posts in preparation for mechanical loading (Figure 4-9). A uniaxal strain was applied using the Flexcell® FX-4000TM tension system, non-strain controls included. The uniaxial strain applied was in sinusoidal wave form cycling between 0 and 5% elongation at 1 Hz for 8, 24 and 48 h. After the application of strain, the cell-gel constructs were washed three times with PBS and stored in RNAlater® for RNA extraction and qRT-PCR (refer to section 4.1.3.9).

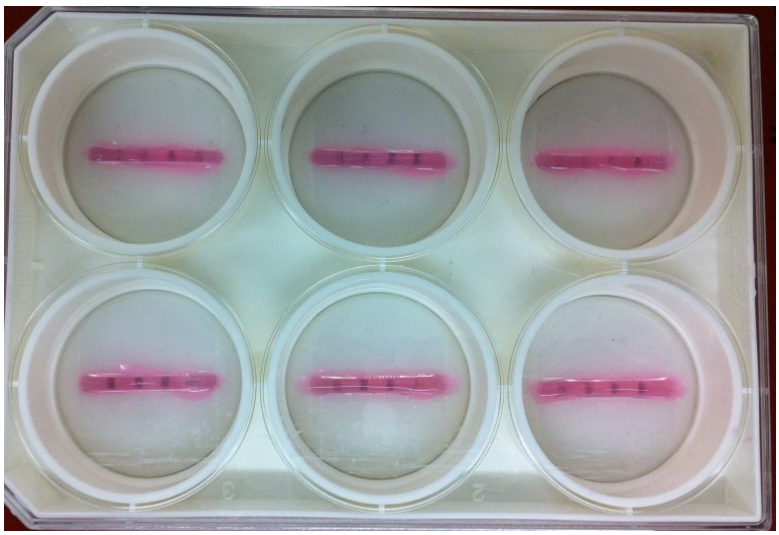

Figure 4-7: HPDLFs in 3D collagen gels before being strained.

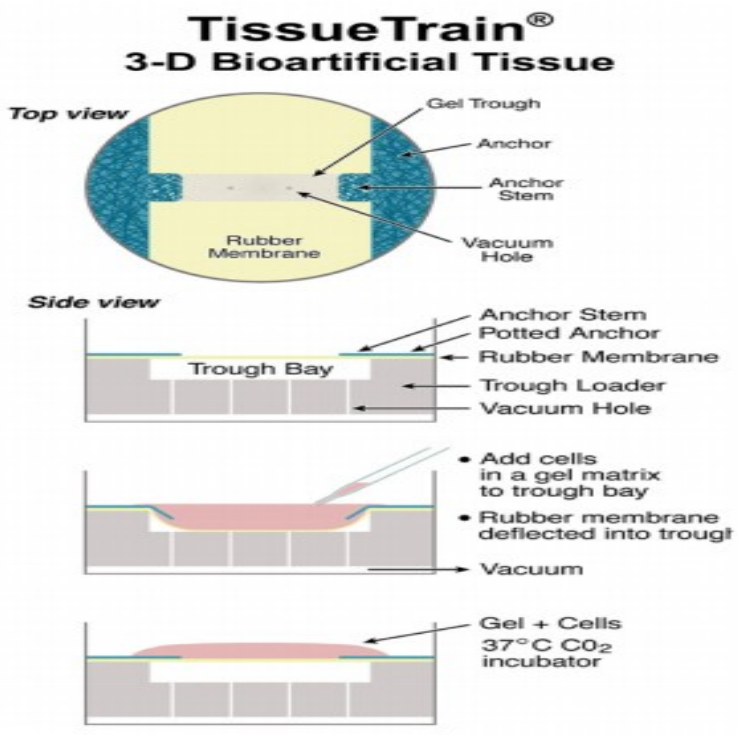

Figure 4-8: Schematic of protocol for making cell seeded gel constructs with the Tissue Train Culture system http://www.flexcellint.com/**.**

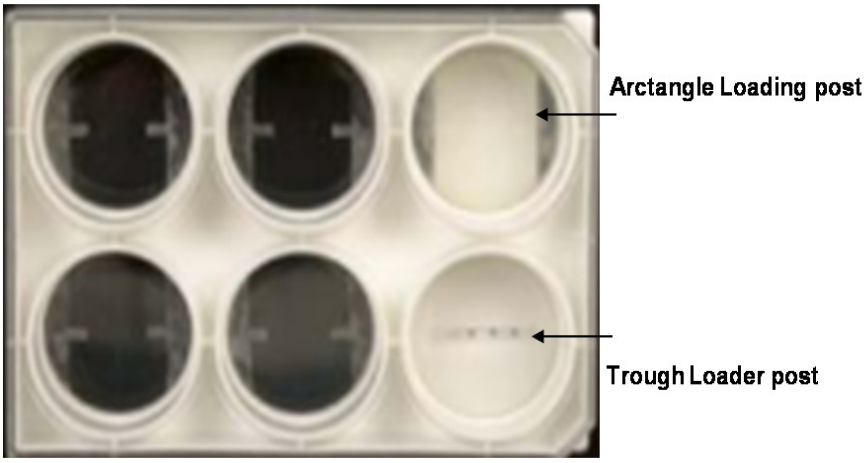

Figure 4-9: Tissue Train culture plate with nylon mesh anchors, Trough Loader, and Arctangle Loading post.

Gel Contraction in Flexcell® System

The 3D cell-gel constructs will remodel with time under strain. This remodelling is observed as gel contraction. ScanFlex™ is an automated image system used to determine the change in the 3D cell-gel construct. The change in gel width was measured in controlled and loaded constructs over time using image J analysis software.

4.2.6 The Effect of EMD and/or TGF- β1 on the Engineered Periodontal ligament Constructs

Growth factors can modulate cell proliferation, differentiation, and matrix synthesis. In this experiment, HPDLFs were stimulated with EMD, EMD+TGF-β1 or TGF-β1 to evaluate their effect on HPDLFs gene expression and protein synthesis. Poly(L-lactic acid) scaffolds were seeded with HPDLFs at a

density of $2x10^6$ and cultured for 7 and 14 days with medium changes twice per week.

The constructs were cultured in medium containing:

- ***EMD group:*** 100 µg/ml EMD
- ***EMD+TGF-β1 group:*** combination of 100 µg/ml EMD and 10 ng/ml TGF-β1
- ***TGF-β1 group:*** 10 ng/ml TGF-β1
- ***Control group:*** no EMD or TGF-β1

4.2.6.1 Cellular Activity Assay

To assess the effect of EMD and TGF-β1 alone or in combination on HPDLF activity, the reduction of alamarBlue® was used (refer section 4.2.4.5).

4.2.6.2 DNA Quantification Assay

To assess whether EMD and/or TGF-β1 have any influence on cellular proliferation, the DNA content of the cell/scaffold constructs was measured at day 14 using the assay decribed in section 4.2.4.5.

4.2.6.3 Total Protein Assay

At day 14, constructs stimulated with EMD and/or TGF-β1 were washed with PBS and processed to measure the total protein using a BCA Protein Assay kit as described previously in section 4.2.4.6.

4.2.6.4 Gene Expression

The change in gene expression of HPDLFs seeded on random and aligned-fibre PLLA scaffolds stimulated with EMD and/or TGF-β1 was assessed at day 7 and 14. HPDLFs were seeded on PLLA scaffolds at a density of $2x10^6$ cells/scaffold and cultured as described previously in section 4.2.6. At day 7 and 14, the constructs were washed twice with PBS and processed for gene expression.The detailed qRT-PCR protocol was described in section 4.2.4.10.

4.2.6.5 Western Blots

Western blots (WB) were performed to detect collagen I, periostin, RUNX2 and osteocalcin proteins in the *in vitro* engineered periodontal ligament constructs treated with EMD and/or TGF-β1 for 14 days. The proteins were extracted from HPDLFs using a RIPA buffer combined with EDTA-free Protease Inhibitor Cocktail and the total protein concentrations of the samples quantified using the Bicinchoninic Acid Protein Assay (BCA) kit as described in section 4.2.4.6. Protein samples were prepared for loading in the gel wells by combining 2 µL of a reducing agent with 5 µL SDS buffer, and added to a volume of the protein samples which contained a total of 40 µg of protein. The total sample volume was made up to 20 µL using dH_2O after which, the samples were incubated at 94˚C for 5 min to denature the proteins. A ready-made SDS-PAGE gel was then inserted into the Mini-Protean Tetra System followed by assembling the system and pouring SDS-running buffer. A Pre-stained protein ladder (5 µL) was added to the first lane to be used as a reference for protein molecular weights. 20 µl of each sample was then

loaded into the remaining wells before running the electrophoresis at 150 V for 1 h to induce protein separation. A nitrocellulose transfer membrane was used to transfer the protein from the gel. The gel, nitrocellulose membrane and 6 filter papers were soaked in a 10% NuPage transfer buffer. The gel and nitrocellulose membranes were then sandwiched between the 6 filter papers, placed in the transfer cassette, before running electro-blotting at a constant 30 V for 1 h. After transferring the proteins to the nitrocellulose membrane, the membranes were incubated for 1 h at room temperature in a 5% skimmed milk/TBST blocking buffer in order to block any unoccupied protein binding sites. The blocking buffer was then removed and a suitable dilution of the primary antibody diluted in a fresh blocking buffer (see Table 4-8) was added to the membrane in a universal tube, and incubated overnight at 4˚C on a rotator. On the following day, the primary antibody was removed and the membrane was washed three times, in TBST (with 10 min for each wash) before adding the biotin-conjugated secondary antibody diluted in fresh blocking buffer at a 1:3000 ratio (Table 4-8). After 1 h incubation at room temperature, the membrane was washed three times in TBST (with 10 min for each wash). Super Signal West Pico Chemiluminescence reagent was used to bind to the biotin sites of the secondary antibody and visualise the antibody/protein complex. A working solution of the chemiluminescence reagent was prepared as per the manufacturer's guidelines and added onto the membrane and incubated for 3 min at room temperature to generate a detectable light signal. Amersham Hyperfilm X-ray films were then exposed to the membrane for different time intervals from 2 to 5 min, in a dark room in

order to detect the chemiluminescence signal. Finally, the films were placed in a film processor machine to produce visualised black bands, which reflected the detected proteins.

Table 4-8: list of the antibodies used in western blots.

Primary antibody	Concentration	Dilution	Secondary antibody
Collagen type I Goat monoclonal to collagen type I (Southern Bioscience)	1 µg/ml	1:1000	Anti-goat IgG (A-5420, Sigma-Aldrich, UK)
Periostin Rabbit polyclonal to periostin (ab14041, ABCAM)	1 µg/ml	1:3000	Anti-rabbit IgG (A-9169, Sigma-Aldrich, UK)
RUNX2 Rabbit polyclonal to RUNX2 (ab23981, ABCAM)	1 µg/ml	1:3000	Anti-rabbit IgG (A-9169, Sigma-Aldrich, UK)
β-actin Mouse monoclonal to β-actin (Cell Signalling)	1 µg/ml	1:3000	Anti-mouse IgG (A-9044, Sigma-Aldrich, UK)

4.2.7 Statistical Analysis

Data are expressed as the mean ± SD from three independent experiments carried out in triplicate and all experimental/assay values were derived from triplicate measurements, unless otherwise specified. Significance for multiple comparisons was determined by one-way analysis of variance (ANOVA) with post hoc comparison by Tukey's multiple comparisons test when equal variance was assumed; otherwise Games-Howell was used. For pair-wise comparisons, two-tailed, unpaired Student's t-tests were used. The statistical analyses were carried out using the SPSS statistical package and statistical significance was set at $P \leq 0.05$. All statistical methods used were reviewed with statisticians at the Mathematics and Statistics Help (MASH) counseling services, The University of Sheffield (http://www.shef.ac.uk/mash).

5. RESULTS

5.1 Scaffold Characterisation

5.1.1 Polymer Based Scaffolds

Electrospun synthetic polymers are one of the most widely used scaffold materials in tissue engineering. Random and aligned-fibre PLLA scaffolds were fabricated by electrospinning using the methodology described in section 4.2.1.1.

5.1.1.1 Optimising the Electrospinning Parameters to Fabricate Aligned PLLA Fibres

Poly(L-lactic acid) solutions were electrospun using standardised electrospinning conditions as given below:

8% wt/vol PLLA dissolved in DCM

1.5 ml of the polymer solution was used per scaffold

20 cm distance between the needle tip and the ground collector

18 kV electrical potential

3 ml/h polymer flow rate

20 G needle

Rotating dremel speed at 5000 rpm

The morphology of the electrospun aligned-fibre PLLA scaffolds was examined by scanning electron microscopy (SEM). SEM micrographs (Figure 5-1) showed that the degree of fibre alignment varied according to the flow rate of the PLLA solution and the voltage used during the electrospinning. The aligned-fibre scaffolds spun at 18kV with a PLLA flow rate of 3 ml/h exhibited the most favourable fibre alignment. Therefore, these parameters were used throughout the study to fabricate the aligned-fibre PLLA scaffolds.

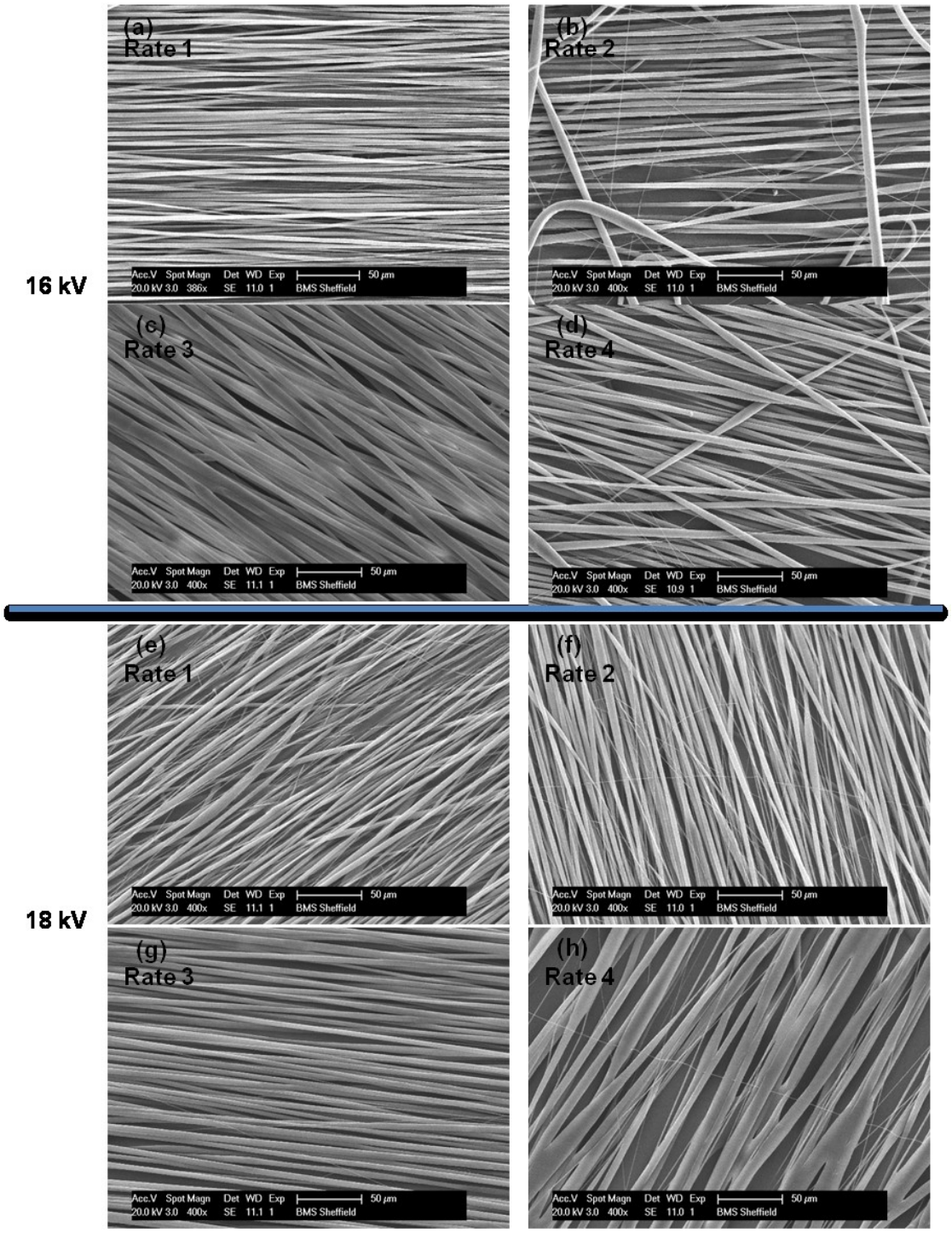

Figure 5-1: Scanning electron micrographs (SEM) of the aligned-fibre PLLA scaffolds showing alignment of the fibres at different PLLA flow rates of 1 ml/h (a, e), 2 ml/h (b, f), 3 ml/h (c, g) and 4 ml/h (d, h) and Voltages 16 kV (a, b, c& d) and 18 kV (e, f, g& h). Scale bars = 50µm

5.1.1.2 PLLA Scaffold Characterisation

The average diameter of the electrospun PLLA fibres was measured using Image J software. The values obtained were 2.1± 1.2 μm and 2.3 ± 1.3 (mean± SD) for random and aligned-fibre scaffolds respectively. The aligned-fibre group had fibres of PLLA which ran in a parallel alignment. No obvious alignment of fibres was observed in the random-fibre groups (Figure 5-2, a & b).

Fast Fourier transform analysis (FFT) was performed to analyse the fibre-alignment of the PLLA scaffolds. Fast Fourier transform analysis of the aligned-fibre scaffold group showed pixels forming a straight line in one definite direction which indicated a high level of fibre-alignment (Figure 5-2, d). In contrast, the random-fibre scaffolds generated an output image containing pixels distributed in a circular pattern, which confirmed the random nature of the fibres in this group (Figure 5-2, c).

These results confirm that highly aligned-fibre PLLA scaffolds were successfully fabricated using the electrospinning method.

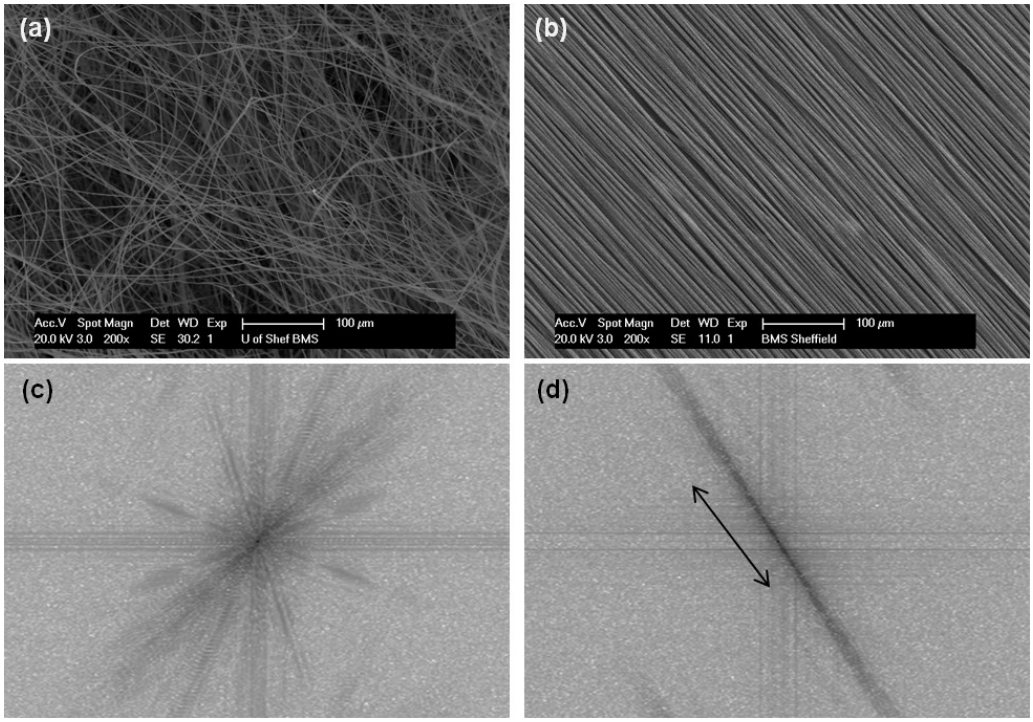

Figure 5-2: SEM micrographs of electrospun PLLA scaffolds. The scaffolds shown are random-fibre PLLA scaffold (a) and aligned-fibre PLLA scaffold (b). The lower part of the figure shows Fast Fourier Transform (FFT) images of both a random-fibre PLLA scaffold (c) and an aligned-fibre PLLA scaffold (d). The images show a high level of fibre orientation in the aligned-fibre PLLA scaffolds which is confirmed by the FFT images. Scale bars in a and b = 100 µm.

5.1.2 Decellularised Skin and Ligament Tissue

Two commonly used detergents, namely Triton X-100 and sodium deoxycholate, were utilised to decellularise samples of bovine skin and ligament. Both detergents were successfully used to decellularise porcine aortic and pulmonary roots (Rieder et al., 2004).

5.1.2.1 Efficacy of Decellularisation Method

Samples of bovine ligament and skin were decellularised as described in section 4.2.2.2. To investigate the degree of decellularisation, samples of the native (control) and decellularised tissues were analysed using light microscopy, SEM and quantitative measurement of DNA.

H&E stained sections of native skin and ligament tissues (Figure 5-3, a& b respectively) showed nuclei stained in blue and a normal distribution of collagen fibres. In contrast, H&E staining of decellularised skin (decell-skin) and decellularised ligament (decell-ligament) exhibited an apparent absence of nuclei and no observable disruption in the collagen integrity of the extracellular matrix was observed (Figure 5-3, c& d). SEM micrographs showed that the network of collagen fibres remained intact in the decell- skin and decell-ligament (Figure 5-3, e& f).

Fluorescent images of native and decellularised tissues were stained with Hoechst dye to visualise nuclei. In contrast to the native tissues, no detectable fluorescence, indicative of nuclei, was observed in the decellularised tissues. These results suggested that during the

decellularisation procedure the nuclei were removed and no nuclei fragments were retained within both decellularised skin and ligaments (Figure 5-4, c& d respectively).

The degree of decellularisation was further confirmed and quantified by measuring the amount of DNA in the native tissues compared to the decellularised tissues. DNA measurements from the decellularised skin and ligament showed that 95% of the DNA content was removed compared to the DNA levels of the native, non-decellularised tissue (Figure 5-5).

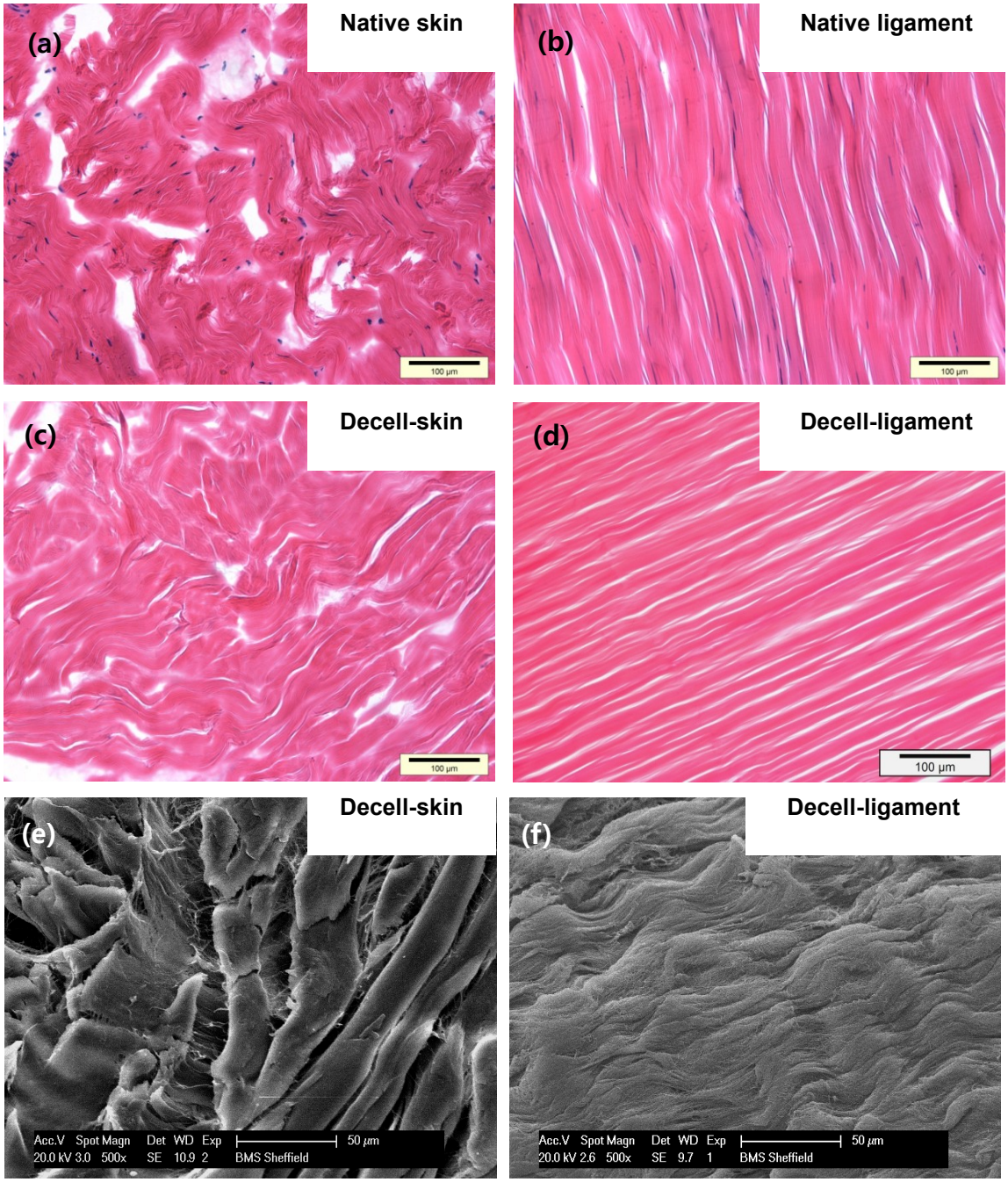

Figure 5-3: Hematoxylin and eosin stained longitudinal sections of non-decellularised skin (a) non-decellularised ligament (b), decellularised skin (c) decellularised ligament (d). SEM micrographs show decellularised skin (e) and decellularised ligament (f). Scale bars shown in the H&E stained sections = 100 µm, scale bars shown in the SEM micrographs = 50 µm.

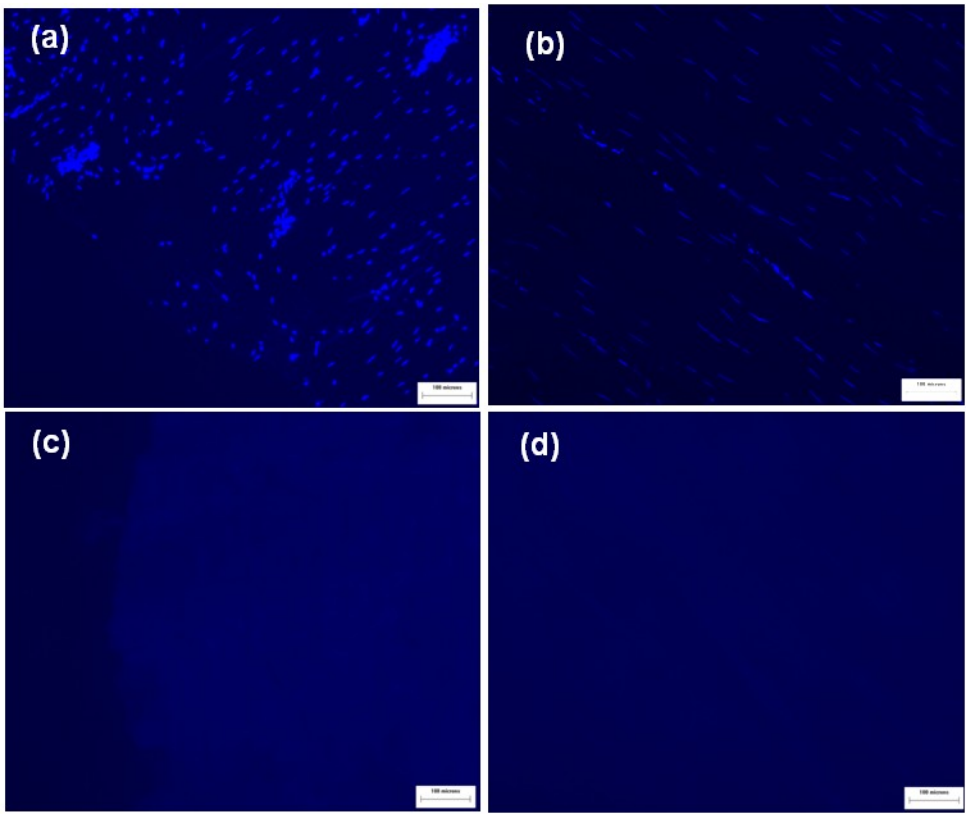

Figure 5-4: Fluorescent images of tissue sections stained with Hoechst reagent to detect intact nuclei which show pale blue fluoresence (a) native skin (b), native ligament, (c) decellularised skin and (d) decellularised ligament. Scale bars = 100 µm.

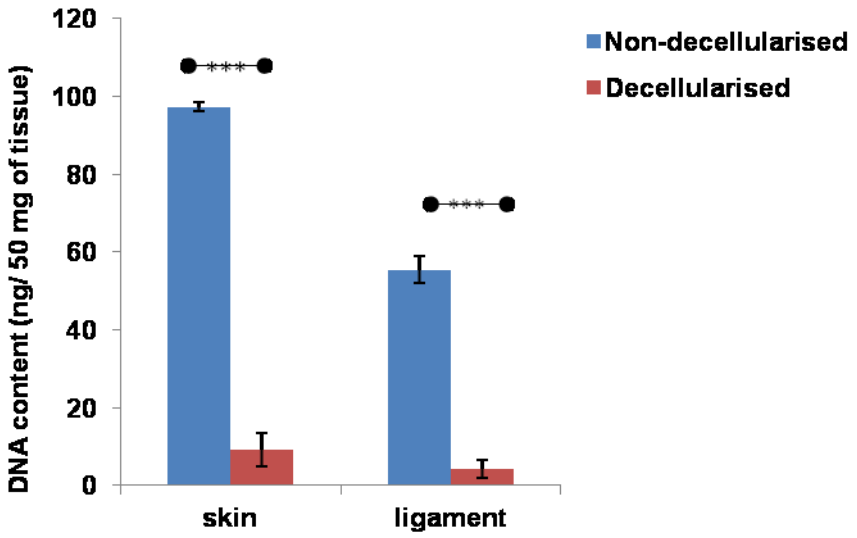

Figure 5-5: Histogram showing the DNA content of skin and ligament samples before and after the decellularisation process. P values were calculated by independent samples T test, *** p≤0.001. The data is presented as mean ± SD of 3 experiments, each assayed in duplicate.

5.2 Cell Sources

In this study periodontal ligament fibroblasts were investigated from three tissue sources. These sources were: 1). porcine periodontal ligament, 2). rat periodontal ligament, and 3). a commercial source of human PDLFs. PDLFs isolated from each of these tissue sources has been used in previous studies (Jacobs et al., 2013, Shirai et al., 2009, Kato et al., 2011). The objective of these experiments was to select the most appropriate tissue source of PDLFs based on factors such as availability, ease of culture and expansion and the cultures of cells that demonstrated the classical properties of PDLFs.

5.2.1 Porcine Periodontal Ligament Fibroblasts (PPDLFs)

Periodontal ligament tissue was successfully harvested from porcine anterior teeth using enzyme digestion and explant techniques (section 4.2.3.2). The use of enzymatic digestion with collagenase yielded a greater cell number and confluent monolayers were achieved at a faster rate than when using the explant technique. Porcine PDLFs grown in monolayers were spindle-shaped, which is a characteristic morphology of periodontal ligament fibroblasts (Figure 5-6). The PPDLFs rapidly lost their fibroblastic spindle shape during culture assuming a more-rounded cell shape. Early infection by yeast, a commensal normally found in porcine oral cavity, was a frequent occurrence. A further complication was that, only 40% of the collected samples yielded living cells. This was probably related to the time that had elapsed since slaughter, which was a difficult variable for us to fully control. For all these reasons porcine periodontal fibroblasts were not used in this project.

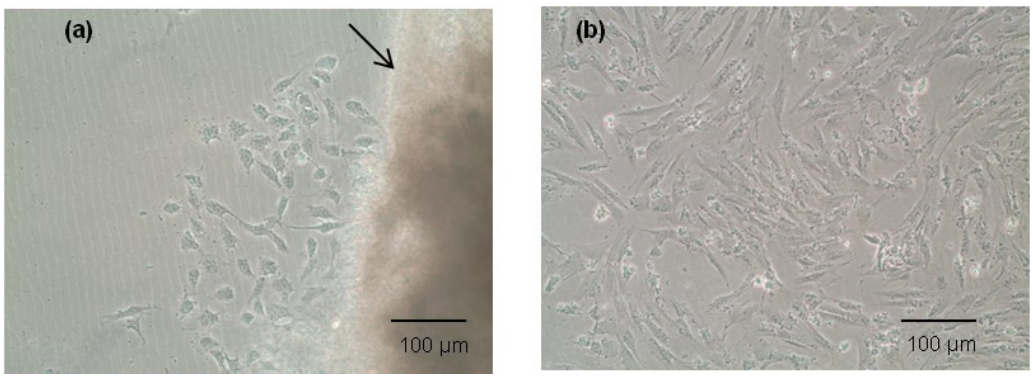

Figure 5-6: Phase contrast microscopy Images showing PPDLFs in monolayer cultured using (a) direct explant technique (arrow points to tissue explant) and (b) cultures of cells isolated by the enzymatic digestion technique. Scale bars = 100 µm.

5.2.2 Rat Periodontal Ligament Fibroblast (RPDLFs)

Periodontal ligament tissue was collected from rat incisor teeth using only the enzymatic approach as the amount of tissue extracted is usually minimal. Also, based on the observation with porcine tissue, the enzymatic approach yielded a greater cell number in a shorter time period. The RPDLFs exhibited the classic fibroblastic spindle shape in monolayer culture under basal conditions (Figure 5-7, a). The RPDLFs stained with SIGMAFAST™ for ALPL showed dense ALPL staining (Figure 5-7, b). When cultured in osteogenic medium for 21 days, the RPDLFs showed mineralised nodule formation which stained positively for calcium deposition with Alizarin Red S (Figure 5-7, c). Immunohistolocalisation showed a dense staining of both collagen type I and periostin of RPDLFs cultured in monolayer (Figure 5-8, a& b respectively). Rat PDLFs were easier to extract and their numbers could be expanded *in vitro* compared to porcine PDLFs. However, it was unfeasible to use these cells in the project as this would have been an expensive option requiring large numbers of animals to yield sufficient cells needed for the whole project.

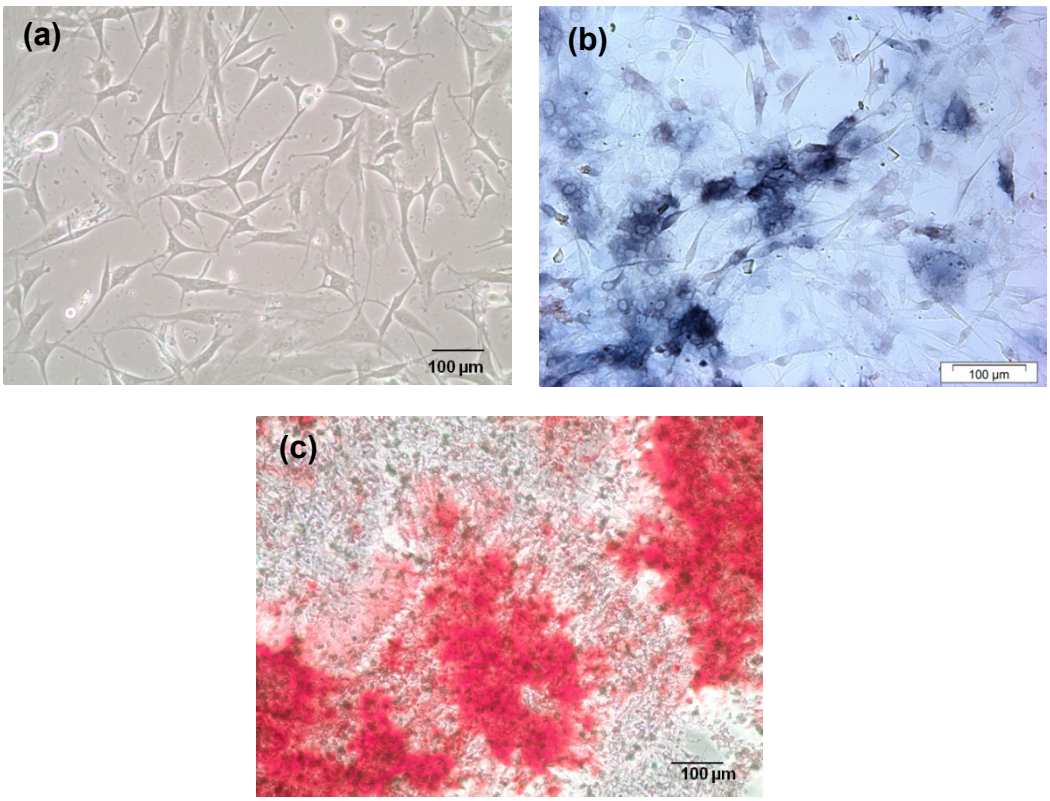

Figure 5-7: Light microscopic images showing RPDLFs cultured in monolayer cultured under basal conditions (a) phase contrast image showing the typical spindle-shaped morphology characteristic of fibroblast cells, (b) alkaline phosphatase (ALPL) localisation and (c) mineralised nodules stained with Alizarin Red S of RPDLFs cultured under osteogenic conditions. Scale bars = 100 µm.

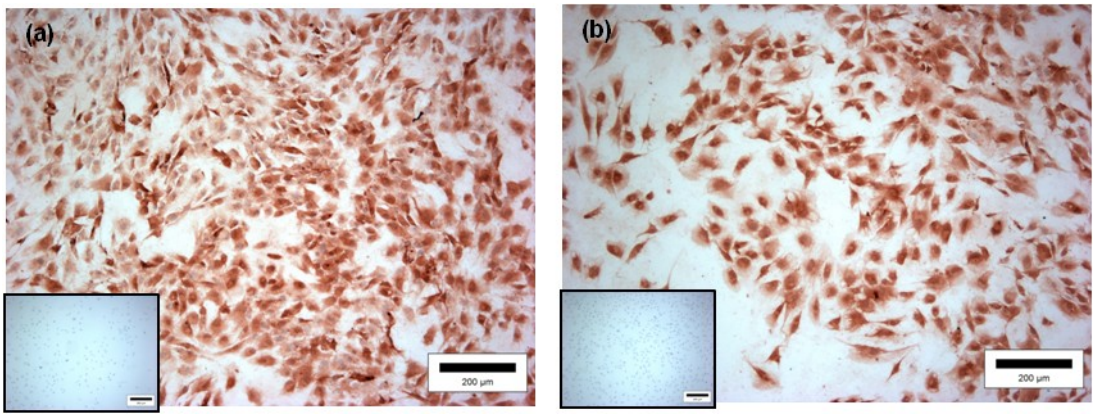

Figure 5-8: Light microscopy images showing immunostaining of collagen type I (a), periostin (b). RPDLFs showed a strong positive stain for collagen type I and periostin in monolayer culture. The images inserted at the bottom left-hand side of each large image show the non-specific staining controls. Scale bars = 200 µm

5.2.3 Human Periodontal Ligament Fibroblasts (HPDLFs)

Commercially available HPDLFs were cultured as monolayers as described in section 4.2.3.1. HPDLF cultures showed a spindle-shaped morphology, which is characteristic of fibroblast cells (Figure 5-9, a). The cultured HPDLFs stained positively for ALP (Figure 5-9, b). Nodules were formed by the HPDLFs when cultured in osteogenic media for 21 days which stained with Alizarin Red S showing that they were mineralised (Figure 5-9, c). Immunohistochemical assays showed a dense staining of both collagen type I and periostin in HPDLFs cultured in monolayer (Figure 5-10, a& b). Only faint staining was seen for RUNX2 and no staining was detectable for osteocalcin (Figure 5-10, c& d respectively).

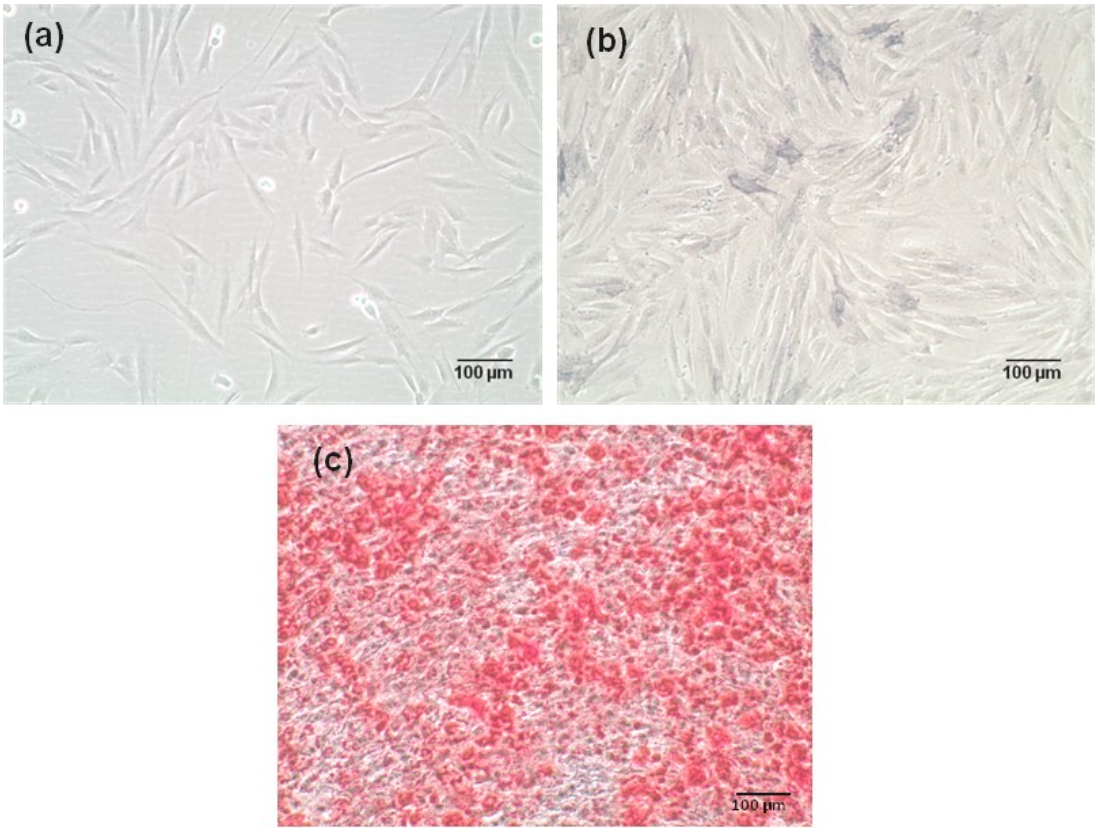

Figure 5-9: Light microscope images showing HPDLFs in monolayer cultured under basal conditions (a) spindle shaped morphology of fibroblast (b) an ALPL staining and (c) Alizarin Red S staining of HPDLFs cultured under osteogenic condition staining mineralised nodules. Scale bars = 100 µm.

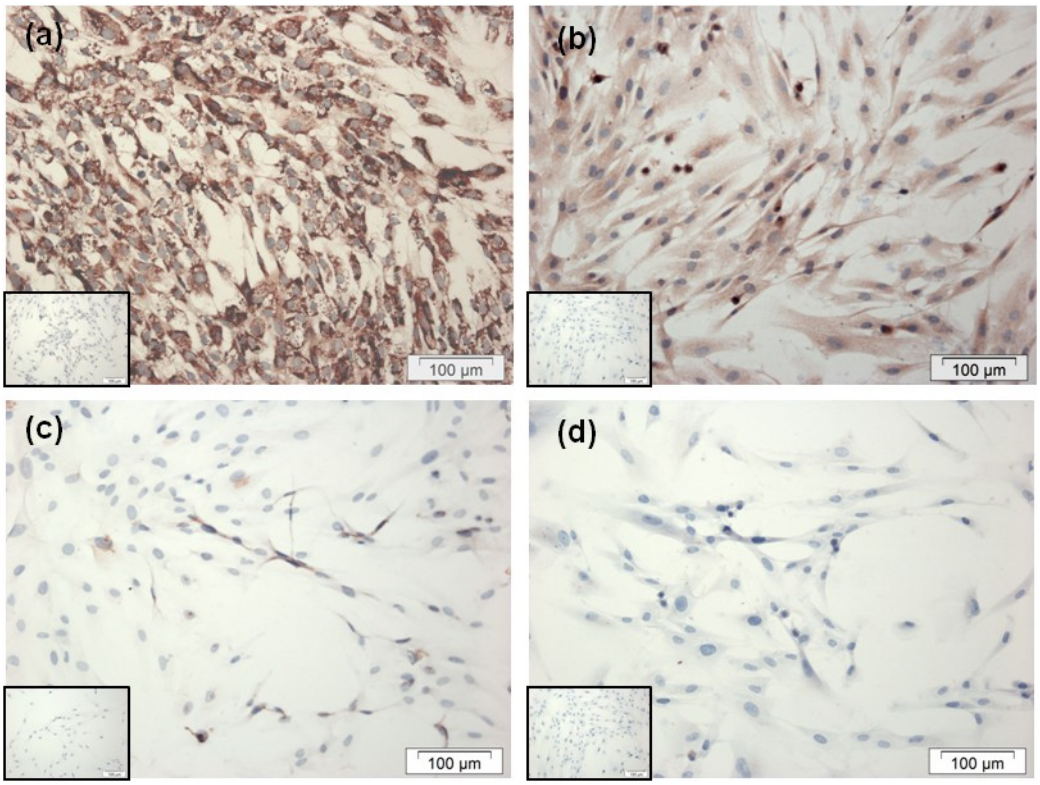

Figure 5-10: Light microscopy images showing immunostaining for collagen type I (a), periostin (b), RUNX2 (c) and osteocalcin (d). HPDLFs showed a strong positive stain for collagen type I and periostin in monolayer. The images inserted at the bottom left-hand side of each large image show the non-specific staining controls Scale bars = 100 µm

5.3 *In vitro* Tissue Engineered Periodontal Ligament Constructs

5.3.1 Cell Attachment and Morphology

The attachment of the HPDLFs seeded on the electrospun PLLA scaffolds and decell-skin and ligament was investigated using SEM. The SEM images (Figure 5-11 & Figure 5-12) revealed that the HPDLFs were successfully seeded on all scaffold types. At day one, the HPDLFs clustered and formed small aggregates on both the random and the aligned-fibre PLLA scaffolds (Figure 5-11 a, b). By day 7, the HPDLFs were spread over both random and aligned-fibre scaffolds. In aligned-fibre PLLA scaffolds, the HPDLFs had a flattened morphology and were elongated along the fibres. In contrast, HPDLFs cultured on the random-fibre PLLA scaffolds were polygonal in shape, with no specific orientation (Figure 5-11 c, d). Meanwhile, HPDLFs seeded on decell-skin and decell-ligament formed a smooth confluent layer as early as day 1 and by day 7 HPDLFs completely covered the scaffolds (Figure 5-12).

Cell morphology was also studied using phalloidin which binds to the α-actin cytoskeleton and Hoechst reagent to stain the nuclei as described previously in 4.2.4.3. Fluorescence images for HPDLFs seeded on both aligned-fibres of PLLA and decell-ligament confirmed that HPDLFs were elongated in shape and oriented parallel to the direction of the fibres (Figure 5-11, e and Figure 5-12, f). HPDLFs cultured on aligned-fibre PLLA scaffold were more

elongated in shape and thinner compared to the cells cultured on decell-ligament, which may suggest that fibre diameter influenced HPDLF morphology.

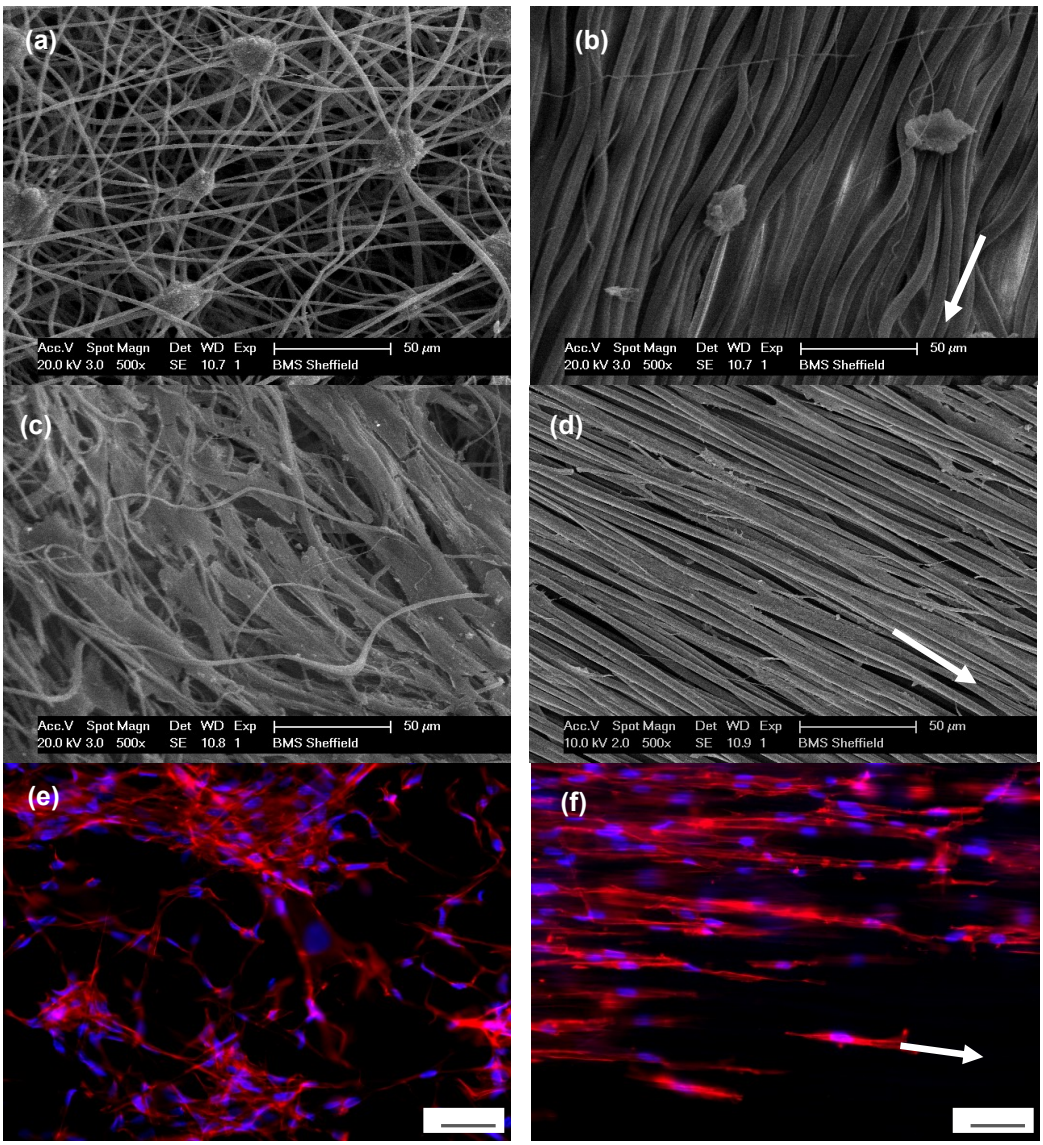

Figure 5-11: SEM micrographs showing HPDLFs seeded on (a, c) random-fibre PLLA scaffolds and (b, d) aligned-fibre PLLA scaffold for 1 day (a, b) and 7 days (c, d). Fluorescence images (e, f) show phalloidin-stained actin filaments (red) and Hoechst-stained nuclei (blue). White arrows indicate the direction of the scaffold fibres. For images a& d scale bars = 50 µm, For images e& f, scale bars = 100 µm.

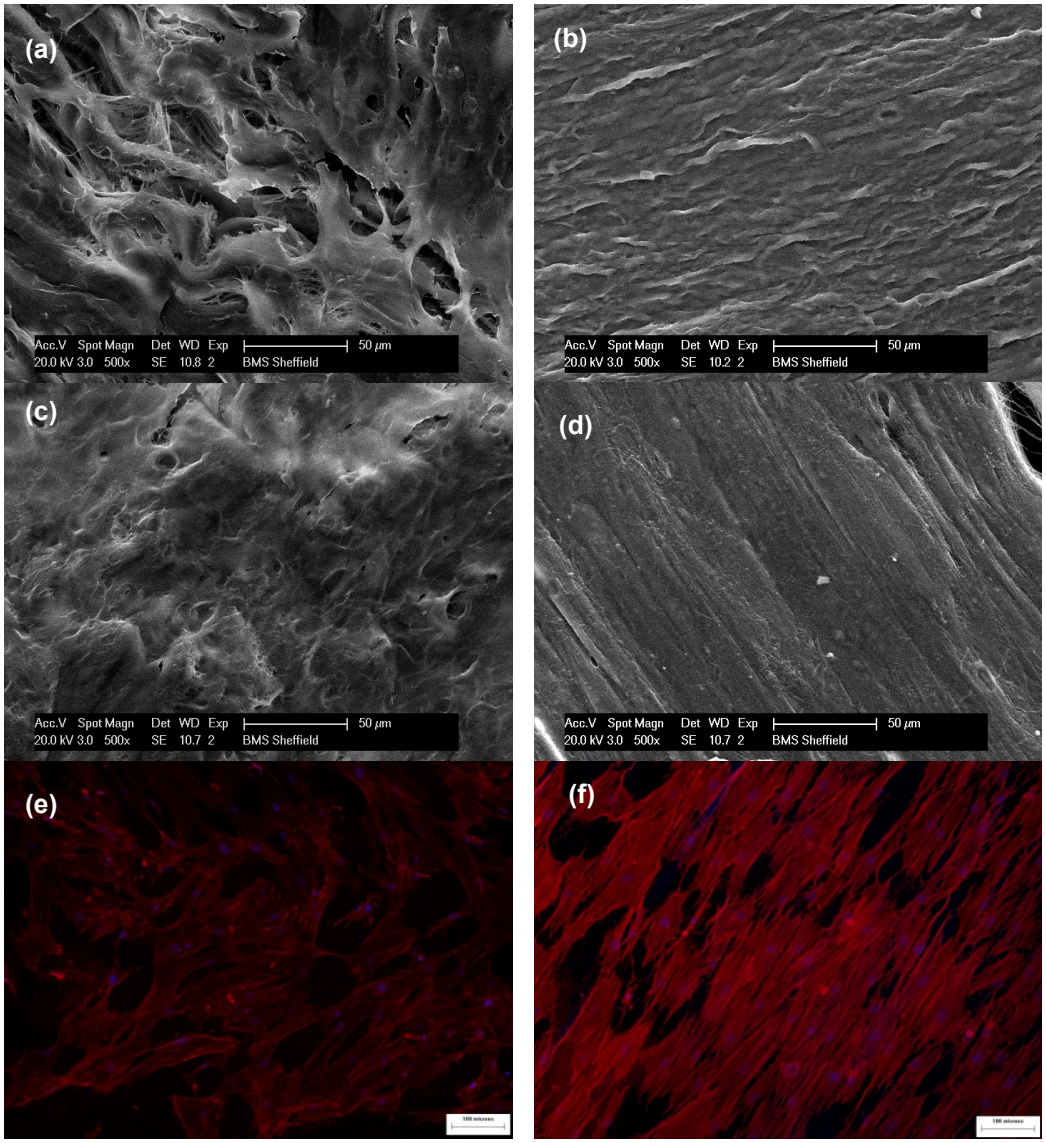

Figure 5-12: SEM micrographs showing HPDLFs seeded on (a, c) decell-skin and (b, d) decell-ligament for 1day (a,b) and 7 days (c,d). Fluorescence images (e,f) show phalloidin and Hoechst-stained HPDLFs. The actin filaments are stained red and nuclei are stained blue. White arrows indicate fibre direction, scale bars = 100 µm.

5.3.2 Cellular Activity

HPDLFs were seeded onto PLLA and decellularised scaffolds and cultured for 20 days. The level of cell activity (an indicator of cell proliferation) was determined using alamarBlue® (as described in section 4.2.4.4) on days 0, 7 and 20.

At day 0, in cells transferred from monolayer to 3D model, no difference was observed in the cellular activity of HPDLFs cultured on random and aligned PLLA scaffolds (Figure 5-13). However, the activity was significantly decreased in HPDLFs cultured in random and aligned-fibre PLLA scaffolds at 7 and 20 days compared to day 0 ($p \leq 0.001$). At day 7, the decrease in cellular activity was equal in both scaffold types. At day 20, the levels of cellular activity were significantly higher in constructs formed from random-fibre PLLA compared to aligned-fibre PLLA scaffolds ($p \leq 0.001$).

A similar pattern was observed when HPDLFs were cultured on decell-skin and decell-ligament. There was reduced cellular activity at day 7 and 20 in both scaffolds compared to day 0. However, at day 0, HPDLFs cultured on decell-skin scaffolds showed significantly greater cellular activity than those seeded on decell-ligament scaffolds ($p \leq 0.05$). The difference in cellular activity between decell-skin and decell-ligament at both day 7 and day 20 was not statistically significant (Figure 5-14).

There was a general reduction in the level of cellular activity over the period of time the constructs were cultured. This reduction was irrespective of fibre alignment or the type of scaffold. This fall in cellular activity could either be a result of a decrease in cell numbers or increased differentiation of HPDLFs. To evaluate the cell numbers over culture time, the total DNA content in each scaffold was measured.

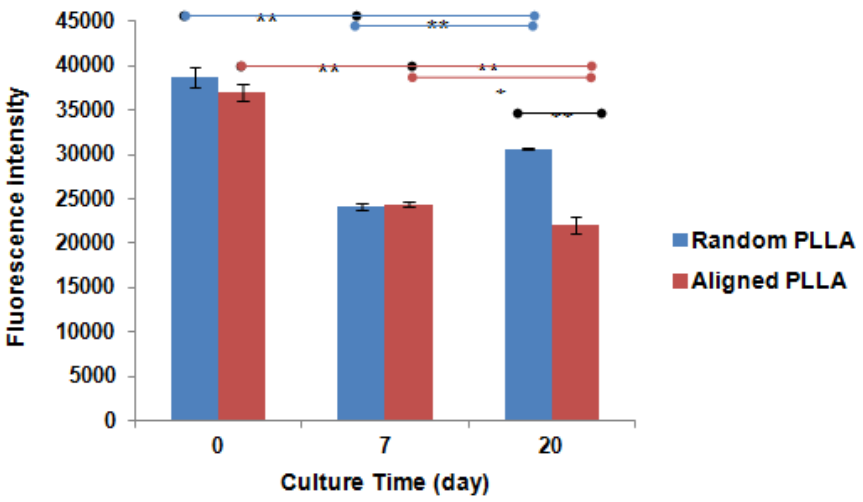

Figure 5-13: Cellular activity of HPDLFs seeded on aligned and random fibres PLLA scaffolds, for 0, 7 and 20 days, after 4 h incubation in alamarBlue®. P values were calculated using ANOVA and independent samples T test, *(P≤0.05), ** (P≤0.01) and * (P≤0.001) denotes significant differences. Data is presented as mean ± SD of 3 experiments, each performed in triplicate.**

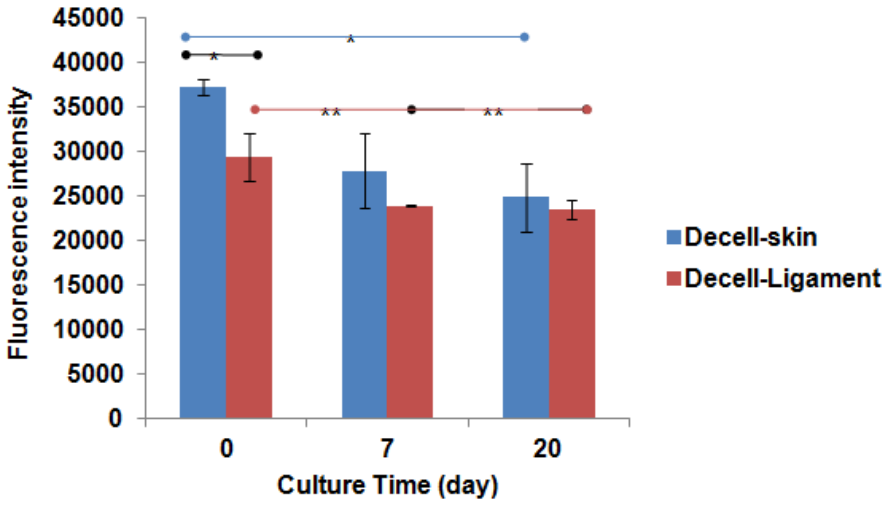

Figure 5-14: Cellular activity of HPDLFs seeded on decellularised skin and ligaments for 0, 7 and 20 days. The histogram shows the levels of reduced dye formed after 4 h incubation in alamarBlue®. P values were calculated using ANOVA and independent samples T test. *(P≤0.05) and ** (P≤0.01) denote significant differences. Data is presented as mean ± SD of 3 experiments, each performed in triplicate.

5.3.3 Cellular Proliferation

The total DNA was quantified using a DNA quantification assay in cell digests prepared from constructs of HPDLFs seeded on PLLA and decellularised scaffolds (see section 4.2.4.5).

At seeding time (day 0), total DNA was similar in both random and aligned PLLA scaffolds. At day 7, the DNA content was significantly increased in aligned-fibre scaffolds compared to day 0. However, there was no difference in DNA content of these constructs between day 7 and day 20 (Figure 5-15).

In HPDLFs seeded in random-fibre scaffolds, there was no statistically significant change in the DNA content of the constructs over the culture period. There was a trend towards a decrease in the DNA content of constructs on day 20, but this was not statistically significant (Figure 5-15). These results suggested that cell viability was maintained over the culture period but no cell proliferation had occurred. In decell-skin constructs, the DNA content significantly decreased from day 0 to day 20 ($p \leq 0.001$), suggesting death of the cells. Conversely, the DNA content significantly increased over culture time in decell-ligament constructs, suggesting cell proliferation (Figure 5-16).

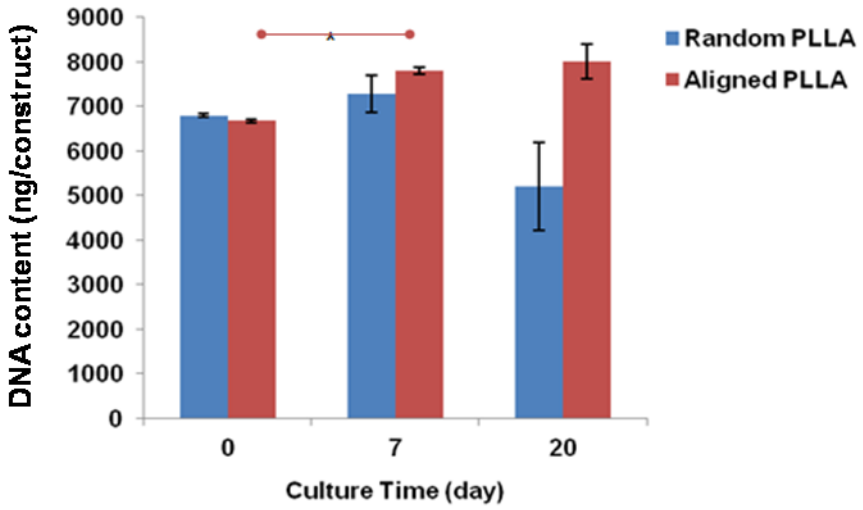

Figure 5-15: The total DNA of HPDLFs cultured on random and aligned-fibre PLLA scaffolds for 0, 7 and 20 days. P values were calculated using ANOVA and independent samples T test, * $p \leq 0.05$, ** $p \leq 0.01$, *** $p \leq 0.001$. Data is presented as mean ± SD of 3 experiments, each performed in triplicate.

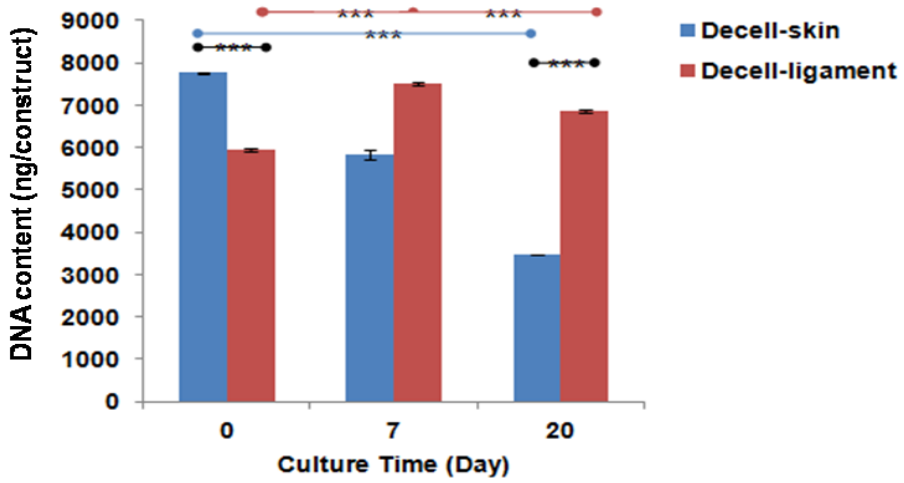

Figure 5-16: The total DNA of HPDLFs cultured on decellularised skin and ligaments for 0, 7 and 20 days. P values were calculated using ANOVA and independent samples T test, * p≤0.05, ** p≤0.01, *** p≤0.001. Data is presented as mean ± SD of 3 experiments, each performed in triplicate.

5.3.4 Total Protein

HPDLFs were seeded on PLLA scaffolds and cultured for 7, 14 and 20 days before the total protein in the construct was measured using the BCA assay (see section 4.2.4.6).

In aligned-fibre constructs, the total protein was significantly increased at day 20 compared to day 0 (p≤0.05) (Figure 5-17). Comparing aligned and random-fibre constructs at day 7 and day 14, the difference in total protein was not statistically significant. However, the amount of total protein was significantly higher in aligned-fibre constructs compared to random-fibre constructs at day 20 (p≤0.05). These results suggested that, as no cell

proliferation was observed during this time (section 5.3.3); the increase in total protein is due to an increase in ECM production.

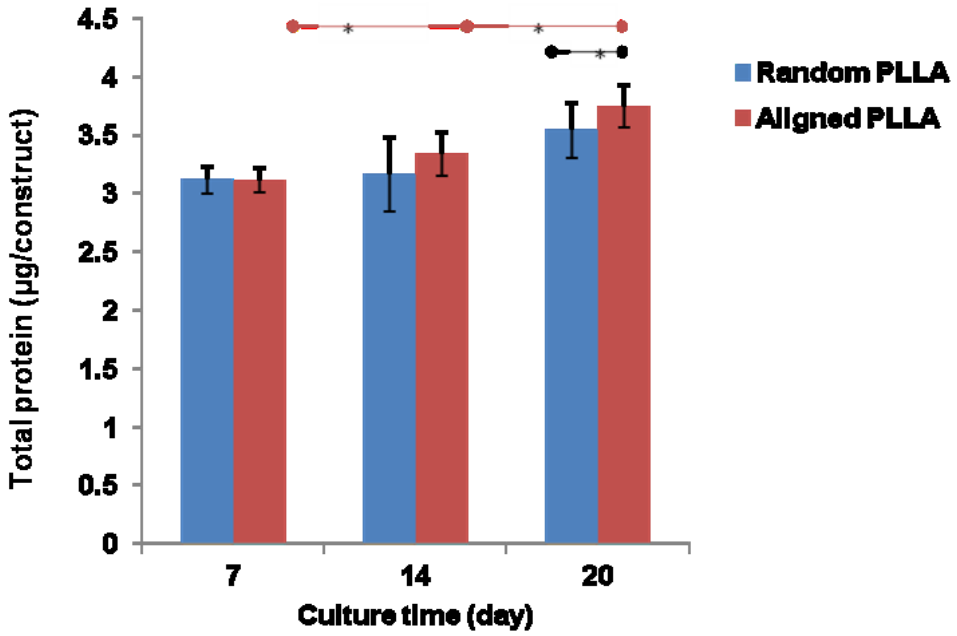

Figure 5-17: Total protein of HPDLFs seeded on random and aligned-fibre PLLA scaffolds and cultured for 7, 14 and 20 days. P values were calculated using ANOVA and independent samples T test, * p≤0.05, ** p≤0.01, *** p≤0.001. Data is presented as mean ± SD of 3 experiments, each in performed in triplicate.

5.3.5 Histological Evaluation

Poly(L-lactic acid) and decellularised scaffolds were seeded with $2x10^6$ cells/scaffold and cultured in tissue engineering medium for 2 weeks (see section 4.2.4.8). The constructs were then stained with H&E and examined under light microscope.

The H&E images showed a thin layer of HPDLFs on the outer surface along with vertical migration into the depth of the scaffold in both random and aligned-fibre PLLA scaffolds (Figure 5-18). In aligned-fibre constructs, the HPDLFs acquired a more stretched, fibroblast-like morphology with flattened and elongated nuclei. Scant extracellular matrix was observed in both random and aligned-fibres constructs.

H&E staining of the decellularised constructs demonstrated that HPDLFs were attached and distributed in the recellularised tissues (Figure 5-19).

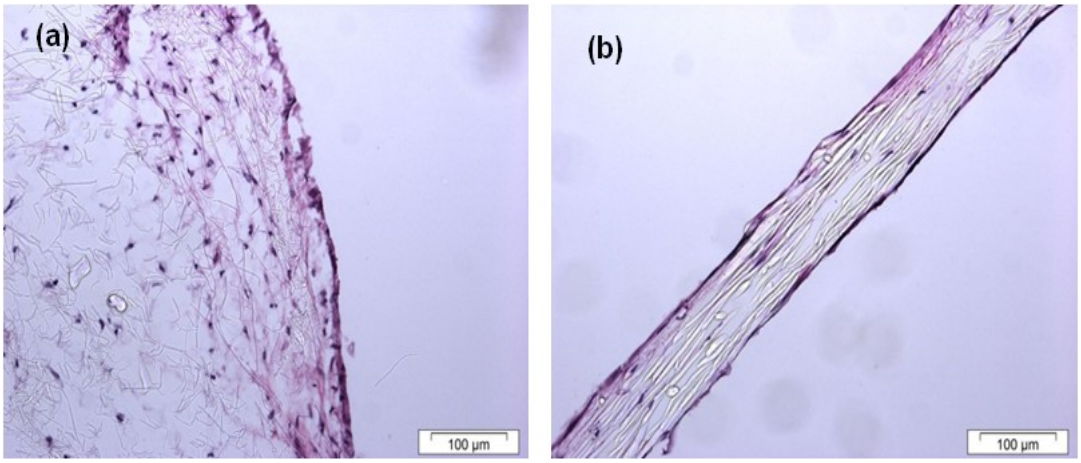

Figure 5-18: Light microscope images showing H&E stained section of (a) HPDLFs seeded on random-fibre PLLA scaffold, (b) HPDLFs seeded on aligned-fibre PLLA scaffold cultured under tissue engineing medium for 2 weeks. Scale bars = 100 µm.

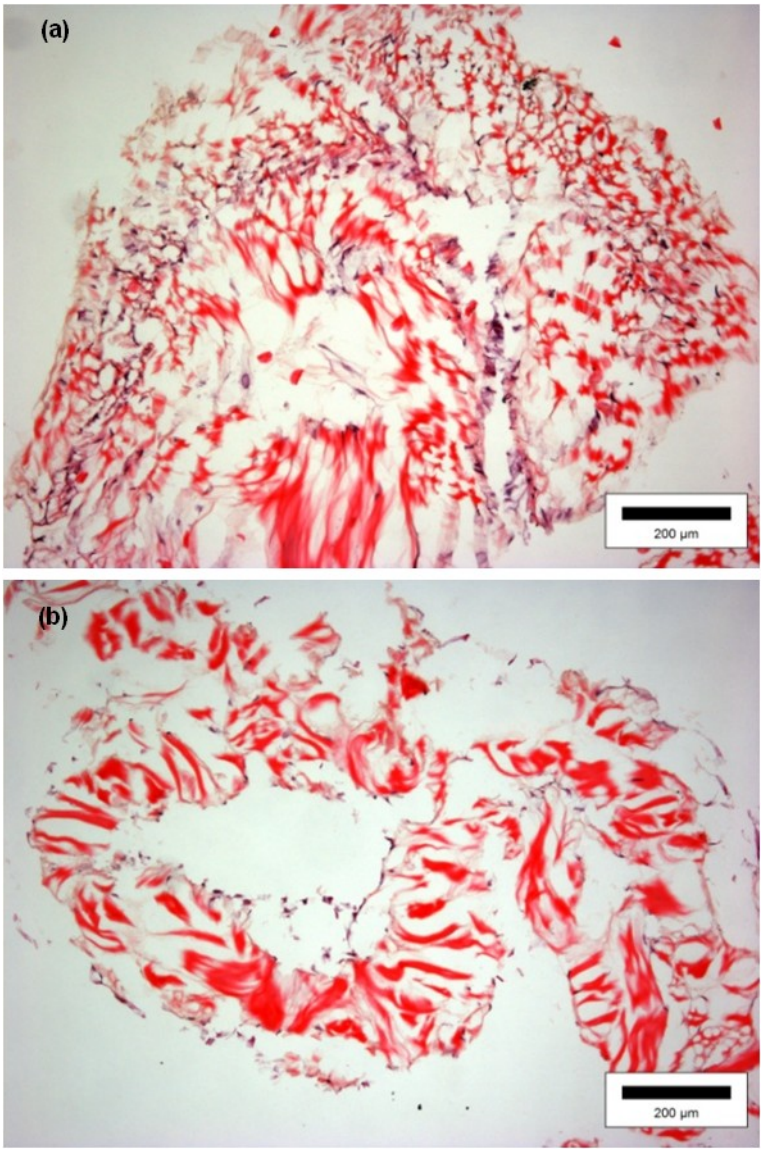

Figure 5-19: Light microscope images showing H&E stained section of (a) HPDLFs seeded on decell-skin, (b) HPDLFs seeded on decell-ligament cultured under tissue engineering medium for 4 weeks. Scale bar = 200 µm.

5.3.6 Effect of Scaffold Topography on HPDLF Gene Expression

5.3.6.1 PLLA Based Tissue Engineered Periodontal Ligament Constructs

To investigate the effect of fibre-alignment on gene expression, HPDLFs were cultured on PLLA and decellularised scaffolds for 0, 7, 14 and 20 days (section 4.2.4.10). The expression of the genes of interest (COL1A1, POSTN, SCXA, ALPL, RUNX2, IL6 and BGLAP) was determined using qRT-PCR. Human beta-2-microglobulin (β2M) mRNA was used as the 'housekeeping' gene/endogenous control as described in section 4.2.5.1.

Collagen type I (COL1A1)

Collagen type I is the most abundant extracellular matrix protein in periodontal ligament. Collagen synthesis is carried out by periodontal ligament fibroblasts and is an essential event in periodontal ligament and alveolar bone remodelling processes. Interestingly, the highest level of expression of COL1A1 was observed on day 0 in both the PLLA constructs (Figure 5-20). At this time point, the HPDLFs had been transferred from a 2D monolayer to 3D culture and the higher level is most likely due to the effect of previous culture in monolayer. At day 7, COL1A1 was significantly down-regulated compared to day 0 ($p \leq 0.01$) in both aligned and random constructs. COL1A1 expression was significantly up-regulated over the remaining culture period in both constructs ($p \leq 0.01$) compared to day 7. At days 14 and 20, COL1A1 expression was significantly higher in HPDLFs

seeded in aligned-fibre scaffolds compared to random-fibre scaffolds ($p \leq 0.01$).

Periostin (POSTN)

Periostin is highly expressed in collagen rich connective tissues and recently identified as a key factor in the regulation of collagen fibrillogenesis and fibroblast differentiation. In PLLA constructs, the pattern of POSTN expression was similar to the COL1A1 expression. At Day 7, POSTN expression was significantly down-regulated ($p \leq 0.01$) in both random and aligned-fibre constructs compared to day 0 (Figure 5-20). In the aligned-fibre constructs, POSTN expression was up-regulated over the culture period ($p \leq 0.001$). At days 14 and 20, POSTN expression was significantly higher in the aligned-fibre constructs compared to random-fibre constructs ($p \leq 0.01$).

Scleraxis (SCXA)

Scleraxis is a tendon and ligament-specific transcription factor essential for cell differentiation and matrix organisation and expressed by periodontal ligament stem cells. At days 0 and 7, both random and aligned-fibre constructs showed similar SCXA expression (Figure 5-20). In aligned-fibre constructs, SCXA expression was maintained over the culture time. However, it was significantly down-regulated in the random-fibre constructs by day 14 and 20 ($p \leq 0.01$, $p \leq 0.001$ respectively). In aligned-fibre constructs, SCXA expression was significantly higher than that in random-fibre constructs on both day 14 and day 20 ($p \leq 0.001$). These results indicated

that the PDLFs in the aligned-fibre scaffolds maintained a more ligament phenotype than the random-fibre constructs.

Alkaline phosphatase (ALPL)

Alkaline phosphatase is a glycoprotein hydrolase that plays an essential role in the mineralisation of hard tissues. ALPL expression was significantly down-regulated in both random and aligned-fibre constructs at days 7, 14, 20 compared to day 0 ($p \leq 0.01$, $p \leq 0.001$, $p \leq 0.001$ respectively) (Figure 5-20). Very low expression of ALPL was observed at days 7 and 14 in both constructs. These results suggested that the PDLFs in monolayer culture (indicted by day 0 data) had a more osteogenic phenotype than the 3D constructs. At day 20, ALPL expression was significantly up-regulated in aligned-fibre constructs compared to random-fibre constructs ($p \leq 0.01$).

Runt-related transcription factor 2 (RUNX2)

Runt-related transcription factor 2 is a transcription factor that regulates osteoblast differentiation and is expressed in bone and periodontal ligament. In random-fibre constructs, RUNX2 was significantly up-regulated at day 7 ($p \leq 0.01$) and then significantly down-regulated over the remaining culturing time ($p \leq 0.001$) (Figure 5-20). In contrast, RUNX2 expression was maintained at a relatively constant level in aligned-fibre constructs over the entire culture time. At days 14 and 20, RUNX2 expression in the aligned-fibre constructs was significantly higher compared to that in random-fibre constructs ($p \leq 0.01$).

Osteocalcin (BGLAP)

Osteocalcin is a calcium-binding bone matrix protein and known to be a marker for late stage osteoblast differentiation. No BGLAP expression was detected in either aligned or random fibre constructs. Therefore, the constructs did not contain any mature osteoblastic cells.

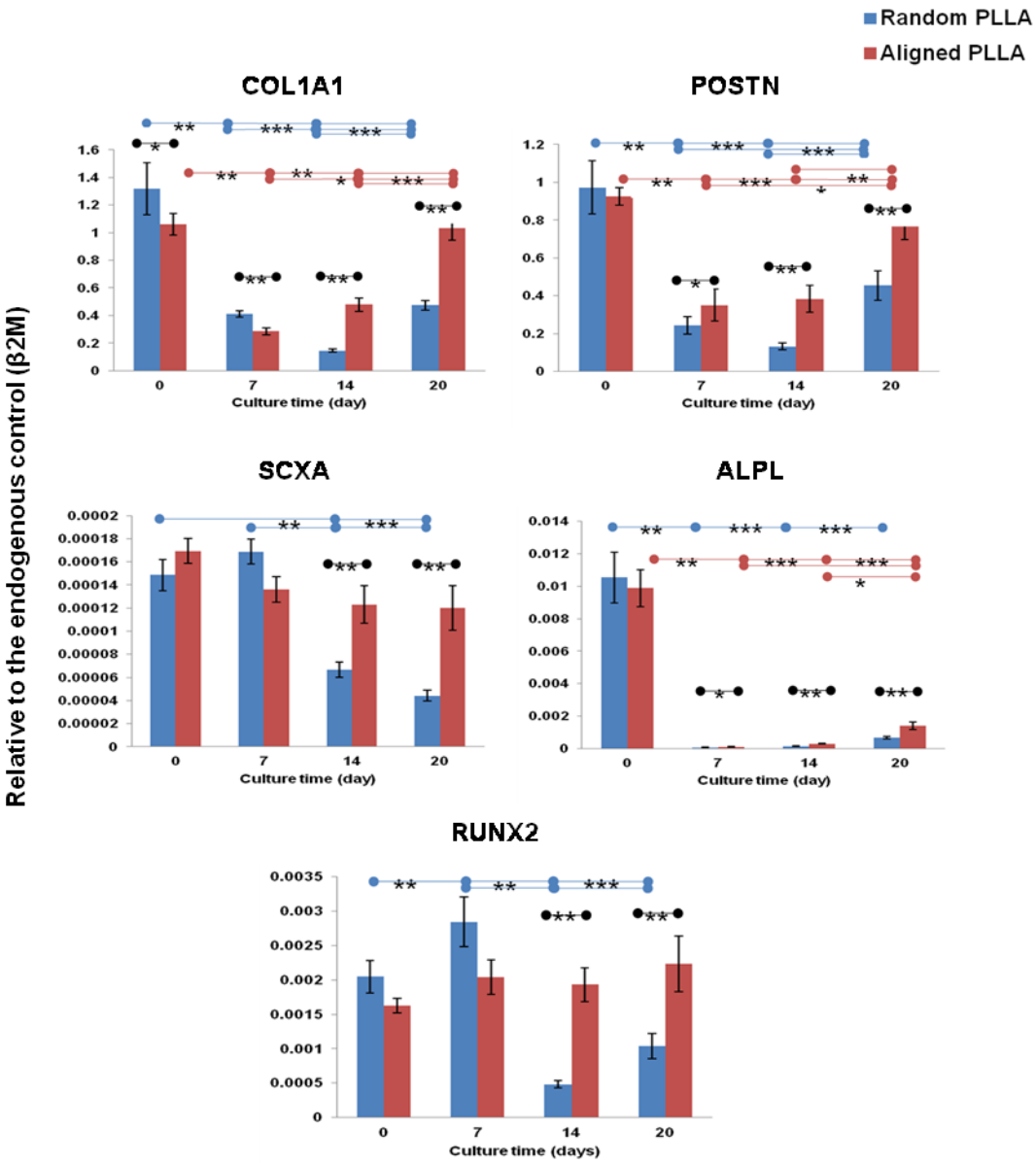

Figure 5-20: Fold change in mRNA expression of COL1A1, POSTN, SCXA, ALPL and RUNX2 genes with time in culture for random-fibre (blue columns) and aligned-fibre (red columns) PLLA-based tissue engineered ligament constructs seeded with HPDLFs and cultured for different periods of time points. Data was normalised to the endogenous control (β2M). P values were calculated using ANOVA and independent samples T test, *P≤0.05, **P≤0.01, ***P≤0.001. n = 3 separate experiments, each performed in triplicate.

5.3.6.2 Decellularised Skin and Ligament-Based Tissue Engineered Periodontal Ligament Constructs

The pattern of gene expression observed in decellularised constructs was found to be similar to that of PLLA-based constructs (Figure 5-21). At day 7, COL1A1, POSTN and ALPL were significantly down-regulated ($p \leq 0.01$) in both decell-skin and decell-ligament constructs. At day 20, COL1A1 and POSTN were expressed significantly higher in decell-ligament constructs compared to decell-skin constructs ($p \leq 0.01$). ALPL expression was very low and virtually undetectable over the entire culture period in both decell-skin and decell-ligament constructs.

At day 7, SCXA and RUNX2 were significantly up-regulated in both decell-skin and decell-ligament constructs ($p \leq 0.01$). In decell-skin constructs, SCXA and RUNX2 were down-regulated at days 14 and 20 ($p \leq 0.01$). In decell-ligament, SCXA and RUNX2 expression were down-regulated at day 14. However, by day 20 the expression of both genes was significantly up-regulated again ($p \leq 0.0$, $p \leq 0.05$ respectively). At day 20, SCXA and RUNX2 expression was significantly higher in decell-ligament constructs compared to decell-skin constructs ($p \leq 0.05$).

These results suggested that on day 0 (indicative of the 2D monolayer culture) the cells expressed a more osteogenic phenotype (suggested by the high ALPL) which on transfer to the 3D environment, the cells expressed a more ligament-like phenotype indicated by COL1A1 and POSTN expression.

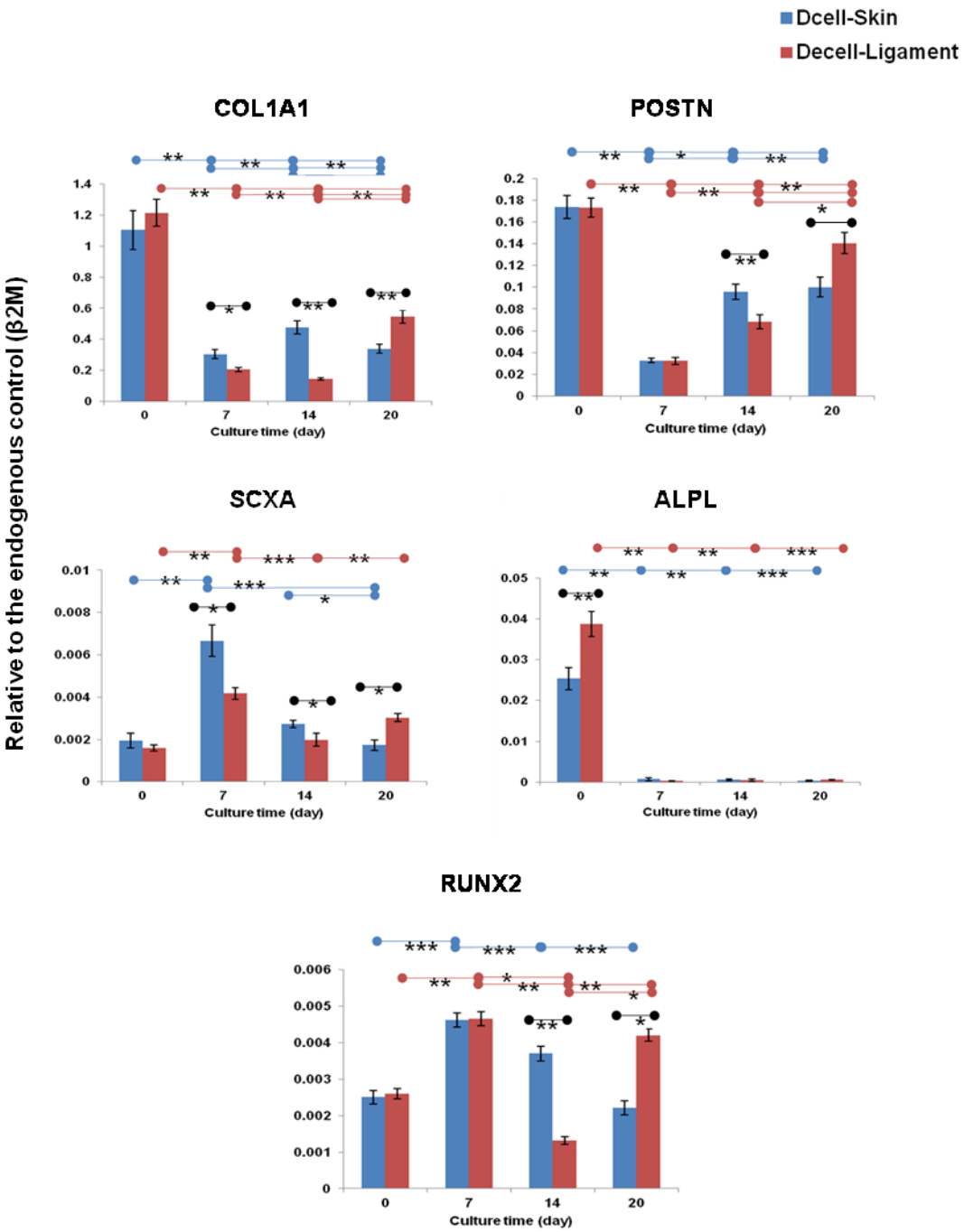

Figure 5-21: Fold change in mRNA expression of COL1A1, POSTN, SCXA, ALPL and RUNX2 genes with time in culture for non loaded decell-skin (blue columns) and decell-ligament (red columns) based tissue engineered ligament constructs seeded with HPDLFs and cultured for different periods of time points. Data was normalised to the endogenous control (β2M). P value was calculated using ANOVA and independent samples T test, *P≤0.05, **P ≤0.01, ***P≤0.001. n = 3 separate experiments, each performed in triplicate.

5.3.7 Immunohistolocalisation Staining

Poly(L-lactic acid) scaffolds seeded with HPDLFs and cultured for 30 days, as described in detailed in section 4.2.4.8, were examined for the effects of fibre-alignment on the deposition of collagen type I and periostin.

Immunohistolocalisation images showed denser collagen type I staining in the ECM of aligned-fibre compared to random-fibre constructs (Figure 5-22). Positive staining of periostin was observed in both aligned and random constructs. The expression of periostin was denser in aligned-fibre constructs. The staining in both constructs was denser and more organised at the superficial layer than around cells deep within the scaffold (Figure 5-23). Therefore, fibre-aligment appeared to enhance collagen type I and periostin deposition.

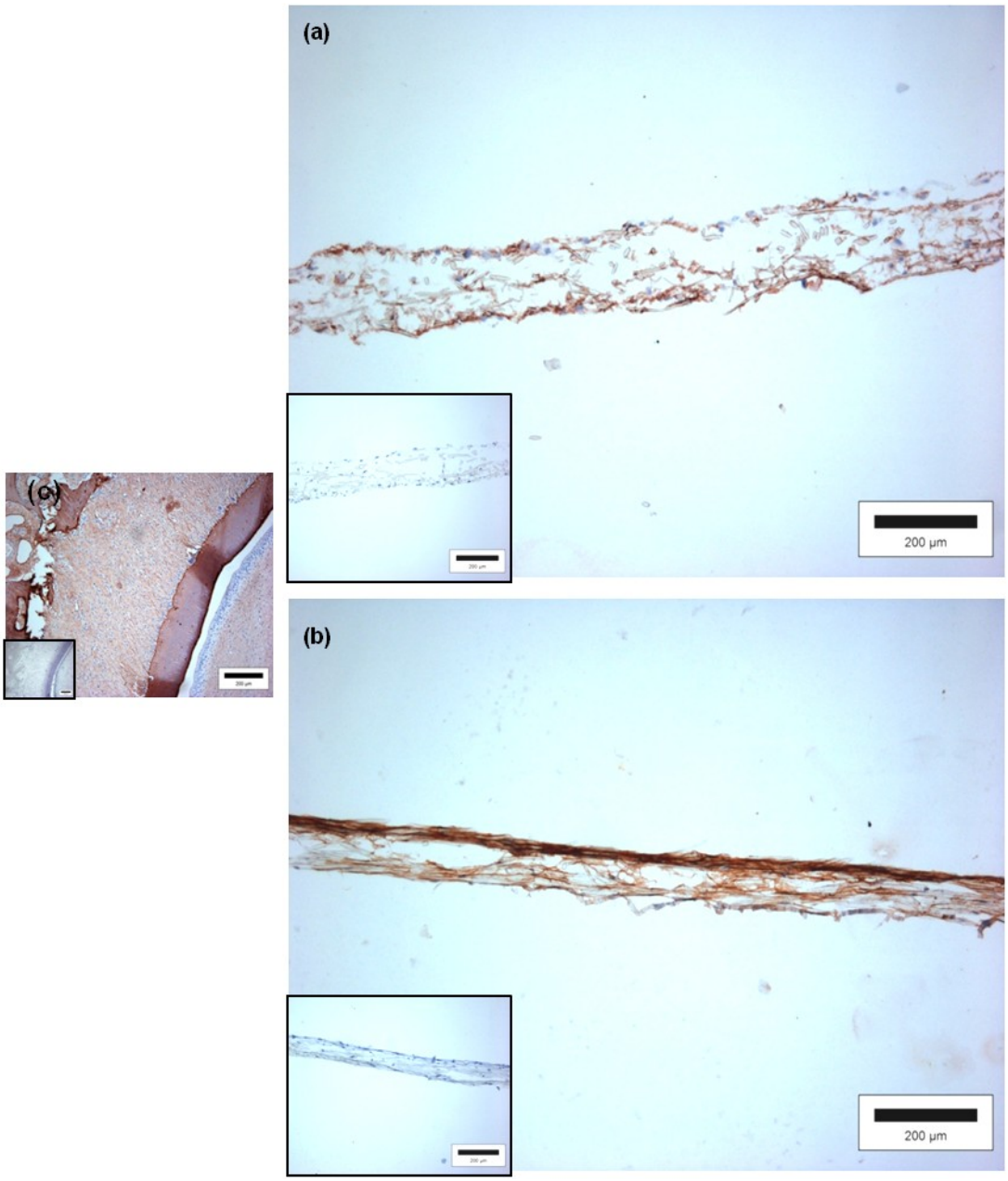

Figure 5-22: Immunohistolocalisation images show collagen type I staining (a) in random-fibre PLLA constructs (b) aligned-fibre PLLA constructs and (c) native periodontal ligament tissue. The images inserted at the lower left hand corners of the main images show the non-specific staining controls. (Scale bars = 200 µm).

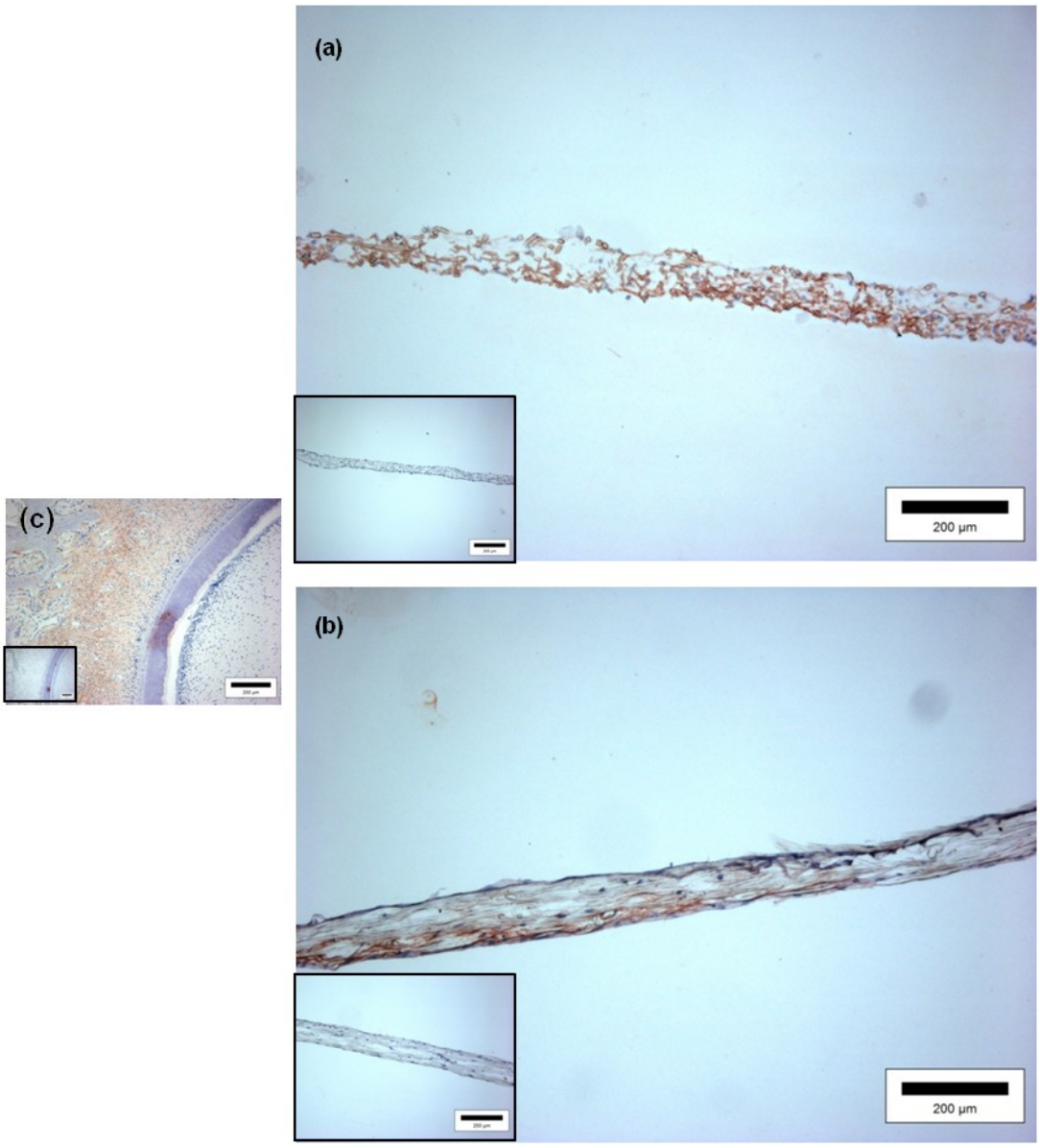

Figure 5-23: Immunohistolocalisation images show periostin staining (a) random-fibre PLLA constructs (b) anti-periostin aligned-fibre PLLA constructs and (c) native periodontal ligament. The images inserted at the lower left hand corners of the main images show the non-specific staining controls. (Scale bars = 200 µm).

5.3.8 Ossifying Nodules Formation

Alizarin Red S staining was used to investigate whether the HPDLF random and aligned-fibre constructs could mineralise in osteogenic media (see 4.2.4.9). Both random and aligned-fibre constructs showed positive staining with Alizarin Red S. However, HPDLFs seeded in aligned-fibre scaffold showed a greater depth of staining than cells seeded in random-fibre scaffolds. These results suggest that the HPDLFs differentiate into osteoblast-like cells to a greater extent in aligned-fibre construct than they did in random-fibre constructs (Figure 5-24).

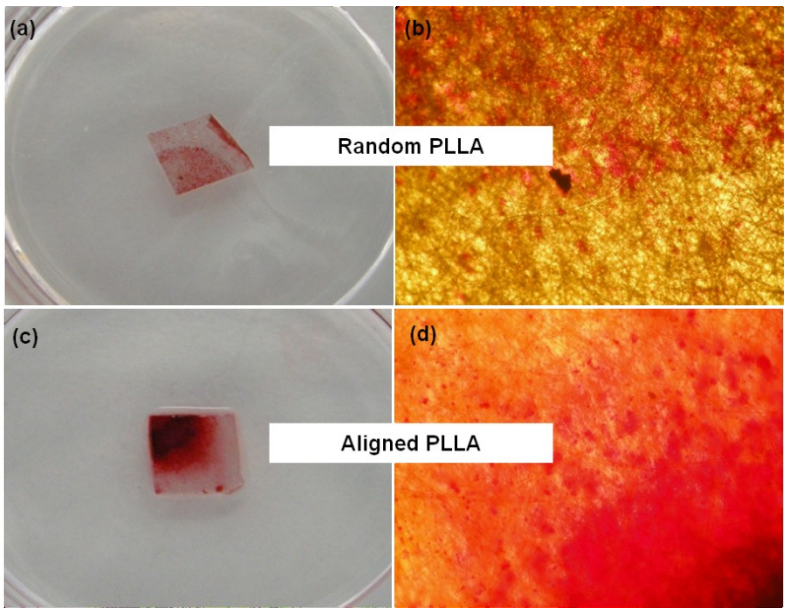

Figure 5-24: Photographs and light microscopy images showing Alizarin Red S staining of the mineralised structure formed on random (a, b) and aligned-fibre PLLA scaffolds (c, d).

5.3.9 Mechanical Strain Application

5.3.9.1 Effect of Static Strain and Fibre-alignment on Gene Expression

Most studies of the effect of mechanical strain have been undertaken on 2D monolayers of PDLFs. In the experiments detailed below, customised, loading chambers were used to investigate the effects of uniaxial strain on the tissue engineered constructs. The chambers had been customised to subject tendon fascicles to strain. Use of this equipment was kindly provided by Dr Graham Riley (University of East Anglia).

PLLA Based Tissue Engineered Periodontal Ligament Constructs

Human PDLFs were seeded on random and aligned scaffolds and cultured for 2 weeks *in vitro*. The tissue engineered periodontal ligaments were subjected to 3 h static strain using custom-made loading chambers. This was the first time these loading chambers were used to load an *in vitro* tissue engineered periodontal ligament construct (4.2.5.1). Quantitative RT-PCR was performed to quantify relative expression levels of genes of interest, namely COL1A1, POSTN, SCXA, ALPL, RUNX2 and IL6. Constructs that were not subjected to strain served as controls.

Collagen type I (COL1A1)

Collagen synthesis and turnover in periodontal ligament is considered to be an adaptive mechanism in response to mechanical loading.

In random-fibre constructs, COL1A1 was significantly up-regulated at 14% strain ($p \leq 0.05$) and significantly down-regulated at the highest strain of 20% ($p \leq 0.05$) (Figure 5-25). In aligned-fibre constructs, COL1A1 was significantly up-regulated at 9, 14 and 20% strain compared to the control construct ($p \leq 0.05$). COL1A1 expression was significantly higher in aligned-fibre constructs at lower strain (9%) and the highest strain (20%) compared to their counterpart random-fibre constructs ($p \leq 0.05$). Generally, it was observed that COL1A1 expression was significantly affected by the different strain applied on both random and aligned-fibre constructs.

Periostin (POSTN)

Periostin is a secreted ECM protein involved in the recruitment and adhesion of cells and plays a significant role in hard tissue formation.

A similar pattern of COL1A1 expression under strain was observed in POSTN expression. In random-fibre constructs, POSTN was significantly up-regulated at 14% strain compared to either control or 9% strained constructs ($p \leq 0.05$) (Figure 5-25). At 20% strain, POSTN expression was significantly down-regulated compared to 14% strained constructs ($p \leq 0.05$).

In aligned-fibre constructs, POSTN expression was significantly up-regulated at 9, 14 and 20% compared to control constructs ($p \leq 0.05$). The

difference in POSTN expression between strains was not statistically significant. POSTN was significantly expressed higher in aligned-fibre constructs strained at 9% and 20% compared to their counterparts' random constructs ($p \leq 0.05$). Generally, strain up-regulate POSTN expression compared to non-strained constructs.

Scleraxis (SCXA)

Scleraxis is a transcription factor mostly expressed in tendon and ligament cells, but not in differentiated cartilage or bone cells. Aligned-fibre constructs strained at 9% and 14% showed significant up-regulation of SCXA compared to control constructs ($p \leq 0.05$) (Figure 5-25). At 20% strain, SCXA expression was significantly down-regulated compared to 9% and 14% strained constructs (Figure 5-25). In random-fibre constructs, SCXA was significantly up-regulated at 14% and 20% strain compared to control constructs ($p \leq 0.05$). At 20% strain, SCXA expression was significantly down-regulated compared to 14% strained constructs. These results indicated that HPDLFs cultured in aligned-fibre scaffolds were more sensitive to the effects of strain as low as 9%.

Alkaline phosphatase (ALPL)

Alkaline phosphatase plays an essential role in the mineralisation of hard tissues. ALPL expression was barely detectable in control constructs regardless of the orientation of the scaffold fibres. However, ALPL expression was significantly up-regulated in random-fibre constructs subjected to 9% ($p \leq 0.05$) and 20% ($p \leq 0.01$) strain (Figure 5-25). In contrast,

in aligned-fibre constructs, ALPL gene expression was not changed by any of the strain levels applied. These results indicated that the HPDLF aligned-fibre constructs retained a more ligament phenotype under strain than random-fibre constructs.

Runt-related transcription factor 2 (RUNX2)

RUNX2 is a vital transcription factor required for osteoblasts differentiation and hard tissue formation. In aligned-fibre constructs, RUNX2 was significantly up-regulated only at the highest strain (20%) ($p \leq 0.05$) (Figure 5-25). In random-fibre constructs, RUNX2 was significantly up-regulated at 14% strained group compared to either control constructs or constructs strained at 9% and 20% ($p \leq 0.05$, $p \leq 0.05$ and $p \leq 0.01$ respectively). At 20% strain, RUNX2 expression was significantly higher in aligned-fibre constructs compared to random constructs ($p \leq 0.05$). This may suggests that HPDLFs cultured in aligned-fibre scaffolds and strained at the highest strain started to differentiate to osteogenic-like cells.

Interleukin 6 (IL6)

IL6 expression was significantly up-regulated in aligned-fibre constructs strained at 14% compared to control or 9% strained constructs ($p \leq 0.05$). In random-fibre constructs, IL6 expression was down-regulated at 20% strain compared to its expression in control, 9% and 14% strain. At 20% strain, Il6 expression was significantly higher in aligned-fibre constructs compared to random constructs. However, its expression in aligned-fibre constructs at 20% strain is comparable to that in control constructs.

Osteocalcin (BGLAP)

Osteocalcin is a marker for late stage osteoblast differentiation. No BGLAP expression was detected in either random or aligned-fibre constructs nor was the gene expression influenced by application of uniaxial strain. Hence, the HPDLFs did not express osteocalcin, a protein indicative of a mature osteoblast phenotype.

The expression patterns of ALPL, RUNX2 and BGLAP (osteogenic genes) in HPDLFs cultured in aligned-fibre scaffolds suggested that HPDLFs in an aligned topographical substrate and strained at “low or medium” strain maintained their ligament phenotype.

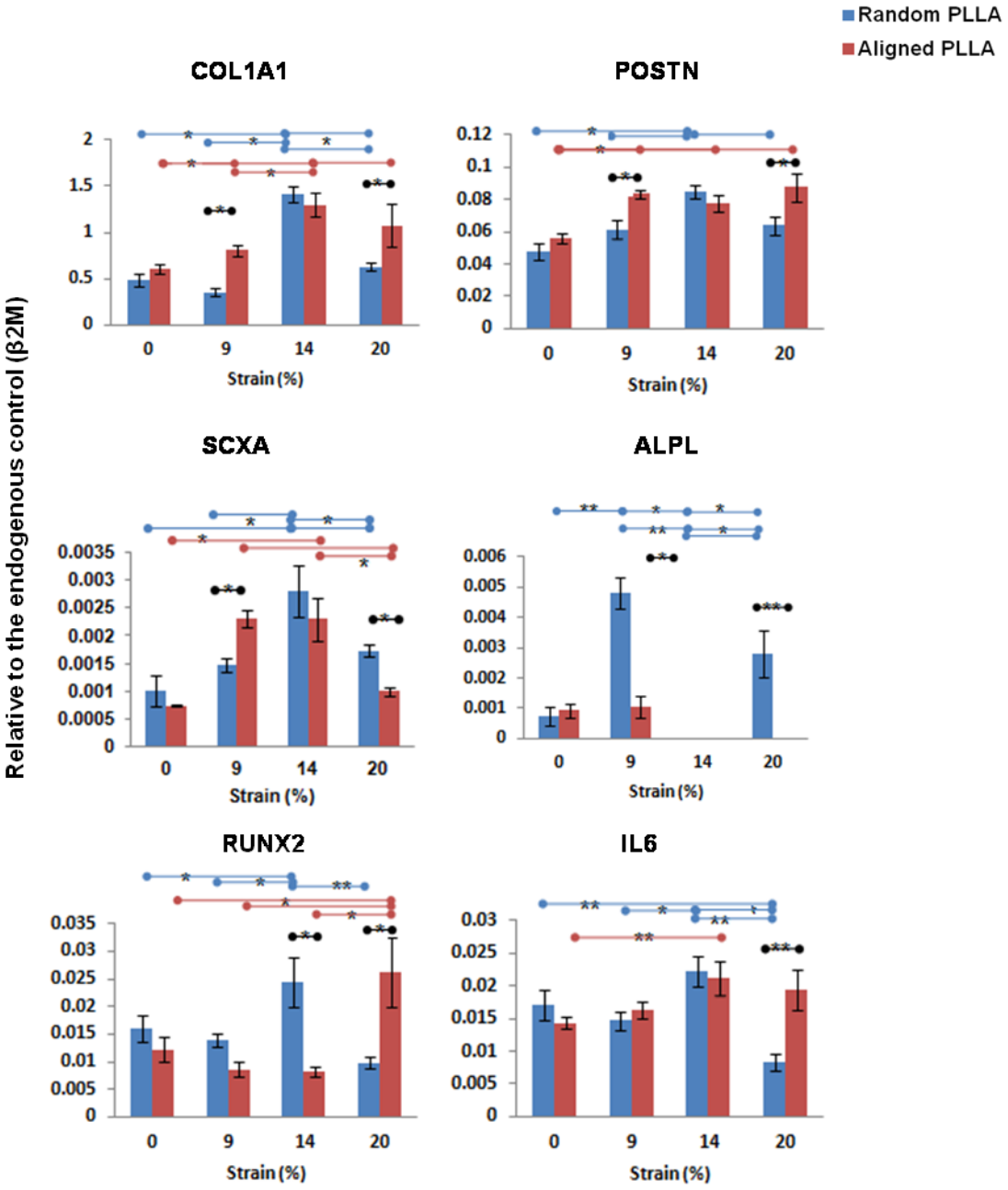

Figure 5-25: Fold change in mRNA expression of COL1A1, POSTN, SCXA, ALPL, RUNX2 and IL6 genes of mechanical loaded random and aligned-fibre PLLA constructs relative to endogenous control (β2M). P values were calculated using ANOVA and independent samples T test, * p≤0.05, ** p≤0.01, *** p≤0.001. Data is presented as mean ± SD. n=3 separate experiments, each performed in triplicate.

Decellularised skin and Ligament Based Tissue Engineered Periodontal Ligament Constructs

Decellularised bovine skin and ligaments were seeded with HPDLFs and cultured for 14 days before being subjected to static strain for 3 h (see 4.2.5.1). The expression of COL1A1, POSTN, SCXA, ALPL, RUNX2 and IL6 were assessed using qRT-PCR technique and the results are shown in Figure 5-26.

In both decell-skin and decell-ligament constructs, COLA1A, POSTN and IL6 expression were not affected by any level of the strain applied. Difference in the expression of COL1A1 and POSTN between strained decell-skin and decell-ligament constructs was statistically insignificant. SCXA was significantly up-regulated in decell-ligament constructs strained at 20% ($p \leq 0.05$). Its expression was significantly higher compared to that in decell-skin constructs strained at the same level ($p \leq 0.05$). On the other hand, strain had little effect on SCXA expression in decell-skin constructs. ALPL expression was significantly up-regulated in both decell-ligament and decell-skin constructs strained at 14% ($p \leq 0.05$) with a higher expression in the decell-skin constructs ($p \leq 0.05$). RUNX2 was significantly up-regulated in both decell-skin and decll-ligament constructs strained at 20% ($p \leq 0.05$) and its expression was significantly higher in decell-ligament compared to that in decell-skin constructs ($p \leq 0.05$). No BGLAP was detected in either the decell-skin or decell-ligament constructs at any strain levels.

Interestingly, the expression of COL1A1, POSTN, SCXA, ALPL, RUNX2 and IL6 in strained decell-skin and decell-ligament constructs was different from their expression in strained PLLA-fibre constructs. The difference in the expression of these genes between the PLLA-based and the native collage/tissue-based constructs may be due to the difference in their mechanical properties.

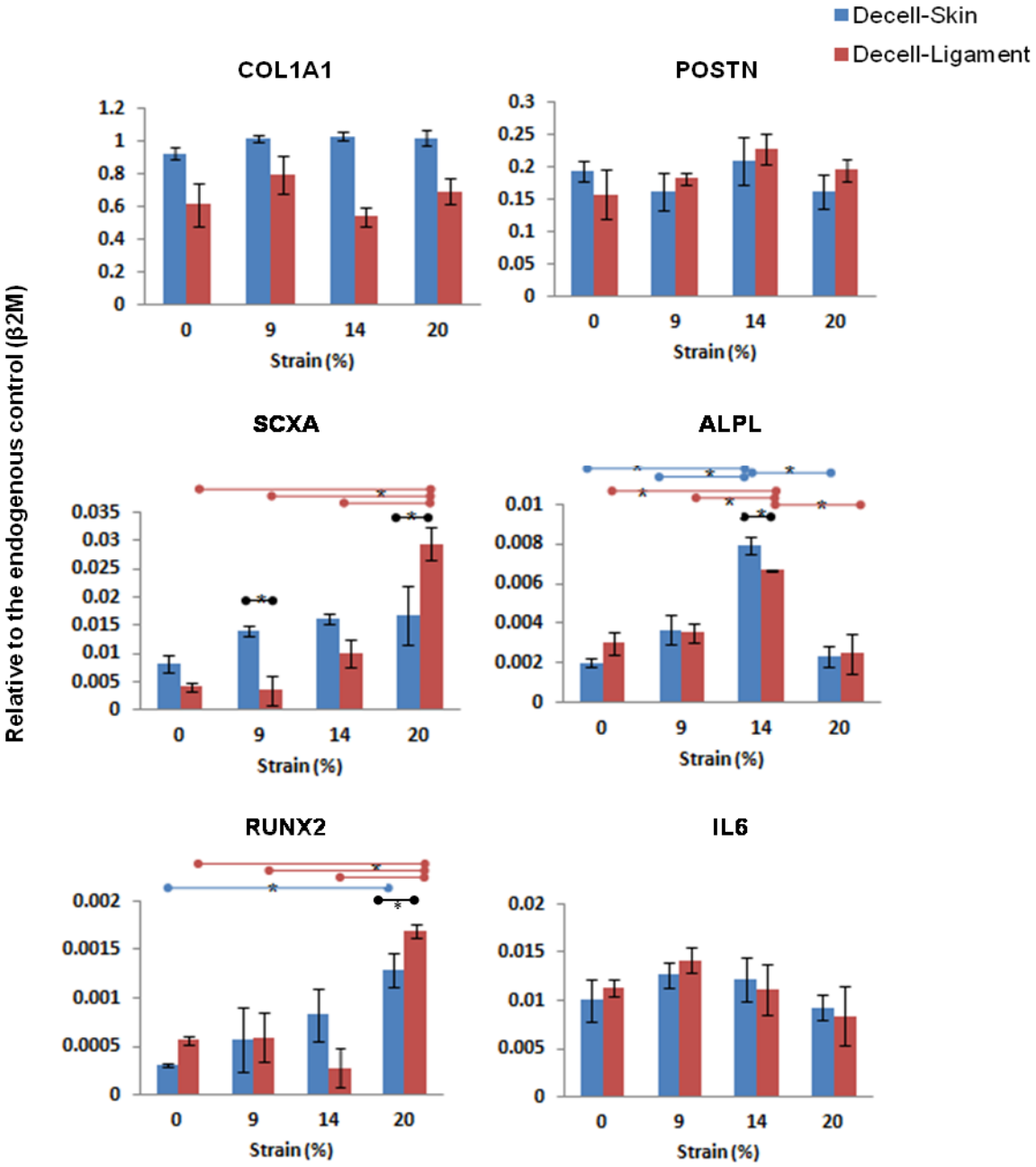

Figure 5-26: Fold change in mRNA expression of COL1A1, POSTN, SCXA, ALPL, RUNX2 and IL6 genes of mechanically strained decellularised skin and ligament constructs relative to the endogenous control (β2M). P values were calculated using ANOVA and independent samples T test, * p≤0.05, ** p≤0.01, *** p≤0.001. Data is presented as mean ± SD. N = 3 separate experiments, each performed in triplicate.

5.3.9.2 Collagen Gel Based 3D Periodontal Ligament Model

Few studies investigating the effect of mechanical loading/straining on PDLFs have used 2D monolayer cultures of cells. Very few studies have addressed the effect of mechanical loading on PDLFs cultured in a 3D environment and these studies have used PDLFs encapsulated in collagen gels (Ku et al., 2009, Berendsen et al., 2009). Collagen is the most abundant protein in periodontal ligament. Compared to periodontal ligament, collagen gels are less stiff and therefore have different mechanical properties. These differences may lead PDLFs to respond differently to strain.

Contraction of the 3D Collagen Gel Constructs

Optimising cell density in gel constructs before loading application.

The maximum number of HPDLFs that could be encapsulated in the collagen gels and cause minimal gel contraction was $1.5x10^6$ cells/ml (300,000 HPDLFs per individual gel construct). Therefore, this cell density was used to form the the gel constructs used to study the effect of cyclic strain on HPDLFs.

Gel contraction after loading application

After 48 h of loading, analysis of images revealed that 3D gel constructs contracted to about 50% of the original constructs size ($p \leq 0.001$) (Figure 5-27).

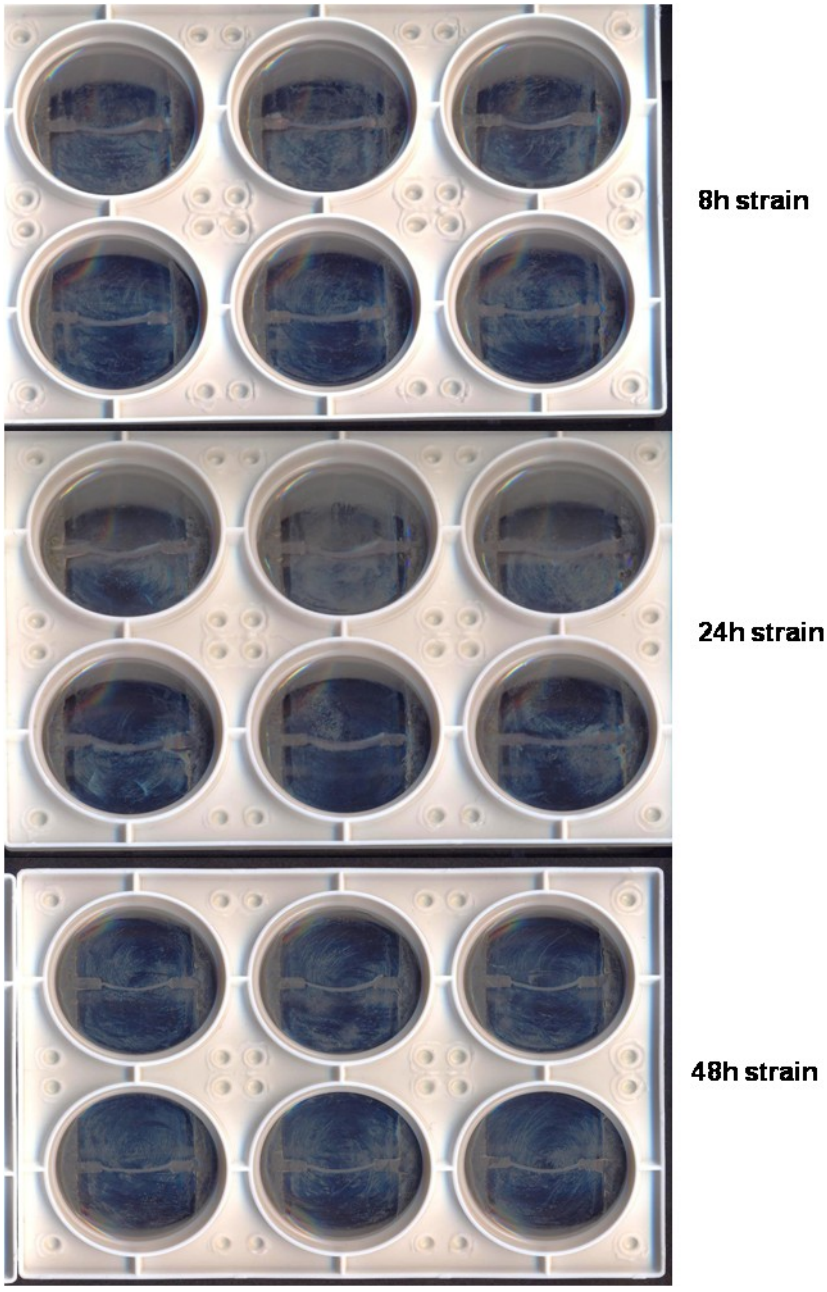

Figure 5-27: Photographs showing the 3D HPDLFs-loaded gels in the Flexcell® Tissue-Train™ plates. The gels were strained for for 8 h (a), 24 h (b) and 48 h (c). Gel contraction and remodelling was obsreved during the culture period.

Effect of Cyclic Mechanical Strain on Gene Expression

The 3D HPDLFs-gel constructs were exposed to 5% cyclic strain at 1Hz for 8, 24 and 48 h. Non-strained constructs were used as control. The gene expression was assessed by loading application as described in section 4.2.5.2 and results are presented in Figure 5-28.

COL1A1 and POSTN were significantly up-regulated in 24 and 48 h strained HPDLFs-gel constructs compared to control constructs ($p \leq 0.001$). Both COL1A1 and POSTN showed significantly higher expression in HPDLFs-gel constructs strained for 24 and 48 h compared to 8 h strained constructs ($p \leq 0.001$).

SCXA was significantly up-regulated in HPDLFs-gel constructs strained for 8, 24 and 48 h compared to the control constructs ($p \leq 0.001$). HPDLFs-gel constructs strained for 48 h expressed a higher level of SCXA compared to that strained for 8 or 24 h ($p \leq 0.001$).

ALPL expression sharply increased in HPDLFs-gel constructs strained for 24 h ($p \leq 0.001$). At 48 h, ALPL expression dropped significantly and was level with that in control constructs ($p \leq 0.001$).

RUNX2 was significantly up-regulated at all time points in strained HPDLFs-gel constructs, compared to the control constructs ($p \leq 0.001$). The difference of RUNX2 expression in 8, 24 and 48 h strained constructs was not statistically significant.

IL6 was significantly up-regulated in strained HPDLFs-gel constructs at all time points compared to the control constructs ($p \leq 0.01$). However, IL6 expression was significantly reduced over the strain period ($p \leq 0.01$).

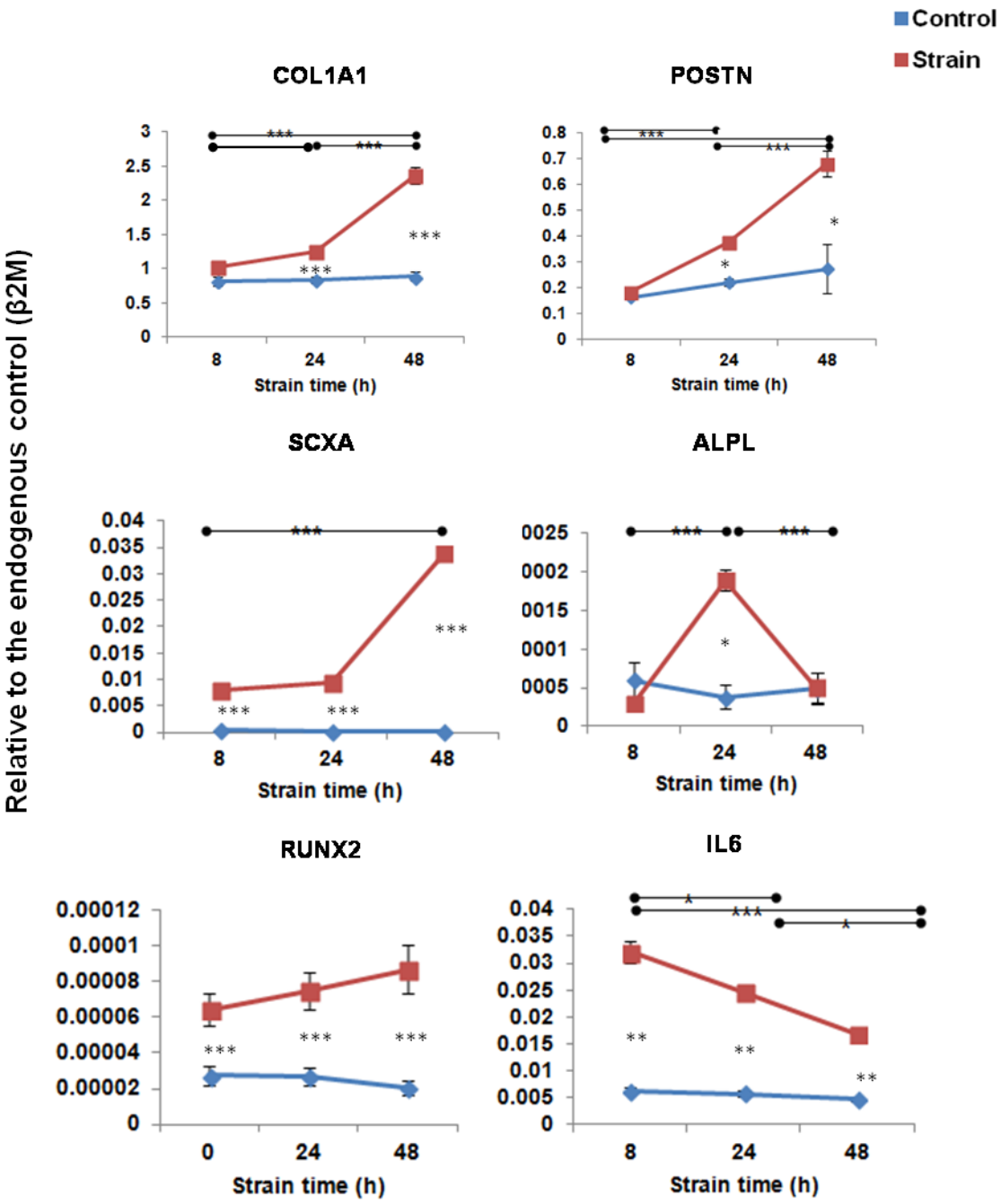

Figure 5-28: Fold change in expression of COL1A1, POSTN, SCXA, ALPL, RUNX2 and IL6 mRNA of strained HPDLFs-loaded collagen gels relative to endogenous control (β2M). P values were calculated using ANOVA and independent samples T test, * p≤0.05, ** p≤0.01, *** p≤0.001. Data is presented as mean ± SD of 3 separate experiments, each performed in triplicate.

5.3.10 EMD and/or TGF-β1 Stimulated Tissue Engineered Periodontal Ligament Constructs

Regeneration of the periodontal ligaments *in vivo* is an active process involving cell- cell and cell-ECM interactions. Growth factors are biologically active proteins that can affect the differentiation of PDLFs and the synthesis of extracellular matrix components. To assess the effect of growth factors on HPDLFs, two of the most commonly used growth factors in periodontal regeneration namely Enamel matrix derivative [Emdogain® (EMD)] and Transforming growth factor beta 1 (TGF-β1) were used. HPDLFs cultured on random and aligned-fibre PLLA scaffolds were stimulated by EMD and/or TGF-β1 as described in section 4.2.6.

5.3.10.1 Cellular Activity

alamarBlue® was used to investigate the cellular activity of HPDLFs cultured on random and aligned-fibre PLLA scaffolds and stimulated with either EMD, EMD+TGF-β1 or TFG-β1 as described in section 4.2.6.1.

At day 14, cellular activity was significantly higher in aligned-fibre constructs treated with EMD+TGF-β1 compared to the control constructs ($p \leq 0.05$). The difference in cellular activity of EMD or TGF-β1 treated aligned-fibre constructs compared to the control constructs was not statistically significant (Figure 5-29). In the random-fibre constructs, a greater cellular activity was observed in constructs stimulated by EMD compared to the control constructs ($p \leq 0.001$). The difference in cellular activity between the EMD or TGF-β1 treated groups and the control in random-fibre constructs was not

statistically significant. The cellular activity was significantly higher in aligned-fibre constructs stimulated with EMD+TGF-β1 or TGF-β1 alone compared to random-fibre constructs (P≤0.001) (Figure 5-29). To confirm whether the cellular activity is due to cell proliferation, the total DNA content in each scaffold was measured.

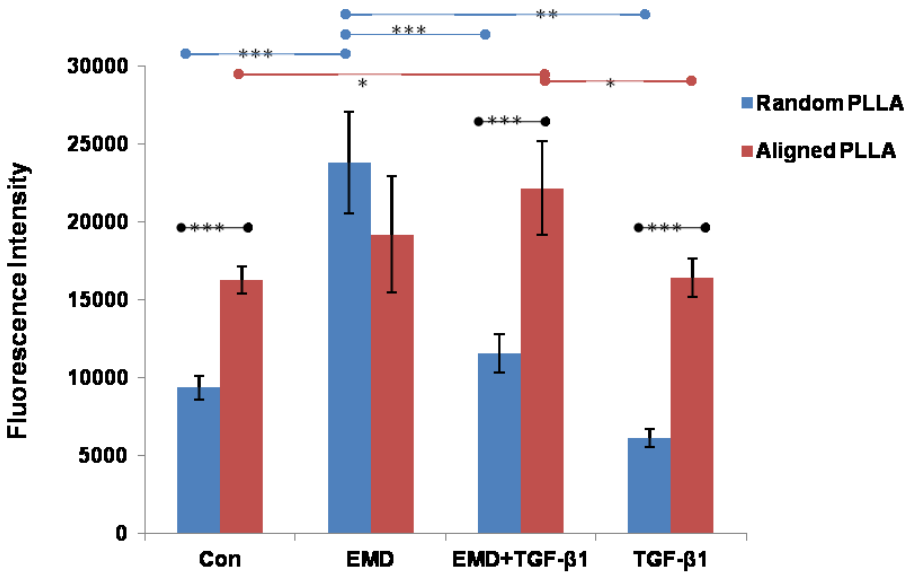

Figure 5-29: Cellular activity of HPDLFs seeded on random and aligned-fibre PLLA scaffolds and stimulated with EMD (100 µg/ml), TGF-β1 (10 ng/ml) and a combination of EMD (100 µg/ml) and TGF-β1 (10 ng/ml) for 14 days. Data shows the cellular activity after 4 h incubation in alamarBlue®. P values were calculated using ANOVA and independent samples T test, *(P≤0.05), ** (P≤0.01) and * (P≤0.001) denotes significant differences. Data is presented as mean ± SD of 3 separate experiments, each performed in triplicate.**

5.3.10.2 Cellular Proliferation

The total DNA content was quantified using the DNA quantification assay to assess the degree of HPDLF proliferation in random and aligned-fibre constructs stimulated with EMD and/or TGF-β1 (section 4.2.4.5).

The DNA content was significantly increased in random-fibre constructs stimulated with EMD or EMD+TGF-β1 compared to the control constructs ($p \leq 0.001$) (Figure 5-30). In aligned-fibre constructs, stimulation with EMD and/or TGF-β1 had no significant effect on the total DNA content of the constructs. Comparing the DNA content of aligned-fibre constructs with random-fibre constructs, EMD-stimulated random-fibre constructs showed a significantly higher DNA content ($p \leq 0.001$).

It appears that EMD and/or TGF-β1 had different effects on random-fibre constructs and aligned-fibre constructs (Figure 5-30). Neither EMD, TGF-β1 nor the EMD and TGF-β1 combination had effect on HPDLF proliferation in aligned-fibre constructs.

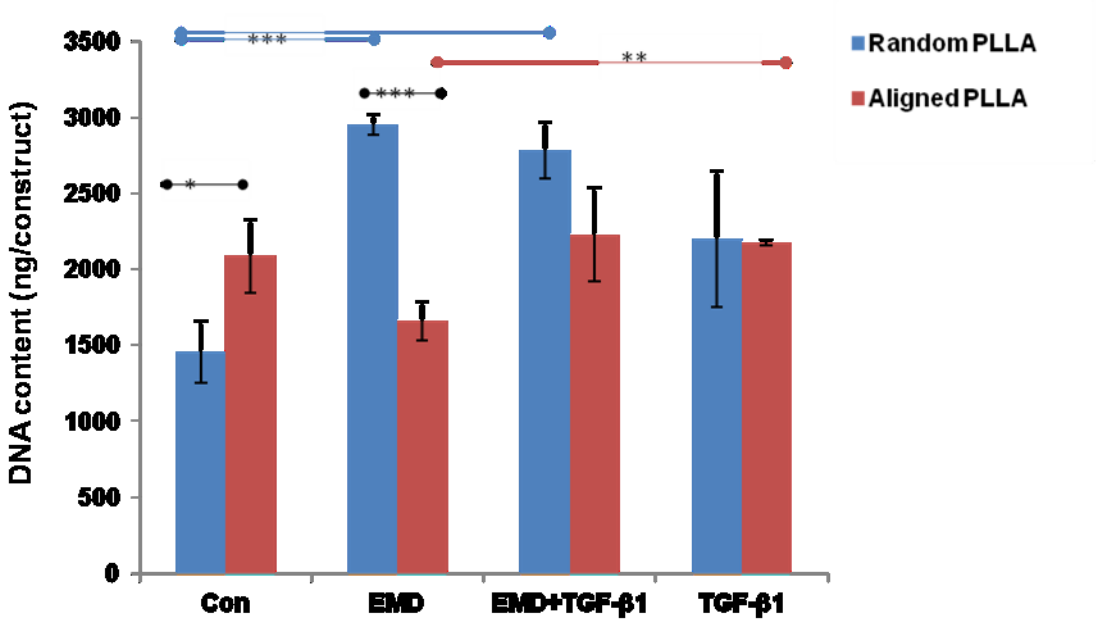

Figure 5-30: The total DNA of HPDLFs cultured on random and aligned-fibre PLLA scaffolds and stimulated with EMD (100 µg/ml), TGF-β1 (10 ng/ml) and a combination of EMD (100 µg/ml) and TGF-β1(10 ng/ml) for 14 days. P values were calculated using ANOVA and independent samples T test, * p≤0.05, ** p≤0.01, *** p≤0.001. Data is presented as mean ± SD of 3 separate experiments, each performed in triplicate.

5.3.10.3 Total Protein

The effect of EMD and/or TGF-β1 stimulation on protein synthesis of HPDLFs constructs formed on random and aligned-fibre PLLA scaffolds was investigated. The constructs were cultured for 14 days (section 4.2.4.5). The EMD and/or TGF-β1 treated constructs were processed to measure total protein using BCA Protein Assay kit as described in section 4.2.6.3.

Total protein was significantly higher in the aligned-fibre constructs stimulated with EMD, EMD+TGF-β1 or TGF-β1 compared to the unstimulated control constructs ($p \leq 0.01$, $p \leq 0.001$, $p \leq 0.001$ respectively) (Figure 5-31). Random-fibre constructs stimulated with EMD or EMD+TGF-β1 also showed significantly higher total protein content compared to control constructs ($p \leq 0.001$). A higher total protein content was observed in aligned-fibre constructs treated with TGF-β1 compared to their counterpart random-fibre constructs ($p \leq 0.05$).

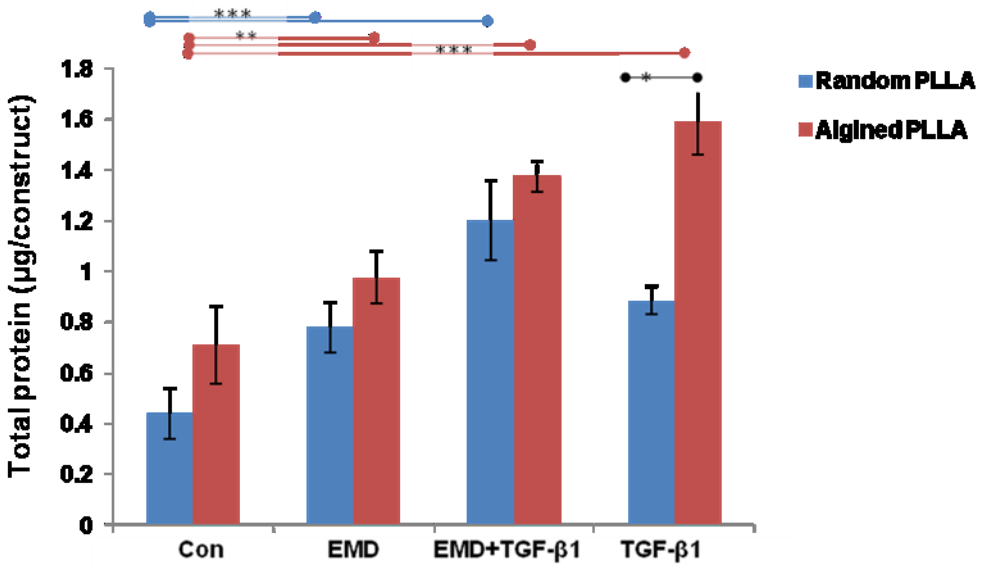

Figure 5-31: Total protein in random and aligned-fibre constructs stimulated with EMD (100 µg/ml), TGF-β1 (10 ng/ml) and a combination of EMD (100 µg/ml) and TGF-β1 (10 ng/ml) for 14 days. P values were calculated using ANOVA and independent samples T test, * p≤0.05, ** p≤0.01, *** p≤0.001. Data is presented as mean ± SD of 3 separate experiments, each performed in triplicate.

5.3.10.4 Gene Expression of EMD and/or TGF-β1 Stimulated Tissue Engineered Periodontal Ligament Constructs

The change in gene expression of constructs of HPDLFs cultured on random and aligned-fibre PLLA scaffolds and stimulated with EMD and/or TGF-β1 for 7 and 14 days was assessed using qRT-PCR. Constructs cultured in PDLFs basic medium with 0.2% FCS were used as control. The results from these experiments are presented in Figure 5-32.

Collagen type I (COL1A1)

At day 7, COL1A1 expression was significantly up-regulated in all stimulated aligned-fibre constructs compared to the control constructs (≤0.001). EMD+TGF-β1 and TGF-β1 stimulated random-fibre constructs showed higher COL1A1 expression compared to the control constructs (≤0.001). Aligned-fibre constructs showed significantly higher COL1A1 expression compared to random-fibre constructs stimulated with EMD, EMD+TGF-β1 or TGF-β1 (≤0.001).

At day 14, COL1A1 continued to be up-regulated in both random and aligned-fibre stimulated constructs compared to the control constructs (≤0.001). COL1A1 expression was higher in aligned-fibre constructs stimulated with TGF-β1 compare to their counterpart random constructs (≤0.001).

Periostin (POSTN)

A similar pattern to COL1A1 expression was observed in POSTN. In comparison to control random-fibre constructs, TGF-β1 stimulated constructs showed POSTN up-regulated at day 7 (≤0.001). POSTN expression was significantly up-regulated in aligned-fibre constructs stimulated with EMD+ TGF-β1 and TGF-β1 compared to control constructs (≤0.001). Aligned-fibre constructs stimulated with EMD and/or TGF-β1 showed significantly higher POSTN expression compared to random-fibre constructs (≤0.001).

At day 14, POSTN was up-regulated in both aligned and random fibre constructs stimulated with EMD and/or TGF-β1 compared to the control constructs (≤0.001). TGF-β1 treated aligned-fibre constructs showed significantly higher POSTN expression compared to random constructs (≤0.001).

Scleraxis (SCXA)

A pattern similar to both COL1A1 and POSTN expression was also observed in SCXA expression. At day 7, SCXA expression was significantly up-regulated in both aligned and random fibre constructs stimulated with EMD+TGF-β1 and TGF-β1 (≤0.001). Yet, SCXA expression was significantly higher in aligned-fibre constructs compared to random-fibre constructs (≤0.001).

At day 14, SCXA continued to be up-regulated in both aligned and random fibre constructs stimulated with EMD+TGF-β1 and TGF-β1 compared to control constructs (≤0.001). Aligned-fibre constructs stimulated with EMD+TGF-β1 showed a significantly higher SCXA expression compared random-fibre constructs (≤0.001).

Alkaline phosphatase (ALPL)

At day 7, ALPL was significantly up-regulated in EMD stimulated aligned-fibre constructs compared to control or random-fibre constructs (≤0.001). At 14 days, ALPL expression was significantly up-regulated in EMD and EMD+ TGF-β1 stimulated aligned-fibre constructs (≤0.001). TGF-β1 had almost no effect on ALPL expression in random-fibre constructs at both days 7 and 14.

Runt-related transcription factor 2 (RUNX2)

At day 7, RUNX2 was significantly up-regulated in both random and aligned constructs stimulated with TGF-β1 and EMD+ TGF-β1 (≤0.001). TGF-β1 treated random-fibre constructs showed higher RUNX2 expression compared to aligned-fibre constructs and this difference was statistically significant (≤0.001).

At day 14, RUNX2 expression was reduced compare to its expression at day 7. Higher RUNX2 expression was observed in random-fibre constructs stimulated with TGF-β1 and EMD+ TGF-β1 compared to control constructs (≤0.001).

Osteocalcin (BGLAP)

No BGLAP expression was observed in either random or aligned-fibre constructs stimulated with EMD and/or TGF-β1 for 7 and 14 days.

EMD and/or TGF-β1 had different effects on HPDLF proliferation, total protein synthesis and gene expression in tissue engineered periodontal ligaments. In this study, EMD showed a tendency to up-regulate genes involved in bone formation and osteoblast differentiation, such as ALPL. Meanwhile, TGF-β1 was observed to up-regulate ligament related genes, i.e. COL1A1, POSTON and SCXA. The results of TGF-β1+EMD-treated constructs followed a trend that was similar to TGF-β1-only treated constructs. Therefore, the influence of TGF- β1 was greater than EMD when these growth factors were used together. The effect of growth factors on gene expression was accentuated by the fibre-alignment of the constructs at day 7.

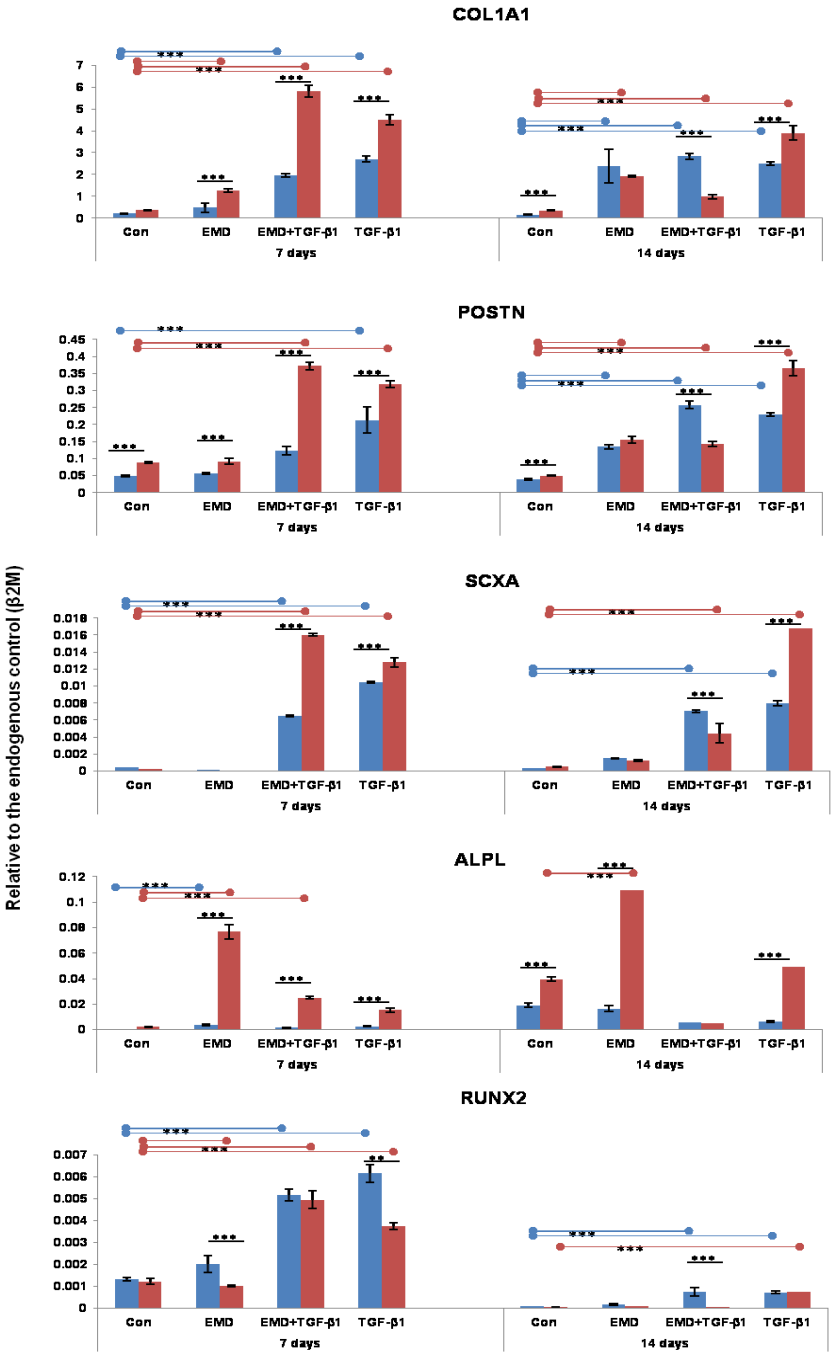

Figure 5-32: Fold change in mRNA expression of COL1A1, POSTN, SCXA, ALPL and RUNX2 genes with time in culture for at different culture time points for random-fibre (blue columns) and aligned-fibre (red columns) PLLA-based engineered ligament constructs seeded with HPDLFs and stimulated with EMD (100 µg/ml), TGF-β1 (10 ng/ml) and a combination of EMD (100 µg/ml) and TGF-β1 (10 ng/ml) for 7 and 14 days. Data was normalised to the endogenous control (β2M). P values were calculated using ANOVA and independent samples T test, *$P \leq 0.05$, **$P \leq 0.01$, ***$P \leq 0.001$. n = 2 separate experiments, performed in triplicate.

5.3.10.5 Western Blots

Western blots were performed to assess whether the up-regulated expression of collagen type I, periostin, and runt-related transcription factor 2 genes in the *in vitro* tissue engineered periodontal ligaments stimulated with EMD and/or TGF-β1 for 14 days (section 4.2.6.5) resulted in the expression of the relevant proteins also.

Western blots results showed that all EMD and/or TGF-β1 treated constructs had expressed collagen type I, periostin, and runt-related transcription factor 2 proteins (Figure 5-33). The loading control protein, β-actin, was detected in all the tested samples and showed a highly similar band intensity among all of them which confirms that an equal amount of the total protein was loaded in every lane during the WB procedure.

Collagen type I

Collagen type I protein band was detected at a molecular weight around 130 kDa, which matches the molecular weight (MW) predicted by the antibody supplier. Aligned-fibre constructs treated with EMD and/or TGF-β1 showed a more strongly stained collagen type I band, visually, in comparison to the control or their counterparts random-fibre constructs.

Periostin

Periostin protein bands were detected at the predicted size, which is around 90 kDa. Visually, EMD and/or TGF-β1 treated constructs showed more strongly staining periostin bands compared to the control constructs in both random and aligned-fibre constructs.

Runt-related transcription factor 2 (RUNX2)

RUNX2 protein bands were detected at approximately 55 kDa on the blots. All treated groups including the controls showed a distinct band of RUNX2. However, stronger staining RUNX2 bands were observed in random-fibre constructs treated with EMD and/or TGF-β1.

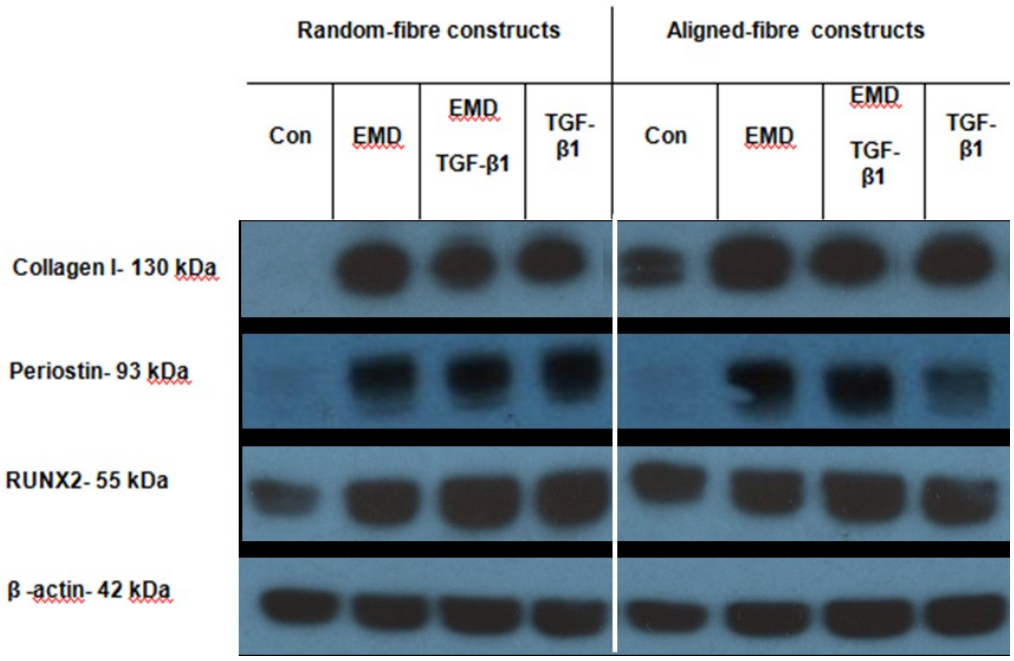

Figure 5-33: Western blot analysis of collagen type I, periostin and RUNX2 of HPDLFs cultured on random and aligned-fibre PLLA scaffolds and stimulated with EMD (100 µg/ml), EMD (100 µg/ml) in combination with TGF-β1 (10 ng/ml) or TGF-β1 (10ng/ml) alone. β-actin was used as a control and distinct bands of β-actin was observed in all lanes.

6. DISCUSSION

The ultimate goal of periodontal treatment is to fully regenerate the periodontal ligament and bone tissue lost as a consequence of periodontal disease. A variety of procedures including bone grafting, guided tissue regeneration and growth factors have been used to treat periodontal defects (Nygaard Østby et al., 2010, Esposito et al., 2010). While bone regeneration was reported, the amount of regenerated periodontal ligament tissue was neither predictable nor site-specific. Therefore, as concluded in Chapter 2, there remains a great clinical need for a novel therapeutic strategy that can overcome the limitations of the existing periodontal therapies.

Periodontal tissue engineering is a relatively new field with enormous potential to fully regenerate the lost periodontal tissues including the periodontal ligament and cementum. In the broader field of tissue engineering to regenerate tissues which have a highly aligned native ECM such as nerve and muscle, much interest has been directed towards the production of aligned scaffolds which mimic the general topographic arrangement of collagen fibres in the ECM. In periodontal ligament, the collagen fibres are highly oriented along the fibre axis and it may be desirable to maintain this feature when designing scaffolds for periodontal ligament tissue engineering. There are few reports of researchers fabricating aligned-fibre scaffolds for periodontal ligament tissue engineering. To the best of my knowledge, there have been no detailed investigations addressing the impact of fibre-alignment on PDLF gene

expression, extracellular matrix production and response of the cells to mechanical loading and growth factors. Therefore, tissue engineered periodontal ligament constructs were developed *in vitro* using aligned-fibre and random-fibre scaffolds to evaluate the impact of fibre-alignment on PDLF cellular behaviour and on the response of the cells to mechanical loading and growth factors. Such an *in vitro* system may also provide a valuable experimental tool to study different aspects of periodontal ligament including mechanisms of repair and regeneration.

6.1 Cell Sources

The *in vitro* isolation and characterisation of primary PDLFs is usually based on the source of the tissue, animal or human, the anatomical site of harvesting the tissue and finally the protocol used to establish cell cultures (outgrowth of cells from tissue explants or enzymatic digestion of the periodontal ligament tissue to release the cells). Three different sources of PDLFs were investigated in this study to evaluate which would be most suitable for tissue engineering PDL constructs. The PDLF sources evaluated were: porcine (PPDLFs), rat (RPDLFs) and human (HPDLFs). Animal-derived PDLs were investigated because of the relative ease of obtaining tissue. This was an important consideration when large numbers of cells were required to prepare the PDLF constructs. In addition, the provenance of the PDL tissue could be fully known and use of different batches of animal PDLFs would overcome animal to animal variation. The use of HPDLF is clinically relevant, however human PDL tissue could not be

obtained locally due to not having the appropriate ethical approvals in place at the time and patient to patient variation can have significant impact. The commercial source of HPDLFs used in this study were derived from the pooled periodontal ligament tissue of several patients which should have reduced an impact of patient-to-patient variation.

Both PPDLFs and RPDLFs were successfully extracted and expanded *in vitro* using both outgrowth of cells from tissue explants and isolation of PDLFs by enzymatic digestion of periodontal ligament tissue. However, a greater cell number could be readily obtained using enzymatic digestion. These PDLFs also showed a higher proliferative rate and reached confluency at a faster rate. These observations were in agreement with those of Tanaka and colleagues who reported that PDLFs isolated using enzymatic digestion had a higher proliferative rate, colony-forming activity and the ability to differentiate into osteoblasts, chondrocytes or adipocytes, which is a characteristic of mesenchymal stem cells (Tanaka et al., 2011). During enzymatic extraction, cells are isolated from the PDL and cultured at sub-confluent densities in the absence of intact PDL tissue. This minimises the effect of paracrine growth factors and cell–cell contact on the differentiation of PDLFs and therefore, may possibly help to retain their mesenchymal stem-like behaviour. Hence, the enzymatic method was used throughout the study to expand rat and porcine PDLFs. However, PPDLF cultures had a high rate of infection and less than half of the PDL samples gave viable cells.

PDLFs from all sources (porcine, rat, human) showed the spindle shape-characteristic of periodontal fibroblasts when examined by light microscopy. Also, cultured PDLFs from all the species stained positive for ALPL staining and formed mineralised nodules when cultured in osteogenic differentiation medium. These observations were also found by other researchers who reported that PDLFs isolated from rat, porcine and human are a heterogeneous population of cells expressing osteoblastic properties which could differentiate into bone-forming cells (Arceo et al., 1991, Nohutcu et al., 1997, Nohutcu et al., 1996, Somerman et al., 1988, Somerman et al., 1990).

To date, there is no defined marker that specifically identifies periodontal ligament fibroblasts. Ideally, PDLF identification *in vitro* should be confirmed by their morphological appearance and the presence of various proteins and mRNA markers including collagen type I, periostin, runt-related transcription factor 2, cementum attachment protein, cementum protein-23, scleraxis, periodontal-ligament associated protein (PLAP)-1/asporin, osteopontin or osteocalcin.

Using PDLFs from animals have advantages in terms of cell availability. Periodontal ligament fibroblasts from porcine (PPDLFs) and rat (RPDLFs) were successfully expanded and characterised *in vitro*, yet they were not used in the project for the following reasons:

a). PPDLFs had a high rate of infection and their viability was unpredictable as a result of an often prolonged time between slaughtering and tissue harvesting which was outside the researcher’s control.

b). RPDLFs were easier to extract and the slaughter to tissue harvesting time was in the researcher's control. However, this tissue source would be an expensive cell source to use in this project as large number of cells was needed for each experiment. Also the need for large cell numbers raises ethical questions as it necessitates the use of significant numbers of animals.

Using HPDLFs for regenerative studies provides data that is more valuable as these cells are more relevant to clinical application. The HPDLFs used in the study were commercially available primary cells (ScienCell, USA) that have been used very recently for several *in vitro* studies (Seo et al., 2011, Chae et al., 2011, Premaraj et al., 2011, Seo et al., 2012, Dai et al., 2012, Saminathan et al., 2013, Kim et al., 2013). In this study, early cell passages between 4 and 7 were used. Primary PDLF cultures used at early passages have the advantage of maintaining the phenotypic and functional heterogeneity of PDLFs. It was reported that PDLFs used at late passages exhibited different morphology and biological activity when compared to those at early passages (Itaya et al., 2009).

In conclusion, PDLFs from different sources (porcine, rat, human) were successfully expanded and characterised *in vitro.* However, HPDLFs were selected for use in advanced tissue engineering studies for the reasons described above.

6.2 3D Tissue Engineered Periodontal Ligament Constructs

Monolayer culture systems (i.e. 2D culture systems) have been commonly used to study periodontal ligament fibroblasts *in vitro*. However, PDLFs normally exist in a 3D environment, embedded in an extracellular matrix of proteins and glycosaminoglycans. It is well known that the topography of the extracellular micro-environment has an essential role in cellular behaviour, from attachment and morphology to proliferation and differentiation through contact guidance (Curtis et al., 2006, Xie et al., 2010). Therefore, developing a 3D model that more-closely resembles the native ECM of periodontal ligament tissue could provide a better *in vitro* model system in which to study PDLF behaviour. *In vivo*, PDLFs exist in a mechanically active environment where ECM plays a role in their response to mechanical loading such as mastication forces. *In vitro*, PDLFs in conventional 2D culture systems lack the mechanical stimuli they would have been exposed to *in vivo*. Therefore, there is still a need for a better *in vitro* 3D periodontal ligament system that can be mechanically loaded to recreate periodontal ligament tissue.

6.2.1 Scaffold Fabrication

6.2.1.1 PLLA Scaffolds

Poly lactic acid (PLA) is known to be a biocompatible and biodegradable polymer which has been approved by the Food and Drug Administration (FDA) (Rasal et al., 2010). Poly lactic acid exists in mainly two enantiomeric forms: the left-handed poly(L-lactic acid) and the right-handed poly(D-L-lactic acid) (Rasal et al., 2010). Poly(L-lactic acid) is a semicrystalline polymer that has high mechanical strength and low degradation rate. Previous studies have shown that PLLA supports the growth and differentiation of many cell types *in vitro* such as tissue engineered tendon (Yin et al., 2010), nerve (Yang et al., 2004), periodontal ligament (Liao et al., 2013).

An 8% (wt/vol) PLLA dissolved in DCM was used to fabricate random and aligned-fibres PLLA scaffolds in this study. It was reported that shrinkage rate is decreased with increasing the concentration of PLLA to 5- 10% (wt/vol) (Yang et al., 2004). Poly glycolic acid (PGA) is one of the most commonly used polymers in tissue engineering. However, although PGA is known to be highly compatible and supports ECM production, it degrades rapidly and shrinks disproportionally as a result of hydrolytic degradation (Reichardt et al., 2012). Poly(L-lactic acid) was used in this study, as it slowly degrades compared to PGA and maintains the scaffolds' structural integrity for a longer time *in vitro*. Rahman and Tsuchiya demonstrated that PLLA has better mechanical stability and degradation rate, over other

polymer scaffolds and was able to maintain cell phenotype (Rahman and Tsuchiya, 2001). Mechanical stability and controlled degradation rate were key requirements of this project because, (a) constructs were subjected to mechanical strain, so maintaining scaffold integrity was crucial to enable proper fitting of constructs into the loading chambers (b) in some of the experiments, a prolonged culture time was required which could last up to 40 days.

Highly aligned PLLA fibres were successfully fabricated using electrospinning. The fibre-alignment was confirmed by SEM images and FFT analysis (Figure 5-2). Electrospun aligned-fibre scaffolds have been widely used in tissue engineering of nerves, tendons/ligaments and heart, but there are few reports of the use of aligned-fibre scaffolds for tissue engineering and periodontal ligament tissue. Different methods have been used to create cell culture surfaces with aligned features such as pillars, grooves, or pits (Table 2-2). Electrospinning has the advantage of producing scaffold mats of variable dimensions with aligned or randomly oriented fibres in which the fibre diameter can be controlled.

Aligned PLLA scaffolds were fabricated at a speed of 5000 rpm to yield highly aligned fibres with a uniform morphology. The aligned nature of the scaffolds obtained was similar to aligned scaffolds fabricated by other researchers. Thomas et al. assessed the effect of rotation speed on fibre-alignment using 0, 3000 and 6000 rpm collection speed. He reported that increasing collector rotation speed produced more aligned fibres. Not only did the alignment of the fibres improve, but the tensile strength of the

scaffold along the axis of alignment increased with increasing rotation speed (Thomas et al., 2006). The same was also observed by Li et al., using PCL polymer to tissue engineer musculoskeletal constructs (Li et al., 2007). The increase in the tensile strength of the scaffolds could be explained by denser-fibre packing and minimum inter-fibre space in highly aligned-fibre scaffolds. Also, the fibres have more uniform morphology and diameter at a higher rotational speed which could contribute to the higher tensile strength observed in aligned-fibre scaffolds. Although no experiments were undertaken to study the mechanical properties of the fabricated scaffolds in this project, it was observed that the scaffolds maintained reasonable mechanical properties needed for handling and mechanical loading during the entire study period.

In conclusion, electrospinning was found to be an effective and versatile technique to produce highly aligned-fibre scaffolds for periodontal tissue engineering.

6.2.1.2 Decellularised Scaffolds

Decellularised bovine skin and ligament were used in this study as a natural reference material to compare with the random and aligned-fibre PLLA scaffolds. The decellularisation protocol used Triton X-100 and sodium deoxycholate as described by Rieder et al., (2004). Triton X-100 and sodium deoxycholate have been used successfully to decellularise heart valves (Wen et al., 2012, Tudorache et al., 2007, Booth et al., 2002), kidney

(Ross et al., 2009), lung (Wallis et al., 2012, Jensen et al., 2012), trachea (Haykal et al., 2012) and ligaments (Yoshida et al., 2012).

In this study, histological and fluorescent staining showed that apparent removal of nuclei and their remnants from the decellularised tissue was achieved (Figure 5-3 and Figure 5-4). Quantification of DNA showed that 95% of the DNA content was removed from the decellularised skin and ligaments (Figure 5-5). These results confirmed that Triton X-100 and sodium deoxycholate together worked as an effective decellularising agent for bovine skin and ligament.

Although the decellularisation protocol used in this study brought about complete removal of cells and their components, it effectively preserved the collagen integrity of the ligament and skin as shown in the SEM and histological images (Figure 5-3). This data is in agreement with Yu et al. who reported that low concentrations of Triton X-100 and sodium deoxycholate effectively removed cells from porcine aortic valve leaflets while maintaining collagen matrix integrity (Yu et al., 2013). Laser scanning microscopy has shown significant ECM alterations in porcine pulmonary leaflets decellularised with sodium dodecyl sulfate, trypsin/EDTA, or trypsin–detergent–nuclease protocols. Only decellularisation with sodium deoxycholate maintained extracellular matrix and collagen fibre integrity (Zhou et al., 2010).

The decellularised bovine skin and ligament were cut into 100 μm sections to match the thickness of the PLLA scaffolds. A similar 'slicing' method was used to build-up a composite of multilayers of decellularised tendon followed by seeding with bone marrow stromal cells (BMSCs) to engineer tendon tissue (Omae et al., 2009). Omea et. al, reported that BMSCs cultured on the tendon slices were able to organise along the collagen fibres and expressed tenomodulin, a known tendon phenotype marker (Omae et al., 2009).

HPDLFs were seeded onto decell-skin and decell-ligament and the resulting constructs cultured for 20 days. Cellular activity assays showed that the HPDLFs maintained viability on the decell-skin and decell-ligament up to 20 days in culture (Figure 5-14). These results suggested that no cytotoxicity occurred as a result of using the decellularising agents or sterilising the tissue with PAA. Also, qRT-PCR data showed that HPDLFs expressed COL1A1 and POSTN which are known PDLFs markers. In addition, the expression of SCXA in the constructs, a known marker for ligament and tendon tissue, was increased over day 0. Also, ALPL expression (an osteoblastic marker) was virtually undetectable in the constructs by day 7. These data suggested that decell-skin and decell-ligaments scaffolds supported the growth and the differentiation of the cultured HPDLFs and promoted a ligament phenotype. On day 0, when the HPDLFs had just been transferred from a 2D to 3D environment, the cells had a higher expression levels of COL1A1, POSTN and ALPL suggesting that in monolayer culture the cells expressed a more osteoblastic phenotype.

The decellularised tissues used in this study were used as natural random (decell-skin) and aligned scaffolds (decell-ligament). The decellularisation method using Triton X-100 and sodium deoxycholate preserved the collagen topography in both skin and ligament tissues and maintained PDLF phenotype throughout the culture time.

6.2.2 Effects of Fibre-alignment on HPDLFs

In tissue engineering, scaffolds not only provide mechanical support for cells to grow on but have potential to act as “intelligent surfaces”. These surfaces are capable of providing cues and signals, either chemical or topographical, to guide cell attachment, morphology, proliferation and differentiation. Previous studies have shown that osteoblasts, mesenchymal stem cells, myoblasts, chondrocytes and Schwann cells were influenced by the substrate topography which modified their cellular behaviour and differentiation ability (Table 2-3). Periodontal ligament ECM is composed of highly oriented collagen fibres. It was recently reported that aligned fibres of PLGA modified the morphology of RPDLFs and enhanced their cellular activity, compared to random scaffolds (Shang et al., 2010). To my knowledge, the effect of fibre-alignment on PDLF gene expression and protein matrix synthesis has not been reported.

Results from this study have shown that HPDLFs seeded on aligned-fibre scaffolds oriented themselves along the direction of the fibres (Figure 5-11). A similar trend was observed when HPDLFs were seeded on decell-ligament scaffolds (Figure 5-12). This is consistent with previous findings

which have reported that cells cultured on aligned-fibre scaffolds oriented and elongated along the fibre axes (Yin et al., 2010, Shang et al., 2010). Rat periodontal ligament fibroblasts cultured on aligned PLGA scaffolds for 7 days showed elongated morphology in the direction of the fibre alignment (Shang et al., 2010). Human tendon stem cells seeded on aligned PLLA scaffolds showed greater cellular orientation and expression of tendon specific genes compared to random-fibre scaffolds (Yin et al., 2010). Other cells have also shown the same oriented morphology when seeded on aligned-fibre scaffolds such as human umbilical vein endothelial cells (Whited and Rylander, 2013), mouse myoblasts (Sheets et al., 2013, Liao et al., 2008), human artery muscle cells (Nivison-Smith and Weiss, 2012), human osteoblast-like cells (Tong et al., 2010), neutral stem cells (Yang et al., 2005) and coronary smooth cells (Xu et al., 2004).

Cellular orientation along the alignment of the fibres reported here may be explained by the effect of contact-guidance, which means that cells migrated in the direction of either chemical, structural, or mechanical properties of the substrate. Therefore, the use of aligned fibre scaffolds may be of exceptional value to control cell orientation and migration in engineering tissues in which the native ECM has highly aligned fibres such as tendons, ligaments, cornea, smooth muscle and blood vessels. Sundararaghavan et al., has reported that human umbilical vein endothelial cells, grown on aligned-fibre scaffolds with a chemical gradient of vascular endothelial growth factor (VEGF), migrated along the orientation of the fibres irrespective of the chemical gradient. Importantly, this observation

suggested that topographical cues may be more influential than chemical cues in directing cell motility (Sundararaghavan et al., 2012).

In this study, HPDLFs attached to both random and aligned PLLA scaffolds within 24 h (SEM images- Figure 5-11). These results showed that the PLLA scaffolds were biocompatible and encouraged the early attachment of HPDLFs. Generally, apart from day 20, no differences were observed in the cellular activity or DNA content of random or aligned-fibre constructs. Similar results were observed with HPDLFs cultured on the decell-skin and decell-ligament. Therefore, there was no significant difference in the rate of HPDLFs proliferation on random or aligned-fibre scaffolds. These results are in contrast to those of Shang and colleagues who reported increased cellular activity and proliferation of RPDLFs seeded on aligned PLGA scaffolds cultured for 7 days (Shang et al., 2010). Also, Heath et al., reported a similar observation as Shang et al., with human umbilical vein endothelial cells grown on aligned methacrylic terpolymer scaffolds for 7 days (Heath et al., 2010). Studies by other researchers have shown varied results with regard to cellular proliferation of cells in aligned-fibre constructs. Ma et al., has reported that fibre-alignment had no effect on the cell proliferation of BMSCs seeded on aligned PLLA scaffolds cultured for 21 days (Ma et al., 2011). Also, it has been shown that human osteoblast-like cells seeded on aligned scaffolds for 14 days showed comparable cell numbers to those on random scaffolds (Tong et al., 2010). The discrepancy between the data from the different groups is most likely due to the

difference in cell-types used in the study but could also be the polymer used or the experimental setting.

At day 20, a sharp drop in the DNA content was observed in the random-fibre constructs. The low cell number in the random-fibre constructs in comparison with HPDLFs in aligned-fibre constructs may possibly suggest a selective survival of differentiated cells at longer culture times. The up-regulation of COL1A1, POSTN and SCXA genes at day 7 in aligned-fibres suggested early differentiation of the PDLFs on aligned-fibre scaffolds along a ligament fibroblast phenotype.

No significant difference was initially observed in the levels of cellular activity or proliferation of HPDLFs seeded on either random or aligned-fibre PLLA scaffolds. However, the cellular activity reduced significantly over culture time in aligned-fibre constructs, which suggested differentiation of the HPDLFs. This was also supported by the higher total protein content found in aligned-fibre constructs over the culture period compared that in random-fibre constructs. Contradicting results between data presented here and data published by Shang et al. could be due to the difference in the polymer used to fabricate the scaffold, the cell source and culture time.

In this study, HPDLFs in both random and aligned-fibre constructs expressed three ligament related markers, COL1A1, POSTN and SCXA, with a higher expression found in aligned-fibre constructs. RUNX2, is a transcription factor involved in osteoblastic differentiation, and its expression was maintained in the aligned-fibre constructs. Generally, ALPL expression

was low in both random and aligned-fibre constructs and no osteocalcin, a late marker of osteoblast differentiation, was detected in either. The higher expression of ligament markers, COLA1A1, POSTN and SCXA, along with the low expression of ALPL and the sustained expression of RUNX2 suggests that HPDLFs in aligned-fibre constructs retained their ligament fibroblastic character with osteogenic potential.

RUNX2 has been reported to be expressed in preosteoblasts and immature osteoblasts but its expression was down-regulated in late, mature osteoblasts (Komori, 2005, Komori, 2010). Even though RUNX2 expression was detected in the PDL, calcification does not occur in periodontium which is suggestive of the existence of a mechanism that inhibits the action of RUNX2 (Saito et al., 2002).

A sharp down-regulation of COL1A1, POSTN and ALPL was observed when HPDLFs were transferred from 2D monolayer culture to the 3D PLLA/decellularised scaffolds (Figure 5-25, Figure 5-26). This suggested that HPDLFs in monolayer culture behaved more like osteoblasts. Substrate stiffness has been shown to strongly affect cell behaviours such as migration, proliferation and differentiation in both osteogenic and non-osteogenic cells (Hsiong et al., 2008, Mullen et al., 2013). It has been shown that MSC differentiation along different phenotypic lineages for example, adipogenic, myogenic and osteogenic is influenced in part by substrate stiffness (Engler et al., 2006).

At the protein deposition level, aligned-fibre constructs immunostained for collagen type I and periostin showed denser staining for these matrix proteins, suggesting greater, protein deposition (Figure 5-22, Figure 5-23). It has been shown that fibre-alignment can modulate cell phenotype and differentiation. Aligned-fibre scaffolds have been reported to enhance the maturation of Schwann cells and support their spreading and cell-alignment (Daud et al., 2012, Chew et al., 2008). Also, aligned scaffolds have shown to increase the expression of tenogenic markers in MSCs as well as the production of tendon/ligament related proteins (Teh et al., 2013). Xie et al., has reported that collagen type I was produced in comparable amounts in both random and aligned PLGA scaffolds seeded with tendon fibroblasts, however collagen type I was more organised along the direction of the fibre alignment in aligned-fibre constructs (Xie et al., 2010). Human tendon stem cells seeded on PLLA and transplanted *in vivo* showed denser ECM in aligned-fibre constructs and the collagen fibres were organised in parallel alignment with the fibres (Yin et al., 2010).

Aligned-fibre constructs cultured in osteogenic medium for 40 days showed denser Alizarin Red S staining than random-fibre constructs, indicative of ossifying nodule formation. These results suggested that fibre-alignment enhanced the osteogenic differentiation of HPDLFs when the constructs were cultured under osteogenic condition. This is in agreement with a previous study by Ma et al. who reported increased mineralisation, in terms of a higher calcium content, in aligned-fibre PLLA scaffolds seeded with

bone marrow stromal cells cultured for up to 21 days in osteogenic condition (Ma et al., 2011).

The mechanism by which cell elongation along fibres can influence intracellular pathways of PDLFs is not known. Generally, elongation of cells is associated with nuclear elongation which has been correlated to cell differentiation. Elongated cellular morphology, as a result of substrate topography, can induce changes in Wnt/β-catenin signalling and consequently cell differentiation by influencing the β-catenin availability (Chew et al., 2008). It has been reported that β-catenin signalling can regulate stem cell pluripotency and is involved in mesenchymal tissue development, including tooth formation (Scheller et al., 2008, Nemoto et al., 2009). β-catenin acts as a structural component of the cell cytoskeleton and as a mediator of canonical Wnt signalling which is involved in embryonic development and controls homeostatic self-renewal and differentiation in adult cells (Zechner et al., 2003). Nuclear elongation was observed in mesenchymal stem cells (MSCs) cultured on substrates with a nanotopographically modified surface. These MSCs showed increased cell contractility and up-regulated Wnt gene expression which in turn, leads to promotion of the differentiation of MSCs to distinct cell-lineages (Kilian et al., 2010).

It has been reported that β-catenin enhanced the expression of collagen type I in dental pulp stem cells (DPSCs) and inhibited alkaline phosphatase activity. Hence, β-catenin regulated the odontoblast-like differentiation of DPSCs under specific culture conditions (Scheller et al., 2008). Activation of

endogenous Wnt signalling has been reported to induce increased β-catenin, activity leading to suppression of alkaline phosphatase activity and the expression of cementum-like cell markers such as BGLAP and RUNX2 (Nemoto et al., 2009). This data suggested that canonical Wnt signalling can also control the differentiation of cementoblasts. Periodontal ligament fibroblasts cultured in osteogenic medium in the presence of lithium chloride (LiCl), an activator of the Wnt/β-catenin signalling pathway, showed up-regulation of ALPL gene expression in a dose dependent manner. It was concluded from these experiments that activation of Wnt/β-catenin signalling pathway enhanced the differentiation of PDLFs into an osteogenic lineage when stimulated with osteogenic medium (Nemoto et al., 2009). Although the exact mechanism through which fibre-alignment influenced HPDLF morphology and differentiation is not fully understood, the effect of fibre-alignment on PDLF phenotype through influencing the Wnt/β-catenin signalling pathway could possibly explain the effect of fibre-alignment in promoting PDLF differentiation towards a more ligament phenotype of a more osteoblastic phenotype depending on which other differntiation signals are also presented.

In conclusion, we have demonstrated that fibre-alignment, of synthetic polymer PLLA or as decelullarised native aligned tissue, had a significant impact on HPDLF morphology, gene expression and consequently phenotype. HPDLFs regained a more ligament-like phenotype when cultured in 3D environment, and this was enhanced by culture on aligned-fibre scaffolds.

6.3 Effect of Mechanical Strain and Fibre-alignment on Gene Expression

In vivo, the periodontal ligament is continuously subjected to forces from mastication which play an essential role in maintaining the homeostasis and reparative processes in periodontal tissue. Appropriate biomechanical cues are essential for ECM organisation and alignment especially when engineering load-bearing tissues such as periodontal ligaments and tendon (Jones et al., 2013, Scott et al., 2011). Therefore, mechanical loading is fundamental in developing tissue engineered periodontal ligaments to mimic the biomechanical properties of native periodontal ligaments.

In this study, we have used custom made loading chambers to apply static strain on the *in vitro* tissue engineered periodontal ligament constructs. These loading chambers have been successfully used to load tendon fascicles dissected from the bovine tendons to evaluate the effect of either static or cyclic loading on tenocytes (Legerlotz et al., 2011, Legerlotz et al., 2013).

In this study, PLLA-based tissue engineered periodontal ligaments were subjected to static loading for 3 h using the custom made loading chambers. The qRT-PCR results of gene expression showed that static loading for 3 h had an effect on the gene expression of COL1A1, POSTN, SCXA, ALPL, RUNX2, IL6 and BGLAP. There have been relatively few studies investigating the effect of mechanical loading on PDLFs in 3D system. Most of the data was obtained on monolayer cultures with only several studies

using encapsulation in collagen gels. The results from these studies have shown that mechanical loading can influence PDLF proliferation, differentiation, gene expression, and protein synthesis. However, the effects were variable depending on the experimental conditions and level of mechanical loading (listed in Table 2-5) (Jacobs et al., 2013, Liao et al., 2008, Liu et al., 2012, Tulloch et al., 2011).

In this study, higher expression of the ligamentous markers, COL1A1, POSTN and SCXA, was observed in strained random and aligned-fibre constructs compared to control, non-strained constructs (Figure 5-25). These results suggest that the application of a short period of strain stimulated a more ligament phenotype. The enhanced expression of COL1A1 is also indicative of enhanced ECM, although this would have to be confirmed by quantitative determination of collagen type I in the ECM. Generally a higher gene expression was observed in the aligned-fibre constructs, indicating that HPDLFs cultured in aligned-fibre scaffolds showed a greater enhanced in their ligament phenotype in reponse to mechanical loading. Also, these results suggested that mechanical loading may be an important factor in stimulating ECM production by HPDLF constructs.

The expression of the ligamentous markers was perceived at low strain level (9%) in aligned-fibre constructs and continued to be expressed at 14% and 20% strain. However, only when random-fibre constructs strained at 14% was the expression of COL1A1, POSTN and SCXA appear to be modulated by the loading. These results suggested that HPDLFs cultured in

the aligned-fibre scaffolds were more responsive to strain. Therefore, the aligned-fibre constructs may have been more sensitive to mechanical loading or the aligned nature of the scaffolds may be more efficient in transmitting the strain forces to the cells. Aligned-fibres are reported to be stiffer during tensile loading therefore, fibres oriented along the loading direction experienced the stretching force more than random fibres (Baji et al., 2010).

Alkaline phosphatase plays an essential role in the mineralisation of hard tissue. ALPL gene expression was barely detectable in non-strained control constructs regardless of the orientation of the scaffold fibres. However, ALPL expression was significantly up-regulated in random-fibre constructs subjected to 9% and 20% strain indicating that in random-fibre constructs, the HPDLFs responded to mechanical loading by attaining a more osteogenic phenotype.

In contrast, ALPL gene expression in aligned-fibre constructs was not affected by any of the strain levels applied. RUNX2 was significantly up-regulated only at the highest strain (20%) in aligned-fibre constructs. No BGLAP expression was detected in the HPDLFs cultured in both random and aligned-fibre PLLA scaffolds and neither was the gene expression influenced by application of strain at all levels tested. Hence, the HPDLFs did not express osteocalcin, a protein indicative of a mature osteoblast phenotype. The expression patterns of ALPL, RUNX2 and BGLAP in HPDLFs cultured in aligned-fibre scaffolds suggested that HPDLFs in aligned-fibre constructs and strained at “low or medium” strain maintained

their ligamentous phenotype better than HPDLFs cultured in random-fibre scaffolds. However, the up-regulation of RUNX2 in the aligned-fibre constructs strained at 20% may suggest that HPDLFs cultured in aligned-fibre scaffolds and strained at the highest strain level may have had more osteoblast-like characteristics.

Most of the reported data on the effect of strain on PDLFs showed up-regulation of COL1A1 gene expression. Liu et al., reported an increased COL1A1 gene expression in PDLFs cultured in monolayer and strained at 12% cyclic strain for 24 h. Also, rat PDLFs seeded in collagen gels and strained at 8% showed up-regulation of COL1A1 and sialoprotein and down-regulation of RUNX2 (Oortgiesen et al., 2012). Three dimensional scaffolds seeded with patella tendon fibroblasts and subjected to tensile strain, rotational strain or a combination of both, showed that COL1A1 was expressed at a high level in all loaded groups (Sawaguchi et al., 2010). On the other hand, 5% and 10% static strain for 12 h did not affect COL1A1 expression in PDLFs cultured in monolayer (Jacobe et al. 2013). Despite whether cells were subjected to either cyclic or static loading, the discrepancies between the results could be due to the heterogeneous nature of PDLFs or the difference in loading regimen (Jacobs et al., 2013, Liu et al., 2012). This suggested that PDLFs can perceive different types of mechanical loading and respond in a different way based on the nature and duration of the type of loading used. Rios and colleagues previously reported that periostin gene expression was increased by mechanical strain in murine PDL fibroblasts through a TGF-β1-dependent mechanism (Rios et

al., 2008). They concluded that mechanical strain likely activated latent TGF-β1, which in turn stimulated periostin expression.

Interestingly, the expression of COL1A1, POSTN, SCXA, ALPL, RUNX2 and IL6 in strained decell-skin and decell-ligament constructs was different from their expression in strained PLLA-fibre constructs. The difference in the expression of these genes in both scaffolds may be due to the difference in their mechanical properties.

There are few studies addressing mechanical loading of periodontal fibroblast *in vitro*. Most of the reported studies had utilised monolayer cultures or short term cultures of PDLFs embedded in collagen gels rather than 3D tissue engineered periodontal ligaments (Jacobs et al., 2013, Oortgiesen et al., 2012). The commercial Flexcell® loading system is one of the most commonly used loading systems to apply mechanical strain on PDLFs either in monolayer or in 3D collagen gels. Therefore, HPDLFs encapsulated in collagen type I gels were used in this study to compare the loading chambers with the Flexcell® loading system.

Strained HPDLFs in the 3D cell-gel constructs showed up-regulation of the ligamentous markers, COL1A1, POSTN and SCXA, compared to the control, non-strained constructs. This up-regulation was significantly increased with increasing time of strain application (Figure 5-28). The expression of the early osteoblast marker, ALPL, was highly up-regulated only at 24 h strain and sharply down-regulated to the control level by 48 h. RUNX2 was up-regulated compared to control constructs, however its

expression was not affected by time. These data supported the gene expression data shown in PLLA constructs strained using loading chambers. HPDLFs encapsulated in collagen gels, as those in PLLA constructs, maintained their ligamentous fibroblastic phenotype under mechanical strain.

6.4 Effect of EMD and/or TGF-β1 and Fibre-alignment on Gene Expression

While the effects of growth factors on PDLFs *in vitro* 2D monolayer system are well established, little is known about their effect on the *in vitro* 3D tissue engineered periodontal ligament constructs in longer culture periods. The data presented in this study identified the effect of EMD and/or TGF-β1 on HPDLFs seeded on random and aligned PLLA scaffolds. These results highlighted the advantage of using appropriate growth factors as chemical cues to facilitate cell-cell or cell-matrix interaction which could play an important role in developing 3D tissue engineered periodontal ligaments *in vitro*.

Data in this study showed that EMD and/or TGF-β1 have limited effect on HPDLF proliferation in aligned-fibre constructs at day 14. This has been observed in a previous study which showed that TGF-β1 did not affect the proliferation of a PDLF cell line (Fujii et al., 2010). In contrast, other data showed that TGF-β1 can promote the proliferation of PDLFs (Sant'Ana et al., 2007, Rodrigues et al., 2007, Fujii et al., 2010, Kono et al., 2013). However, these studies were carried out in a monolayer culture system and

for a short culture time of 3 to 7 days. The discrepancies observed between the data may suggest that the effect of TGF-β1 on cell growth is dependent on the differentiation stage of the cells. It is suggested that TGF-β1 may have a dual effect on PDLF proliferation, either inhibitory or stimulatory, depending on the stage of cell (Fujii et al., 2010). Conflicting data has been reported on the effect of EMD on PDLF proliferation; it has been observed in previous studies that EMD had no effect on PDLF proliferation (Chong et al., 2006, Amin et al., 2012, Tanimoto et al., 2012). Yet, Rodrigues et al., and Kémoun et al., showed that stimulating PDLFs with EMD application was associated with an increased cell number (Rodrigues et al., 2007, Kémoun et al., 2011). These inconsistent data may be due to the differences in the experimental setting, the cell differentiation stage and the nature and concentration of the EMD used.

The limited effect of both EMD and/or TGF-β1 on the proliferation of HPDLFs grown on aligned-fibre scaffolds could be related to the early differentiation of HPDLFs grown in aligned-fibre scaffolds compared to that in random-fibre constructs. This was indicated by the higher expression of the ligamentous fibroblastic markers such as COL1A1 and SCXA as early as day 7 in culture. This suggestion is further supported by the total protein data (Figure 5-31) which showed a higher protein content in the aligned-fibre constructs stimulated with EMD and/or TGF-β1 compared to the control and random-fibre constructs. This also suggests that the influence of EMD on HPDLF proliferation appeared to decrease with progress of cell differentiation/maturation.

Quantitative RT-PCR data of *in vitro* tissue engineered periodontal ligaments stimulated with EMD showed that EMD has the ability to promote the osteoblastic phenotype of HPDLFs as reflected by the up-regulation of ALPL and RUNX2. On the other hand, TGF-β1 stimulated tissue engineered periodontal ligaments showed up-regulation of COL1A1, POSTN and SCXA which suggested that TGF-β1 enhanced the ligamentous fibroblastic phenotype of HPDLFs.

Transforming growth factor-β1 is one of the most abundant cytokines in bone matrix and is a potent stimulator of tissue regeneration and a fibrogenic mediator (Shi and Massague 2003). Data presented in this study is in consistence with previous studies which reported that TGF-β1 contributed to PDLF fibroblastic differentiation by up-regulating actin alpha 2 (ACTA2), COL1A1, FBN1 and α-SMA (Fujii et al., 2010, Kono et al., 2013).

EMD has been reported to up-regulate gene expression of osteoblast differentiation markers including ALPL, OPN, RUNX2 and BGLAP in PDLF monolayers *in vitro* (Kémoun et al., 2011, Amin et al., 2012). In contrast, Okubo et al. showed that EMD might not have substantial effect on osteoblastic differentiation of PDLFs. Tanimoto et al., reported that EMD has no effect on ALPL, BGLAP and OPN mRNA level. However, they used an immortalised PDLF cell line which may have affected the osteoblastic potential of the cells as a result of the immortalisation process (Tanimoto et al., 2012). The differences in the available data may be due to the fact that PDLFs are heterogeneous and their phenotype and differentiation greatly depend on the method used for isolation, expansion and culturing.

In this study, it was observed that the up-regulation of genes COL1A1, POSTN, SCXA and ALPL was higher in the HPDLFs grown in the aligned-fibre scaffolds. This suggested that fibre-alignment, as contact guidance and topographical cues, can enhance HPDLF differentiation ability; either as fibroblasts when stimulated with TGF-β1 or osteoblast-like cells when stimulated with EMD. Also, the data suggest that fibre-alignment could potentiate the effect of EMD or TGF-β1. Interestingly, It has been reported that fibre-induced cell alignment can effectively activate canonical Wnt signalling in adult MSCs, and further enhance the differentiation induced by biochemical cues (Lim et al., 2010).

Under selective lineage-specific culture conditions, EMD has the ability to significantly up-regulate osteogenic, chondrogenic and neovasculogenic genes and modulate the multi-lineage differentiation of HPDLFs *in vitro* (Amin et al., 2012). These data suggest that the EMD action is greatly affected by the differentiation status of the cells. It has been reported previously that combining both factors, EMD and TGF-β1, showed that the influence of EMD was greater than TGF-β1, as demonstrated by the results following the same trend as EMD (Rodrigues et al., 2007). Yet in this study the effect of TGF-β1 was more prominent when combining both EMD and TGF-β1. EMD has been reported to stimulate the expression of endogenous TGF-β1 at both protein and mRNA level (Okubo et al., 2003). This might boost the effect of TGF-β1 when combined with EMD. Also it could be that, compared to cells on monolayer culture plates, HPDLFs in aligned-fibre constructs with the presence of TGF-β1 have greater affinity to be

differentiated to a ligament fibroblast phenotype and therefore, the effect of EMD would be limited. It has been reported that EMD has greater effect on PDLFs cultured in osteogenic medium compared to cells in basic culture medium (Amin et al., 2012). Although the exact mechanism by which EMD and/or TGF-β1 affects the cell behaviour is unknown, the data suggest that their effects are enormously dependent on the cell differentiation and phenotype.

7. CONCLUSIONS

In conclusion, this research has made a substantial contribution to the scientific knowledge of the tissue engineered periodontal ligament and the conditions that promote a desired cell phenotype. This section is a summary of the major findings and the conclusions drawn from experiments described in Chapters 3 and 4 directed at the study of 3D periodontal ligament constructs, and in particular the effects of fibre-alignment, applying mechanical strain and adding growth factors. This research conclude:

- Electrospinning was an effective method to fabricate highly aligned-fibre scaffolds of PLLA. Random-fibre scaffolds of PLLA were also electrospun successfully for use as reference material.
- Natural aligned collagen-fibre scaffolds were produced by decellularisation of bovine ligament. Decellularised bovine skin was used as a natural random collagen-fibre scaffold. The decellularisation process removed 98% of the cellular DNA content but preserved the collagen topography in both skin and ligament, and supported the growth of PDLFs throughout the study.
- Several cells sources were evaluated for use in the preparation of a tissue engineered model periodontal ligament. Rat PDLFs were effective, but these were not considered ideal because of limited supply. Porcine PDLFs were difficult to obtain, and in particular it was difficult to dissect out viable tissue. It was concluded that the

human PDLFs from pooled periodontal tissues were best suited to the tissue engineering experiments in this study.

- Tissue engineered periodontal ligament constructs were therefore prepared *in vitro* using human PDLFs. This new tissue construct has potential for use as a 3D model system to study periodontal ligament repair and regeneration, and in the long term, it may itself form the basis for a regenerative therapy.
- Aligned-fibre scaffolds, as a synthetic substrate for HPDLF differentiation, were superior to random scaffolds of the same biomaterial in that they more effectively induced cell alignment and provided strong topographical cues that appeared to enhance HPDLF differentiation towards the ligament fibroblast phenotype. Specific markers were detected including collagen type I, POSTN, SCXA and ALPL and histologically there were better morphological features (greater collagen type I and periostin deposition) which were in common with the native tissue.
- HPDLFs further enhanced their fibroblastic phenotype in constructs subjected to a short period of mechanical strain. Aligned-fibre constructs were more responsive to mechanical strain than random-fibre constructs. This was the first demonstration of the effect of strain on tissue engineered periodontal ligament constructs in a carefully designed study.
- EMD promoted the differentiation of HPDLF constructs towards an osteoblastic phenotype, whereas TGF-β1 promoted a more ligamentous fibroblastic phenotype. These effects of EMD and

TGF-β1 were greater in HPDLF aligned-fibre constructs. The results obtained with EMD and TGF-β1 highlighted the potential role of growth factors in periodontal tissue engineering.

A unique approach was taken to mechanically strain the tissue engineered ligament constructs by applying uniaxial strains was also described. The effect of this mechanical loading on PDLF gene expression was then investigated. In addition, the effect of fibre-alignment on gene expression of HPDLFs in response to mechanical loading was also investigated. Fibre-alignment, controlled mechanical loading, and specific growth factors were all demonstrated to elicit a positive effect on the biological quality and maturity of tissue engineered periodontal ligament. To the best of my knowledge, this is the first detailed study to report on the effect of fibre-alignment on the response of tissue engineered ligament constructs to growth factors and mechanical loading. These 3D aligned-fibre constructs have great potential for use as a model system in which to study PDL biology and regeneration mechanisms, and in time this work will underpin new strategies for the development of new therapies for periodontal ligament regeneration.

8. FUTURE WORK

Based on the results obtained and the challenges encountered throughout this project, the following are suggested to be carried out in the future:

- Further optimising the electrospinning process to fabricate aligned fibres of different materials such as PLGA, polycaprolactone, collagen, etc and study their mechanical properties to optimise the stiffness and strength of the scaffolds.
- Decellularised bovine skin and ligaments were used in this study as native counterparts of the PLLA random and aligned-fibre scaffolds. However, further investigation of the decellularised matrix as scaffolds in periodontal tissue engineering could be of great value.
- The *in vivo* characteristics of these tissue engineered ligament constructs could be investigated in animal models to assess their potential for a tissue engineering therapy.
- Aligned PLLA membranes could be functionalised to carry and release growth factors such as EMD, TGF-β1 or BMPs.
- Fabrication of a multilayered membrane, consisting of aligned-fibre at the inner side resembling periodontal ligament and random-fibre at the outer surface resembling bone, to develop an *in vitro* model for the entire periodontium.

- Study the use of multiple growth factors such as EMD, TGF-β1, bFGF or BMPs with variable dose and culture time for optimising PDLF differentiation pathway and facilitate cell-matrix interaction to further improve the development of tissue engineered periodontal ligaments *in vitro*.
- We have addressed the effect of static strain for only 3 h; therefore it is relevant to investigate the effect of cyclic mechanical strain for variable loading times. Also, further studying the effect of mechanical loading on the production of endogenous TGF-β1 should be undertaken.
- Study the effect of simultaneous application of mechanical loading and EMD and/or TGF-β1 to investigate whether it enhances the functional efficacy of the 3D tissue engineered periodontal ligament constructs developed in this project.

9. REFERENCES

ADAMS, A. M., SOAMES, J. V. & SEARLE, R. F. 1993. Cultural and morphological characteristics of human periodontal ligament cells *in vitro*. *Archives of Oral Biology*, 38, 657-662.

ALVAREZ-PÉREZ, M., NARAYANAN, S., ZEICHNER-DAVID, M., RODRÍGUEZ, C. & ARZATE, H. 2006. Molecular cloning, expression and immunolocalization of a novel human cementum-derived protein (CP-23). *Bone*, 38, 409-419.

AMIN, H., OLSEN, I., KNOWLES, J., DARD, M. & DONOS, N. 2012. Effects of enamel matrix proteins on multi-lineage differentiation of periodontal ligament cells *in vitro. Acta Biomaterialia*, 9, 4796-4805.

ANZAI, J., KITAMURA, M., NOZAKI, T., NAGAYASU, T., TERASHIMA, A., ASANO, T. & MURAKAMI, S. 2010. Effects of concomitant use of fibroblast growth factor (FGF)-2 with beta-tricalcium phosphate ([beta]-TCP) on the beagle dog 1-wall periodontal defect model. *Biochemical and Biophysical Research Communications*, 403, 345-350.

ARCEO, N., SAUK, J. J., MOEHRING, J., FOSTER, R. A. & SOMERMAN, M. J. 1991. Human periodontal cells initiate mineral-like nodules *in vitro*. *Journal of Periodontology*, 62, 499-503.

ARMITAGE, G. 2004. Periodontal diagnoses and classification of periodontal diseases. *Periodontology 2000*, 34, 9-21.

ARMITAGE, G. C. 1999. Development of a classification system for periodontal diseases and conditions. *Annals of periodontology/ the American Academy of Periodontology*, 4, 1-6.

AUBIN, H., KRANZ, A., HÜLSMANN, J., LICHTENBERG, A. & AKHYARI, P. 2013. decellularized whole heart for bioartificial heart. *Cellular Cardiomyoplasty*, 2, 163-178.

AVISS, K., GOUGH, J. & DOWNES, S. 2010. Aligned electrospun polymer fibres for skeletal muscle regeneration. *European Cells and Materials*, 19, 193-204.

AYRES, C. E., JHA, B. S., MEREDITH, H., BOWMAN, J. R., BOWLIN, G. L., HENDERSON, S. C. & SIMPSON, D. G. 2008. Measuring fiber alignment in electrospun scaffolds: a user's guide to the 2D fast Fourier transform approach. *Journal of Biomaterials Science, Polymer Edition*, 19, 603-621.

AYUB, L. G., RAMOS, U. D., REINO, D. M., GRISI, M. F., TABA, M., SOUZA, S. L., PALIOTO, D. B. & NOVAES, A. B. 2012. A Randomized comparative clinical study of two surgical procedures to improve root coverage with the acellular dermal matrix graft. *Journal of Clinical Periodontology*, 39, 871-878.

BAJI, A., MAI, Y.-W., WONG, S.-C., ABTAHI, M. & CHEN, P. 2010. Electrospinning of polymer nanofibers: Effects on oriented morphology, structures and tensile properties. *Composites Science and Technology*, 70, 703-718.

BARTOLD, P. M., WALSH, L. J. & NARAYANAN, A. S. 2000. Molecular and cell biology of the gingiva. *Periodontology 2000*, 24, 28-55.

BECKER, J., SCHUPPAN, D., RABANUS, J. P., RAUCH, R., NIECHOY, U. & GELDERBLOM, H. R. 1991. Immunoelectron microscopic localization of collagens type I, V, VI and of procollagen type III in human periodontal ligament and cementum. *Journal of Histochemistry and Cytochemistry*, 39, 103-110.

BELLOWS, C. G., MELCHER, A. H. & AUBIN, J. E. 1981. Contraction and organization of collagen gels by cells cultured from periodontal ligament, gingiva and bone suggest functional differences between cell types. *Journal of Cell Science*, 50, 299-314.

BERENDSEN, A. D., SMIT, T. H., WALBOOMERS, X. F., EVERTS, V., JANSEN, J. A. & BRONCKERS, A. L. 2009. Three-dimensional loading model for periodontal ligament regeneration *in vitro*. *Tissue Engineering Part C: Methods*, 15, 561-570.

BOOTH, C., KOROSSIS, S., WILCOX, H., WATTERSON, K., KEARNEY, J., FISHER, J. & INGHAM, E. 2002. Tissue engineering of cardiac valve prostheses I: development and histological characterization of an acellular porcine scaffold. *The Journal of Heart Valve Disease*, 11, 457-462.

BOSKEY, A. L. 1996. Matrix proteins and mineralization: An overview. *Connective Tissue Research*, 35, 357-363.

BOSSHARDT, D. D. & NANCI, A. 2004. Hertwig's epithelial root sheath, enamel matrix proteins, and initiation of cementogenesis in porcine teeth. *Journal of Clinical Periodontology*, 31, 184-192.

BOSSHARDT, D., ZALZAL, S., MCKEE, M. & NANCI, A. 1998. Developmental appearance and distribution of bone sialoprotein and osteopontin in human and rat cementum. *The Anatomical Record Part A: Discoveries in Molecular, Cellular, and Evolutionary Biology*, 250, 13-33.

BROOKS, D. N., WEBER, R. V., CHAO, J. D., RINKER, B. D., ZOLDOS, J., ROBICHAUX, M. R., RUGGERI, S. B., ANDERSON, K. A., BONATZ, E. E. & WISOTSKY, S. M. 2012. Processed nerve allografts for peripheral nerve reconstruction: A multicenter study of utilization and outcomes in sensory, mixed, and motor nerve reconstructions. *Microsurgery*, 32, 1-14.

CARNIO, J. & FUGANTI, M. 2013. Clinical long-term evaluation of acellular dermal matrix in the treatment of root recession: case report. *General Dentistry*, 61(1), 42-45.

CARTMELL, J. S. & DUNN, M. G. 2004. Development of cell-seeded patellar tendon allografts for anterior cruciate ligament reconstruction. *Tissue Engineering*, 10, 1065-1075.

CATON, J. G. & GREENSTEIN, G. 1993. Factors related to periodontal regeneration. *Periodontology 2000*, 1, 9-15.

CHAE, H. S., PARK, H.-J., HWANG, H. R., KWON, A., LIM, W.-H., YI, W. J., HAN, D.-H., KIM, Y. H. & BAEK, J.-H. 2011. The effect of antioxidants on the production of pro-inflammatory cytokines and orthodontic tooth movement. *Molecules and Cells*, 32, 189-196.

CHAREST, J., BRYANT, L., GARCIA, A. & KING, W. 2004. Hot embossing for micropatterned cell substrates. *Biomaterials*, 25, 4767-4775.

CHAVARRY, N. 2009. The relationship between diabetes mellitus and destructive periodontal disease: a meta-analysis. *Oral Health and Preventive Dentistry*, 7, 107-27.

CHEN, F., SHELTON, R., JIN, Y. & CHAPPLE, I. 2009. Localized delivery of growth factors for periodontal tissue regeneration: role, strategies, and perspectives. *Medicinal Research Reviews,* 29, 472-513.

CHEN, F., ZHAO, Y., ZHANG, R., JIN, T., SUN, H., WU, Z. & JIN, Y. 2007. Periodontal regeneration using novel glycidyl methacrylated dextran (Dex-GMA)/gelatin scaffolds containing microspheres loaded with bone morphogenetic proteins. *Journal of Controlled Release*, 121, 81-90.

CHEW, S., MI, R., HOKE, A. & LEONG, K. 2007. Aligned protein-polymer composite fibers enhance nerve regeneration: a potential tissue-engineering platform. *Advanced Functional Materials*, 17, 1288-1296.

CHEW, S., MI, R., HOKE, A. & LEONG, K. 2008. The effect of the alignment of electrospun fibrous scaffolds on Schwann cell maturation. *Biomaterials*, 29, 653-661.

CHO, M. I., MATSUDA, N., LIN, W. L., MOSHIER, A. & RAMAKRISHNAN, P. R. 1992. *In vitro* formation of mineralized nodules by periodontal ligament cells from the rat. *Calcified Tissue International*, 50, 459-467.

CHOI, J., LEE, S., CHRIST, G., ATALA, A. & YOO, J. 2008. The influence of electrospun aligned poly (-caprolactone)/collagen nanofiber meshes on the formation of self-aligned skeletal muscle myotubes. *Biomaterials*, 29, 2899-2906.

CHONG, C. H., CARNES, D. L., MORITZ, A. J., OATES, T., RYU, O. H., SIMMER, J. & COCHRAN, D. L. 2006. Human periodontal fibroblast response to enamel matrix derivative, amelogenin, and platelet-derived growth factor-BB. *Journal of Periodontology*, 77, 1242-1252.

CIONCA, N., GIANNOPOULOU, C., UGOLOTTI, G. & MOMBELLI, A. 2010. Microbiologic Testing and Outcomes of Full-Mouth Scaling and Root Planing With or Without Amoxicillin/Metronidazole in Chronic Periodontitis. *Journal of Periodontology*, 81, 15-23.

COOKE, J., SARMENT, D., WHITESMAN, L., MILLER, S., JIN, Q., LYNCH, S. & GIANNOBILE, W. 2006. Effect of rhPDGF-BB delivery on mediators of periodontal wound repair. *Tissue Engineering*, 12, 1441-1450.

CORTELLINI, P. & TONETTI, M. S. 2007. A minimally invasive surgical technique with an enamel matrix derivative in the regenerative treatment of intra-bony defects: a novel approach to limit morbidity. *Journal of Clinical Periodontology*, 34, 87-93.

CRAPO, P. M., GILBERT, T. W. & BADYLAK, S. F. 2011. An overview of tissue and whole organ decellularization processes. *Biomaterials*, 32, 3233-3243.

CURTIS, A. S. G. & VARDE, M. 1964. Control of cell behavior-topological factors. *Journal of the National Cancer Institute*, 33, 15-26.

CURTIS, A., DALBY, M. & GADEGAARD, N. 2006. Cell signaling arising from nanotopography: implications for nanomedical devices. *Nanomedicine*, 1, 67-72.

DAI, L., QIN, Z., DEFEE, M., TOOLE, B. P., KIRKWOOD, K. L. & PARSONS, C. 2012. Kaposi sarcoma-associated herpesvirus (KSHV) induces a functional tumor-associated phenotype for oral fibroblasts. *Cancer Letters*, 318, 214-220.

DAUD, M. F., PAWAR, K. C., CLAEYSSENS, F., RYAN, A. J. & HAYCOCK, J. W. 2012. An aligned 3D neuronal-glial co-culture model for peripheral nerve studies. *Biomaterials*, 33, 5901-5913.

DIJKMAN, P. E., DRIESSEN-MOL, A., FRESE, L., HOERSTRUP, S. P. & BAAIJENS, F. 2012. Decellularized homologous tissue-engineered heart valves as off-the-shelf alternatives to xeno-and homografts. *Biomaterials*, 33, 4545-4554.

ENGLER, A. J., SEN, S., SWEENEY, H. L. & DISCHER, D. E. 2006. Matrix elasticity directs stem cell lineage specification. *Cell*, 126, 677-689.

ESPOSITO, M., GRUSOVIN, M., PAPANIKOLAOU, N., COULTHARD, P. & WORTHINGTON, H. 2010. Enamel matrix derivative (Emdogain®) for periodontal tissue regeneration in intrabony defects. *Australian Dental Journal*, 55, 101-104.

FANG, T., LINEAWEAVER, W. C., SAILES, F. C., KISNER, C. & ZHANG, F. 2013. Clinical Application of Cultured Epithelial Autografts on Acellular Dermal Matrices in the Treatment of Extended Burn Injuries. *Annals of Plastic Surgery*, 1-5.

FUJII, S., MAEDA, H., TOMOKIYO, A., MONNOUCHI, S., HORI, K., WADA, N. & AKAMINE, A. 2010. Effects of TGF-β1 on the proliferation and differentiation of human periodontal ligament cells and a human periodontal ligament stem/progenitor cell line. *Cell and Tissue Research*, 342, 233-242.

FUJITA, T., SHIBA, H., VAN DYKE, T. E. & KURIHARA, H. 2004. Differential effects of growth factors and cytokines on the synthesis of SPARC, DNA, fibronectin and alkaline phosphatase activity in human periodontal ligament cells. *Cell Biology International,* 28, 281-286.

GALLAGHER, J., MCGHEE, K., WILKINSON, C. & RIEHLE, M. 2003. Interaction of animal cells with ordered nanotopography. *NanoBioscience, IEEE Transactions on*, 1, 24-28.

GARVIN, J., QI, J., MALONEY, M. & BANES, A. J. 2003. Novel system for engineering bioartificial tendons and application of mechanical load. *Tissue Engineering*, 9, 967-979.

GAY, I., CHEN, S. & MACDOUGALL, M. 2007. Isolation and characterization of multipotent human periodontal ligament stem cells. *Orthodontics and Craniofacial Research*, 10, 149-160.

GHOSH, A., YUAN, W., MORI, Y. & VARGA, J. 2000. Smad-dependent stimulation of type I collagen gene expression in human skin fibroblasts by TGF-beta involves functional cooperation with p300/CBP transcriptional coactivators. *Oncogene*, 19, 3546-3555.

GIANNOBILE, W., HERNANDEZ, R., FINKELMAN, R., RYARR, S., KIRITSY, C., D'ANDREA, M. & LYNCH, S. 1996. Comparative effects of plateletderived growth factor BB and insulin like growth factor I, individually and in combination, on periodontal regeneration in Macaca fascicularis. *Journal of Periodontal Research*, 31, 301-312.

GIANNOPOULOU, C. & CIMASONI, G. 1996. Functional characteristics of gingival and periodontal ligament fibroblasts. Journal of Dental Research, 75, 895-902.

GILPIN, S., GUYETTE, J., REN, X., GONZALEZ, G., XIONG, L., SONG, J., VACANTI, J. & OTT, H. 2013. Up-Scaling Decellularization and Whole Organ Culture for Human Lung Regeneration. *The Journal of Heart and Lung Transplantation*, 32, 69-70.

GROENEVELD, M. C., EVERTS, V. & BEERTSEN, W. 1993. A quantitative enzyme histochemical analysis of the distribution of alkaline phosphatase activity in the periodontal ligament of the rat incisor*. Journal of Dental Research*, 72, 1344-1350.

GROENEVELD, M. C., EVERTS, V. & BEERTSEN, W. 1994. Formation of afibrillar acellular cementum-like layers induced by alkaline phosphatase activity from periodontal ligament explants maintained *in vitro*. Journal of Dental Research, 73, 1588-1592.

GUPTA, B., REVAGADE, N. & HILBORN, J. 2007. Poly (lactic acid) fiber: An overview. *Progress in Polymer Science*, 32, 455-482.

HAKKINEN, L., OKSALA, O., SALO, T., RAHEMTULLA, F. & LARJAVA, H. 1993. Immunohistochemical localization of proteoglycans in human periodontium. *Journal of Histochemistry and Cytochemistry*, 41, 1689-1699.

HAMILTON, D., OATES, C., HASANZADEH, A., MITTLER, S. & EGLES, C. 2010. Migration of periodontal ligament fibroblasts on nanometric topographical patterns: influence of filopodia and focal adhesions on contact guidance. *PloS one*, 5, 517-532..

HASEGAWA, M., YAMATO, M., KIKUCHI, A., OKANO, T. & ISHIKAWA, I. 2005. Human periodontal ligament cell sheets can regenerate periodontal ligament tissue in an athymic rat model. *Tissue Engineering*, 11, 469-478.

HASEGAWA, N., KAWAGUCHI, H., HIRACHI, A., TAKEDA, K., MIZUNO, N., NISHIMURA, M., KOIKE, C., TSUJI, K., IBA, H. & KATO, Y. 2006. Behavior of transplanted bone marrow-derived mesenchymal stem cells in periodontal defects. *Journal of Periodontology*, 77, 1003-1007.

HASSELL, T. M. 1993. Tissues and cells of the periodontium. Periodontology 2000, 3, 9-38.

HAYKAL, S., SOLEAS, J. P., SALNA, M., HOFER, S. O. & WADDELL, T. K. 2012. Evaluation of the structural integrity and extracellular matrix components of tracheal allografts following cyclical decellularization techniques: comparison of three protocols. *Tissue Engineering Part C: Methods*, 18, 614-623.

HE, Y., MACARAK, E. J., KOROSTOFF, J. M. & HOWARD, P. S. 2004. compression and tension: differential effects on matrix accumulation by periodontal ligament fibroblasts *in vitro*. *Connective Tissue Research*, 45, 28-39.

HEATH, D., LANNUTTI, J. & COOPER, S. 2010. Electrospun scaffold topography affects endothelial cell proliferation, metabolic activity, and morphology. *Journal of Biomedical Materials Research Part A*, 94, 1195-1204.

HOFFMAN-KIM, D., MITCHEL, J. & BELLAMKONDA, R. 2010. Topography, Cell response, and nerve regeneration. *Annual Review of Biomedical Engineering*, 12, 203-231.

HORIUCHI, K., AMIZUKA, N., TAKESHITA, S., TAKAMATSU, H., KATSUURA, M., OZAWA, H., TOYAMA, Y., BONEWALD, L. F. & KUDO, A. 1999. Identification and characterization of a novel protein, periostin, with restricted expression to periosteum and periodontal ligament and increased expression by transforming growth factor. *Journal of Bone and Mineral Research*, 14, 1239-1249.

HSIONG, S. X., CARAMPIN, P., KONG, H. J., LEE, K. Y. & MOONEY, D. J. 2008. Differentiation stage alters matrix control of stem cells. *Journal of Biomedical Materials Research Part A*, 85, 145-156.

HUANG, C., CHEN, R., KE, Q., MORSI, Y., ZHANG, K. & MO, X. 2010. Electrospun collagen-chitosan-TPU nanofibrous scaffolds for tissue engineered tubular grafts. *Colloids and Surfaces B: Biointerfaces*, 82(2), 307-315.

HUANG, Y. H., OHSAKI, Y. & KURISU, K. 1991. Distribution of type I and type III collagen in the developing periodontal ligament of mice. Matrix, 11, 25-35.

IBRAHIM, A. M., AYENI, O. A., HUGHES, K. B., LEE, B. T., SLAVIN, S. A. & LIN, S. J. 2013. Acellular dermal matrices in breast surgery: A comprehensive review. *Annals of Plastic Surgery*, 70, 732-738.

INANC, B., ELCIN, A. E. & ELCIN, Y. M. 2006. Osteogenic induction of human periodontal ligament fibroblasts under two- and three-dimensional culture conditions. *Tissue Engineering*, 12, 257-266.

INANC, B., ELCIN, A. E. & ELCIN, Y. M. 2007. Effect of osteogenic induction on the *in vitro* differentiation of human embryonic stem cells cocultured with periodontal ligament fibroblasts. *Artificial Organs*, 31, 792-800.

INGRAM, J. H., KOROSSIS, S., HOWLING, G., FISHER, J. & INGHAM, E. 2007. The use of ultrasonication to aid recellularization of acellular natural tissue scaffolds for use in anterior cruciate ligament reconstruction. *Tissue Engineering*, 13, 1561-1572.

ITAYA, T., KAGAMI, H., OKADA, K., YAMAWAKI, A., NARITA, Y., INOUE, M., SUMITA, Y. & UEDA, M. 2009. Characteristic changes of periodontal ligament derived cells during passage. *Journal of Periodontal Research*, 44, 425-433.

IVANOVSKI, S., LI, H., HAASE, H. R. & BARTOLD, P. M. 2001. Expression of bone associated macromolecules by gingival and periodontal ligament fibroblasts. *Journal of Periodontal Research*, 36, 131-141.

JACOBS, C., GRIMM, S., ZIEBART, T., WALTER, C. & WEHRBEIN, H. 2013. Osteogenic differentiation of periodontal fibroblasts is dependent on the strength of mechanical strain. *Archives of Oral Biology*, 58, 896-901.

JAYAVEL, K., SWAMINATHAN, M. & KUMAR, S. 2011. Ridge augmentation and root coverage using acellular dermal matrix: a case report. *Dental Research Journal*, 7(2), 88-97.

JENSEN, T., ROSZELL, B., ZANG, F., GIRARD, E., MATSON, A., THRALL, R., JAWORSKI, D. M., HATTON, C., WEISS, D. J. & FINCK, C. 2012. A rapid lung de-cellularization protocol supports embryonic stem cell differentiation *in vitro* and following implantation. *Tissue Engineering Part C: Methods*, 18, 632-646.

JONES, E. R., JONES, G. C., LEGERLOTZ, K. & RILEY, G. P. 2013. Cyclical strain modulates metalloprotease and matrix gene expression in human tenocytes via activation of TGFβ. *Biochimica et Biophysica Acta (BBA)-Molecular Cell Research*, 1833(12), 2596-2607.

KANEDA, T., MIYAUCHI, M., TAKEKOSHI, T., KITAGAWA, S., KITAGAWA, M., SHIBA, H., KURIHARA, H. & TAKATA, T. 2006. Characteristics of periodontal ligament subpopulations obtained by sequential enzymatic digestion of rat molar periodontal ligament. *Bone*, 38, 420-426.

KANZAKI, H., CHIBA, M., SATO, A., MIYAGAWA, A., ARAI, K., NUKATSUKA, S. & MITANI, H. 2006. Cyclical tensile force on periodontal ligament cells inhibits osteoclastogenesis through OPG induction. *Journal of Dental Research*, 85, 457-462.

KANZAKI, H., CHIBA, M., SHIMIZU, Y. & MITANI, H. 2002. Periodontal ligament cells under mechanical stress induce osteoclastogenesis by receptor activator of

nuclear factor kB ligand up-regulation via prostaglandin E2 synthesis. *Journal of Bone and Mineral Research*, 17, 210-220.

KARIMBUX, N. Y., ROSENBLUM, N. D. & NISHIMURA, I. 1992. Site-specific expression of collagen I and XII mRNAs in the rat periodontal ligament at two developmental stages. *Journal of Dental Research*, 71, 1355-1362.

KARRING, T., NYMAN, S., GOTTLOW, J. & LAURELL, L. 1993. Development of the biological concept of guided tissue regeneration-animal and human studies. *Periodontology 2000*, 1, 26-35.

KASAJ, A., WILLERSHAUSEN, B., JUNKER, R., STRATUL, S.-I. & SCHMIDT, M. 2012. Human periodontal ligament fibroblasts stimulated by nanocrystalline hydroxyapatite paste or enamel matrix derivative. An *in vitro* assessment of PDL attachment, migration, and proliferation. *Clinical Oral Investigations*, 16, 745-754.

KATO, T., HATTORI, K., DEGUCHI, T., KATSUBE, Y., MATSUMOTO, T., OHGUSHI, H. & NUMABE, Y. 2011. Osteogenic potential of rat stromal cells derived from periodontal ligament. *Journal of Tissue Engineering and Regenerative Medicine*, 5, 798-805.

KÉMOUN, P., GRONTHOS, S., SNEAD, M., RUE, J., COURTOIS, B., VAYSSE, F., SALLES, J. & BRUNEL, G. 2011. The role of cell surface markers and enamel matrix derivatives on human periodontal ligament mesenchymal progenitor responses *in vitro*. *Biomaterials*, 32, 7375-7388.

KII, I., AMIZUKA, N., MINQI, L., KITAJIMA, S., SAGA, Y. & KUDO, A. 2006. Periostin is an extracellular matrix protein required for eruption of incisors in mice. *Biochemical and Biophysical Research Communications*, 342, 766-772.

KILIAN, K. A., BUGARIJA, B., LAHN, B. T. & MRKSICH, M. 2010. Geometric cues for directing the differentiation of mesenchymal stem cells. *Proceedings of the National Academy of Sciences*, 107, 4872-4877.

KILIAN, M., FRANDSEN, E., HAUBEK, D. & POULSEN, K. 2006. The etiology of periodontal disease revisited by population genetic analysis. *Periodontology 2000*, 42, 158-179.

KIM, T.-I., HAN, J.-E., JUNG, H.-M., OH, J.-H. & WOO, K. M. 2013. Analysis of histone deacetylase inhibitor-induced responses in human periodontal ligament fibroblasts. *Biotechnology Letters*, 35, 129-133.

KISSIN, E., LEMAIRE, R., KORN, J. & LAFYATIS, R. 2002. Transforming growth factor beta induces fibroblast fibrillin-1 matrix formation. *Arthritis and Rheumatism*, 46, 3000-3009.

KLEIN, M. B., YALAMANCHI, N., PHAM, H., LONGAKER, M. T. & CHAN, J. 2002. Flexor tendon healing *in vitro*: Effects of TGF-β on tendon cell collagen production. *Journal of Hand Surgery*, 27, 615-620.

KOMORI, T. 2005. Regulation of skeletal development by the Runx family of transcription factors. *Journal of Cellular Biochemistry*, 95, 445-453.

KOMORI, T. 2010. Regulation of osteoblast differentiation by RUNX2. *Osteoimmunology*, 658, 43-49.

KONO, K., MAEDA, H., FUJII, S., TOMOKIYO, A., YAMAMOTO, N., WADA, N., MONNOUCHI, S., TERAMATSU, Y., HAMANO, S. & KOORI, K. 2013. Exposure to transforming growth factor-β1 after basic fibroblast growth factor promotes the fibroblastic differentiation of human periodontal ligament stem/progenitor cell lines. *Cell and Tissue Research*, 34, 1-15.

KOOK, S.-H., JANG, Y.-S. & LEE, J.-C. 2011. Involvement of JNK-AP-1 and ERK-NF-κB signaling in tension-stimulated expression of Type I collagen and MMP-1 in human periodontal ligament fibroblasts. *Journal of Applied Physiology*, 111, 1575-1583.

KORNMAN, K. S. 2008. Mapping the pathogenesis of periodontitis: a new look. *Journal of Periodontology*, 79, 1560-1568.

KRAMER, P. R., NARES, S., KRAMER, S. F., GROGAN, D. & KAISER, M. 2004. Mesenchymal stem cells acquire characteristics of cells in the periodontal ligament *in vitro*. *Journal of Dental Research*, 83, 27-34.

KU, S.-J., CHANG, Y.-I., CHAE, C.-H., KIM, S.-G., PARK, Y.-W., JUNG, Y.-K. & CHOI, J.-Y. 2009. Static tensional forces increase osteogenic gene expression in three-dimensional periodontal ligament cell culture. *BMB Reports*, 42, 427-432.

KURU, L., PARKAR, M. H., GRIFFITHS, G. S., NEWMAN, H. N. & OLSEN, I. 1998. Flow cytometry analysis of gingival and periodontal ligament cells. *Journal of Dental Research,* 77, 555-564.

LEE, K., SILVA, E. & MOONEY, D. 2010. Growth factor delivery-based tissue engineering: general approaches and a review of recent developments. *Journal of the Royal Society Interface*, 8, 153-170

LEGERLOTZ, K., JONES, G., SCREEN, H. & RILEY, G. 2013. Cyclic loading of tendon fascicles using a novel fatigue loading system increases interleukin-6 expression by tenocytes. *Scandinavian Journal of Medicine and Science in Sports*, 23, 31-37.

LEKIC, P., SODEK, J. & MCCULLOCH, C. A. G. 1996. Relationship of cellular proliferation to expression of osteopontin and bone sialoprotein in regenerating rat periodontium. Cell and Tissue Research, 285, 491-500.

LI, W.-J., MAUCK, R. L., COOPER, J. A., YUAN, X. & TUAN, R. S. 2007. Engineering controllable anisotropy in electrospun biodegradable nanofibrous scaffolds for musculoskeletal tissue engineering. *Journal of Biomechanics*, 40, 1686-1693.

LIAO, I., LIU, J., BURSAC, N. & LEONG, K. 2008. Effect of electromechanical stimulation on the maturation of myotubes on aligned electrospun fibers. *Cellular and Molecular Bioengineering*, 1, 133-145.

LIAO, W., OKADA, M., SAKAMOTO, F., OKITA, N., INAMI, K., NISHIURA, A., HASHIMOTO, Y. & MATSUMOTO, N. 2013. *In vitro* human periodontal ligament-like tissue formation with porous poly-l-lactide matrix. *Materials Science and Engineering: C*, 33(6), 3273-3280.

LIM, S. H., LIU, X. Y., SONG, H., YAREMA, K. J. & MAO, H.-Q. 2010. The effect of nanofiber-guided cell alignment on the preferential differentiation of neural stem cells. Biomaterials, 31, 9031-9039.

LIU, M., DAI, J., LIN, Y., YANG, L., DONG, H., LI, Y., DING, Y. & DUAN, Y. 2012. Effect of the cyclic stretch on the expression of osteogenesis genes in human periodontal ligament cells. *Gene*, 491, 187-193.

LIU, X., CHEN, J., GILMORE, K., HIGGINS, M., LIU, Y. & WALLACE, G. 2010. Guidance of neurite outgrowth on aligned electrospun polypyrrole/poly (styrene isobutylene styrene) fiber platforms. *Journal of Biomedical Materials Research Part A*, 94, 1004-1011.

LIU, Y., JI, Y., GHOSH, K., CLARK, R., HUANG, L. & RAFAILOVICH, M. 2009. Effects of fiber orientation and diameter on the behavior of human dermal fibroblasts on electrospun PMMA scaffolds. *Journal of Biomedical Materials Research Part A*, 90, 1092-1106.

LIU, Y., ZHENG, Y., DING, G., FANG, D., ZHANG, C., BARTOLD, P., GRONTHOS, S., SHI, S. & WANG, S. 2008. periodontal ligament stem cell mediated treatment for periodontitis in miniature swine. *Stem Cells*, 26, 1065-1073.

LONG, P., HU, J., PIESCO, N., BUCKLEY, M. & AGARWAL, S. 2001. Low magnitude of tensile strain inhibits IL-1β-dependent induction of pro-inflammatory cytokines and induces synthesis of IL-10 in human periodontal ligament cells *in vitro*. *Journal of Dental Research*, 80, 1416-1420.

LUCKPROM, P., WONGKHANTEE, S., YONGCHAITRAKUL, T. & PAVASANT, P. 2010. Adenosine triphosphate stimulates RANKL expression through P2Y1 receptor–cyclo-oxygenase-dependent pathway in human periodontal ligament cells. *Journal of Periodontal Research*, 45, 404-411.

LUMPKINS, S. B., PIERRE, N. & MCFETRIDGE, P. S. 2008. A mechanical evaluation of three decellularization methods in the design of a xenogeneic scaffold for tissue engineering the temporomandibular joint disc. *Acta Biomaterialia*, 4, 808-816.

MA, J., HE, X. & JABBARI, E. 2011. Osteogenic differentiation of marrow stromal cells on random and aligned electrospun poly(L-lactide) nanofibers. *Annals of Biomedical Engineering,* 39, 14-25.

MACNEIL, R. L., BERRY, J., D'ERRICO, J., STRAYHORN, C. & SOMERMAN, M. J. 1995. Localization and expression of osteopontin in mineralized and nonmineralized tissues of the periodontium. *Annals of the New York Academy of Sciences*, 760, 166-176.

MARIOTTI, A. & COCHRAN, D. L. 1990. Characterization of fibroblasts derived from human periodontal ligament and gingiva. *Journal of Periodontology*, 61, 103-111.

MARTINEZ, E., ENGEL, E., PLANELL, J. & SAMITIER, J. 2009. Effects of artificial micro-and nano-structured surfaces on cell behaviour. *Annals of Anatomy*, 191, 126-135.

MATSUZAKA, K., FRANK WALBOOMERS, X., YOSHINARI, M., INOUE, T. & JANSEN, J. 2003. The attachment and growth behavior of osteoblast-like cells on microtextured surfaces. *Biomaterials*, 24, 2711-2719.

MCCLURE, M., SELL, S., AYRES, C., SIMPSON, D. & BOWLIN, G. 2009. Electrospinning-aligned and random polydioxanone–polycaprolactone–silk fibroin-blended scaffolds: geometry for a vascular matrix. *Biomedical Materials*, 4, 055010-055018.

MCCULLOUCH, C. A. G. & KNOWLES, G. C. 1993. Deficiencies in collagen phagocytosis by human fibroblasts *in vitro*: A mechanism for fibrosis?. *Journal of Cellular Physiology*, 155, 461-471.

MCKEE, M., ZALZAL, S. & NANCI, A. 1996. Extracellular matrix in tooth cementum and mantle dentin: localization of osteopontin and other noncollagenous proteins, plasma proteins, and glycoconjugates by electron microscopy. *The Anatomical Record Part A: Discoveries in Molecular, Cellular, and Evolutionary Biology*, 245, 293-312.

MEHTA, R., KUMAR, V., BHUNIA, H. & UPADHYAY, S. 2005. Synthesis of poly (lactic acid): A review. *Polymer Reviews*, 45, 325-349.

MEYLE, J., WOLBURG, H. & VON RECUM, A. 1993. Surface micromorphology and cellular interactions. *Journal of Biomaterials Applications*, 7, 362-374.

MONNOUCHI, S., MAEDA, H., FUJII, S., TOMOKIYO, A., KONO, K. & AKAMINE, A. 2011. The roles of angiotensin II in stretched periodontal ligament cells. *Journal of Dental Research*, 90, 181-185.

MULLEN, C., HAUGH, M., SCHAFFLER, M., MAJESKA, R. & MCNAMARA, L. 2013. Osteocyte differentiation is regulated by extracellular matrix stiffness and intercellular separation. *Journal of the Mechanical Behavior of Biomedical Materials*, 28, 183-194.

NAGATOMO, K., KOMAKI, M., SEKIYA, I., SAKAGUCHI, Y., NOGUCHI, K., ODA, S., MUNETA, T. & ISHIKAWA, I. 2006. Stem cell properties of human periodontal ligament cells. *Journal of Periodontal Research*, 41, 303-310.

NAKAO, K., GOTO, T., GUNJIGAKE, K., KONOO, T., KOBAYASHI, S. & YAMAGUCHI, K. 2007. Intermittent force induces high RANKL expression in human periodontal ligament cells. *Journal of Dental Research*, 86, 623-628.

NAKAYAMA, G., CATON, M., NOVA, M. & PARANDOOSH, Z. 1997. Assessment of the Alamar Blue assay for cellular growth and viability *in vitro*. *Journal of Immunological Methods*, 204(2), 205-208.

NANCI, A. & BOSSHARDT, D. D. 2006. Structure of periodontal tissues in health and disease. *Periodontology 2000*, 40, 11-28.

NANCI, A. 2008. Ten Cate's Oral Histology: development, structure, and function, Missouri, *Mosby*.

NEMOTO, E., KOSHIKAWA, Y., KANAYA, S., TSUCHIYA, M., TAMURA, M., SOMERMAN, M. J. & SHIMAUCHI, H. 2009. Wnt signaling inhibits cementoblast differentiation and promotes proliferation. *Bone*, 44, 805-812.

NEMOTO, T., KAJIYA, H., TSUZUKI, T., TAKAHASHI, Y. & OKABE, K. 2010. Differential induction of collagens by mechanical stress in human periodontal ligament cells*. Archives of Oral Biology*, 55, 981-987.

NEWMAN, M. G., TAKEI, H., KLOKKEVOLD, P. R. & CARRANZA, F. A. 2011. Carranza's clinical periodontology, *Elsevier health sciences*.

NIE, Z. & KUMACHEVA, E. 2008. Patterning surfaces with functional polymers. *Nature Materials*, 7, 277-290.

NIVISON-SMITH, L. & WEISS, A. S. 2012. Alignment of human vascular smooth muscle cells on parallel electrospun synthetic elastin fibers. *Journal of Biomedical Materials Research. Part A*, 100, 155-161.

NOHUTCU, R. M., MCCAULEY, L. K., KOH, A. J. & SOMERMAN, M. J. 1997. Expression of extracellular matrix proteins in human periodontal ligament cells during mineralization *in vitro*. *Journal of Periodontology*, 68, 320-327.

NOHUTCU, R. M., MECAULEY, L. K., SHIGEYAMA, Y. & SOMERMAN, M. J. 1996. Expression of mineral-associated proteins by periodontal ligament cells: *In vitro* vs. *ex vivo*. *Journal of Periodontal Research*, 31, 369-372.

NORRIS, R. A., DAMON, B., MIRONOV, V., KASYANOV, V., RAMAMURTHI, A., MORENO-RODRIGUEZ, R., TRUSK, T., POTTS, J. D., GOODWIN, R. L., DAVIS, J., HOFFMAN, S., WEN, X., SUGI, Y., KERN, C. B., MJAATVEDT, C. H., TURNER, D. K., OKA, T., CONWAY, S. J., MOLKENTIN, J. D., FORGACS, G. & MARKWALD, R. R. 2007. Periostin regulates collagen fibrillogenesis and the biomechanical properties of connective tissues. *Journal of Cellular Biochemistry*, 101, 695-711.

NYGAARD ØSTBY, P., BAKKE, V., NESDAL, O., NILSSEN, H., SUSIN, C. & WIKESJÖ, U. 2008. Periodontal healing following reconstructive surgery: effect of guided tissue regeneration using a bioresorbable barrier device when combined with autogenous bone grafting. A randomized controlled clinical trial. *Journal of Clinical Periodontology*, 35, 37-43.

NYGAARD ØSTBY, P., BAKKE, V., NESDAL, O., SUSIN, C. & WIKESJÖ, U. 2010. Periodontal healing following reconstructive surgery: effect of guided tissue

regeneration using a bioresorbable barrier device when combined with autogenous bone grafting. A randomized controlled trial 10 year follow up. *Journal of Clinical Periodontology*, 37, 366-373.

NYMAN, S., GOTTLOW, J., KARRING, T. & LINDHE, J. 1982. The regenerative potential of the periodontal ligament. An experimental study in the monkey. *Journal of Clinical Periodontology*, 9, 257-265.

OKUBO, K., KOBAYASHI, M., TAKIGUCHI, T., TAKADA, T., OHAZAMA, A., OKAMATSU, Y. & HASEGAWA, K. 2003. Participation of endogenous IGF-I and TGF-β1 with enamel matrix derivative-stimulated cell growth in human periodontal ligament cells. *Journal of Periodontal Research*, 38, 1-9.

OMAE, H., ZHAO, C., SUN, Y. L., AN, K. N. & AMADIO, P. C. 2009. Multilayer tendon slices seeded with bone marrow stromal cells: a novel composite for tendon engineering. *Journal of Orthopaedic Research*, 27, 937-942.

ONO, Y., SENSUI, H., OKUTSU, S. & NAGATOMI, R. 2007. Notch2 negatively regulates myofibroblastic differentiation of myoblasts. *Journal of Cellular Physiology*, 210(2), 358-369.

OORTGIESEN, D. A., YU, N., BRONCKERS, A. L., YANG, F., WALBOOMERS, X. F. & JANSEN, J. A. 2012. A three-dimensional cell culture model to study the mechano-biological behavior in periodontal ligament regeneration. *Tissue Engineering Part C: Methods*, 18, 81-89.

OTSUKA, K., PITARU, S., OVERALL, C. M., AUBIN, J. E. & SODEK, J. 1988. Biochemical comparison of fibroblast populations from different periodontal tissues: Characterization of matrix protein and collagenolytic enzyme synthesis. *Biochemistry and Cell Biology*, 66, 167-176.

OZAKI, S., KANEKO, S., PODYMA-INOUE, K., YANAGISHITA, M. & SOMA, K. 2005. Modulation of extracellular matrix synthesis and alkaline phosphatase activity of periodontal ligament cells by mechanical stress. *Journal of Periodontal Research*, 40, 110-117.

PALIOTO, D. B., COLETTA, R. D., GRANER, E., JOLY, J. C. & DE LIMA, A. F. M. 2004. The influence of enamel matrix derivative associated with insulin-like growth factor-I on periodontal ligament fibroblasts. *Journal of Periodontology*, 75, 498-504.

PALIOTO, D. B., COLETTA, R. D., GRANER, E., JOLY, J. C. & DE LIMA, A. F. M. 2004. The influence of enamel matrix derivative associated with insulin-like growth factor-I on periodontal ligament fibroblasts. *Journal of Periodontology*, 75, 498-504.

PALIOTO, D. B., RODRIGUES, T. L., MARCHESAN, J. T., BELOTI, M. M., DE OLIVEIRA, P. T. & ROSA, A. L. 2011. Effects of enamel matrix derivative and transforming growth factor-b1 on human osteoblastic cells. *Head and Face Medicine*, 7, 13-21.

PARK, K. S., LEE, E. G. & SON, Y. 2013. Uniaxial cyclic strain stimulates cell proliferation and secretion of IL-6 and VEGF of human dermal fibroblasts seeded

on chitosan scaffolds. *Journal of Biomedical Materials Research Part A*, 102(7), 2268-2276.

PARKAR, M. H. & TONETTI, M. 2004. Gene expression profiles of periodontal ligament cells treated with enamel matrix proteins *in vitro*: analysis using cDNA arrays. *Journal of Periodontology*, 75, 1539-1546.

PAULANDER, J., WENNSTROM, J. L., AXELSSON, P. & LINDHE, J. 2004. Some risk factors for periodontal bone loss in 50-year-old individuals. A 10-year cohort study. *Journal of Clinical Periodontology*, 31, 489-96.

PERUZZO, D. C., BENATTI, B. B., AMBROSANO, G. M., NOGUEIRA-FILHO, G. R., SALLUM, E. A., CASATI, M. Z. & NOCITI, F. H., JR. 2007. A systematic review of stress and psychological factors as possible risk factors for periodontal disease. *Journal of Periodontology*, 78, 1491-504.

PINKERTON, M. N., WESCOTT, D. C., GAFFEY, B. J., BEGGS, K. T., MILNE, T. J. & MEIKLE, M. C. 2008. Cultured human periodontal ligament cells constitutively express multiple osteotropic cytokines and growth factors, several of which are responsive to mechanical deformation. *Journal of Periodontal Research*, 43, 343-351.

PITARU, S., NARAYANAN, S., OLSON, S., SAVION, N., HEKMATI, H., ALT, I. & METZGER, Z. 1995. Specific cementum attachment protein enhances selectively the attachment and migration of periodontal cells to root surfaces. *Journal of Periodontal Research*, 30, 360-368.

PITARU, S., TAL, H., SOLDINGER, M., AZAR-AVIDAN, O. & NOFF, M. 1987. Collagen membranes prevent the apical migration of epithelium during periodontal wound healing. *Journal of Periodontal Research*, 22, 331-333.

PREMARAJ, S., SOUZA, I. & PREMARAJ, T. 2011. Mechanical loading activates β-catenin signaling in periodontal ligament cells. *The Angle Orthodontist*, 81, 592-599.

PRIDGEN, B. C., WOON, C. Y., KIM, M., THORFINN, J., LINDSEY, D., PHAM, H. & CHANG, J. 2011. Flexor tendon tissue engineering: acellularization of human flexor tendons with preservation of biomechanical properties and biocompatibility. *Tissue Engineering Part C: Methods*, 17, 819-828.

RAHMAN, M. S. & TSUCHIYA, T. 2001. Enhancement of chondrogenic differentiation of human articular chondrocytes by biodegradable polymers. *Tissue Engineering*, 7, 781-790.

RAMAKRISHNA, S., VENUGOPAL, J. & LIAO, S. 2011. Engineered Biomimetic Nanofibers for Regenerative Medicine. *Advances in Science and Technology*, 76, 114-124.

RASAL, R., JANORKAR, A. & HIRT, D. 2010. Poly (lactic acid) modifications. *Progress in Polymer Science*, 35, 338-356.

REICHARDT, A., ARSHI, A., SCHUSTER, P., POLCHOW, B., SHAKIBAEI, M., GRIES, T., HENRICH, W., HETZER, R. & LUEDERS, C. 2012. Custom-made generation of three-dimensional nonwovens composed of polyglycolide or polylactide for the cardiovascular tissue engineering. *Journal of Biomaterials and Tissue Engineering*, 2, 322-329.

RIEDER, E., KASIMIR, M.-T., SILBERHUMER, G., SEEBACHER, G., WOLNER, E., SIMON, P. & WEIGEL, G. 2004. Decellularization protocols of porcine heart valves differ importantly in efficiency of cell removal and susceptibility of the matrix to recellularization with human vascular cells. *The Journal of Thoracic and Cardiovascular Surgery*, 127, 399-405.

RIOS, H. F., MA, D., XIE, Y., GIANNOBILE, W. V., BONEWALD, L. F., CONWAY, S. J. & FENG, J. Q. 2008. Periostin is essential for the integrity and function of the periodontal ligament during occlusal loading in mice. *Journal of Periodontology*, 79, 1480-1490.

RIPAMONTI, U. & RENTON, L. 2006. Bone morphogenetic proteins and the induction of periodontal tissue regeneration. *Periodontology 2000*, 41, 73-87.

RODRIGUES, T. L. S., MARCHESAN, J. T., COLETTA, R. D., NOVAES JR, A. B., GRISI, M. F. M., SOUZA, S. L. S., TABA JR, M. & PALIOTO, D. B. 2007. Effects of enamel matrix derivative and transforming growth factor-β1 on human periodontal ligament fibroblasts. *Journal of Clinical Periodontology,* 34, 514-522.

ROSS, E. A., WILLIAMS, M. J., HAMAZAKI, T., TERADA, N., CLAPP, W. L., ADIN, C., ELLISON, G. W., JORGENSEN, M. & BATICH, C. D. 2009. Embryonic stem cells proliferate and differentiate when seeded into kidney scaffolds. *Journal of the American Society of Nephrology*, 20, 2338-2347.

ROSSA JR, C., MARCANTONIO JR, E., CIRELLI, J., MARCANTONIO, R., SPOLIDORIO, L. & FOGO, J. 2000. Regeneration of Class III furcation defects with basic fibroblast growth factor (b-FGF) associated with GTR. A descriptive and histometric study in dogs. *Journal of Periodontology*, 71, 775-784.

SAITO, M., IWASE, M., MASLAN, S., NOZAKI, N., YAMAUCHI, M., HANDA, K., TAKAHASHI, O., SATO, S., KAWASE, T. & TERANAKA, T. 2001. Expression of cementum-derived attachment protein in bovine tooth germ during cementogenesis. *Bone*, 29, 242-248.

SAITO, Y., YOSHIZAWA, T., TAKIZAWA, F., IKEGAME, M., ISHIBASHI, O., OKUDA, K., HARA, K., ISHIBASHI, K., OBINATA, M. & KAWASHIMA, H. 2002. A cell line with characteristics of the periodontal ligament fibroblasts is negatively regulated for mineralization and Runx2/Cbfa1/Osf2 activity, part of which can be overcome by bone morphogenetic protein-2. *Journal of Cell Science*, 115, 4191-4200.

SAMINATHAN, A., VINOTH, K., LOW, H., CAO, T. & MEIKLE, M. 2013. Engineering three-dimensional constructs of the periodontal ligament in hyaluronan-gelatin hydrogel films and a mechanically active environment. *Journal of Periodontal Research*, 48(6), 790-801.

SANT'ANA, A. C., MARQUES, M. M., BARROSO, E. C., PASSANEZI, E. & DE REZENDE, M. L. R. 2007. Effects of TGF-β1, PDGF-BB, and IGF-1 on the rate of proliferation and adhesion of a periodontal ligament cell lineage *in vitro*. *Journal of Periodontology*, 78, 2007-2017.

SATO, Y., KIKUCHI, M., OHATA, N., TAMURA, M. & KUBOKI, Y. 2004. Enhanced cementum formation in experimentally induced cementum defects of the root surface with the application of recombinant basic fibroblast growth factor in collagen gel *in vivo*. *Journal of Periodontology*, 75, 243-248.

SAWAGUCHI, N., MAJIMA, T., FUNAKOSHI, T., SHIMODE, K., HARADA, K., MINAMI, A. & NISHIMURA, S.-I. 2010. Effect of cyclic three-dimensional strain on cell proliferation and collagen synthesis of fibroblast-seeded chitosan-hyaluronan hybrid polymer fiber. *Journal of Orthopaedic Science*, 15, 569-577.

SCHELLER, E., CHANG, J. & WANG, C. 2008. Wnt/β-catenin inhibits dental pulp stem cell differentiation. *Journal of Dental Research*, 87, 126-130.

SCHNEIDER, T., KOHL, B., SAUTER, T., KRATZ, K., LENDLEIN, A., ERTEL, W. & SCHULZE-TANZIL, G. 2012. Influence of fiber orientation in electrospun polymer scaffolds on viability, adhesion and differentiation of articular chondrocytes. *Clinical Hemorheology and Microcirculation*, 52, 325-336.

SCHWARZ, S., KOERBER, L., ELSAESSER, A. F., GOLDBERG-BOCKHORN, E., SEITZ, A. M., DÜRSELEN, L., IGNATIUS, A., WALTHER, P., BREITER, R. & ROTTER, N. 2012. Decellularized cartilage matrix as a novel biomatrix for cartilage tissue-engineering applications. *Tissue Engineering Part A*, 18, 2195-2209.

SCOTT, A., DANIELSON, P., ABRAHAM, T., FONG, G., SAMPAIO, A. & UNDERHILL, T. 2011. Mechanical force modulates scleraxis expression in bioartificial tendons. *Journal of Musculoskeletal and Neuronal Interactions*, 11, 124-132.

SEO, B. M., MIURA, M., GRONTHOS, S., BARTOLD, P. M., BATOULI, S., BRAHIM, J., YOUNG, M., ROBEY, P. G., WANG, C. Y. & SHI, S. 2004. Investigation of multipotent postnatal stem cells from human periodontal ligament. *Lancet*, 364, 149-155.

SEO, T., CHA, S., KIM, T.-I., LEE, J.-S. & WOO, K. M. 2012. Porphyromonas gingivalis-derived lipopolysaccharide-mediated activation of MAPK signaling regulates inflammatory response and differentiation in human periodontal ligament fibroblasts. *The Journal of Microbiology*, 50, 311-319.

SEO, T., CHA, S., WOO, K. M., PARK, Y.-S., CHO, Y.-M., LEE, J.-S. & KIM, T.-I. 2011. Synergic induction of human periodontal ligament fibroblast cell death by nitric oxide and N-methyl-D-aspartic acid receptor antagonist. Journal *of Periodontal & Implant Science*, 41, 17-22.

SHANG, S., YANG, F., CHENG, X., WALBOOMERS, X. F. & JANSEN, J. A. 2010. The effect of electrospun fibre alignment on the behaviour of rat periodontal ligament cells. *European Cells and Materials*, 19, 180-192.

SHEETS, K., WUNSCH, S., NG, C. & NAIN, A. S. 2013. Shape-dependent cell migration and focal adhesion organization on suspended and aligned nanofiber scaffolds. *Acta Biomaterialia*, 9, 7169–7177.

SHI, S., BARTOLD, P. M., MIURA, M., SEO, B. M., ROBEY, P. G. & GRONTHOS, S. 2005. The efficacy of mesenchymal stem cells to regenerate and repair dental structures. *Orthodontics and Craniofacial Research*, 8, 191-199.

SHI, Y. & MASSAGUÉ, J. 2003. Mechanisms of TGF-β signaling from cell membrane to the nucleus. *Cell*, 113, 685-700.

SHIMONISHI, M., HATAKEYAMA, J., SASANO, Y., TAKAHASHI, N., UCHIDA, T., KIKUCHI, M. & KOMATSU, M. 2007. *In vitro* differentiation of epithelial cells cultured from human periodontal ligament. *Journal of Periodontal Research*, 42, 456-465.

SHIRAI, K., ISHISAKI, A., KAKU, T., TAMURA, M. & FURUICHI, Y. 2009. Multipotency of clonal cells derived from swine periodontal ligament and differential regulation by fibroblast growth factor and bone morphogenetic protein. *Journal of Periodontal Research*, 44, 238-247.

SICILIANO, V. I., ANDREUCCETTI, G., SICILIANO, A. I., BLASI, A., SCULEAN, A. & SALVI, G. E. 2011. Clinical outcomes after treatment of non-contained intrabony defects with enamel matrix derivative or guided tissue regeneration: a 12-month randomized controlled clinical trial. *Journal of Periodontology*, 82, 62-71.

SMITH, P., KROHN, R. I., HERMANSON, G., MALLIA, A., GARTNER, F., PROVENZANO, M., FUJIMOTO, E., GOEKE, N., OLSON, B. & KLENK, D. 1985. Measurement of protein using bicinchoninic acid. Analytical Biochemistry, 150, 76-85.

SOMERMAN, M. 2011. Growth factors and periodontal engineering. *Journal of Dental Research*, 90, 7-8.

SOMERMAN, M. J., ARCHER, S. Y., IMM, G. R. & FOSTER, R. A. 1988. A comparative study of human periodontal ligament cells and gingival fibroblasts *in vitro*. *Journal of Dental Research*, 67, 66-70.

SOMERMAN, M. J., YOUNG, M. F., FOSTER, R. A., MOEHRING, J. M., IMM, G. & SAUK, J. J. 1990. Characteristics of human periodontal ligament cells *in vitro*. *Archives of Oral Biology*, 35, 241-247.

SOWMYA, N., KUMAR, A. & MEHTA, D. 2010. Clinical evaluation of regenerative potential of type I collagen membrane along with xenogenic bone graft in the treatment of periodontal intrabony defects assessed with surgical re-entry and radiographic linear and densitometric analysis. *Journal of Indian Society of Periodontology*, 14(1), 23-29.

STABHOLZ, A., SOSKOLNE, W. & SHAPIRA, L. 2010. Genetic and environmental risk factors for chronic periodontitis and aggressive periodontitis. *Periodontology 2000*, 53, 138-153.

SUNDARARAGHAVAN, H. G., SAUNDERS, R. L., HAMMER, D. A. & BURDICK, J. A. 2012. Fiber alignment directs cell motility over chemotactic gradients. *Biotechnology and Bioengineering*, 110, 1249-1254.

SUZUKI, S., NAGANO, T., YAMAKOSHI, Y., GOMI, K., ARAI, T., FUKAE, M., KATAGIRI, T. & OIDA, S. 2005. Enamel matrix derivative gel stimulates signal transduction of BMP and TGF-β. *Journal of Dental Research*, 84, 510-514.

SZYNKARUK, M., KEMP, S. W., WOOD, M. D., GORDON, T. & BORSCHEL, G. H. 2012. Experimental and clinical evidence for use of decellularized nerve allografts in peripheral nerve gap reconstruction. *Tissue Engineering Part B: Reviews*, 19, 83-96.

TANAKA, K., IWASAKI, K., FEGHALI, K. E., KOMAKI, M., ISHIKAWA, I. & IZUMI, Y. 2011. Comparison of characteristics of periodontal ligament cells obtained from outgrowth and enzyme-digested culture methods. *Archives of Oral Biology*, 56, 380-388.

TANIMOTO, K., KUNIMATSU, R., TANNE, Y., HUANG, Y.-C., MICHIDA, M., YOSHIMI, Y., MIYAUCHI, M., TAKATA, T. & TANNE, K. 2012. Differential effects of amelogenin on mineralization of cementoblasts and periodontal ligament cells. *Journal of Periodontology*, 83, 672-679.

TATAKIS, D., WIKESJÖ, U., RAZI, S., SIGURDSSON, T., LEE, M., NGUYEN, T., ONGPIPATTANAKUL, B. & HARDWICK, R. 2000. Periodontal repair in dogs: effect of transforming growth factor- 1 on alveolar bone and cementum regeneration. *Journal of Clinical Periodontology*, 27, 698-704.

TEH, T. K., TOH, S.-L. & GOH, J. C. 2013. Aligned Fibrous Scaffolds for Enhanced Mechanoresponse and Tenogenesis of Mesenchymal Stem Cells. *Tissue Engineering Part A*, 19, 1360-1372.

THOMAS, V., JOSE, M. V., CHOWDHURY, S., SULLIVAN, J. F., DEAN, D. R. & VOHRA, Y. K. 2006. Mechano-morphological studies of aligned nanofibrous scaffolds of polycaprolactone fabricated by electrospinning. *Journal of Biomaterials Science, Polymer Edition*, 17, 969-984.

THOMBRE, V., KOUDALE, S. & BHONGADE, M. 2012. Comparative evaluation of the effectiveness of coronally positioned flap with or without acellular dermal matrix allograft in the treatment of multiple marginal gingival recession defects. *The International journal of Periodontics and Restorative Dentistry*, 33, 88-94.

TONETTI, M. S., FOURMOUSIS, I., SUVAN, J., CORTELLINI, P., BRÄGGER, U. & LANG, N. P. 2004. Healing, post-operative morbidity and patient perception of outcomes following regenerative therapy of deep intrabony defects. *Journal of Clinical Periodontology*, 31, 1092-1098.

TONETTI, M. S., LANG, N. P., CORTELLINI, P., SUVAN, J. E., ADRIAENS, P., DUBRAVEC, D., FONZAR, A., FOURMOUSIS, I., MAYFIELD, L. & ROSSI, R. 2002. Enamel matrix proteins in the regenerative therapy of deep intrabony defects. *Journal of Clinical Periodontology*, 29, 317-325.

TONG, H., WANG, M. & LU, W. 2010. Electrospun poly (hydroxybutyrate-co-hydroxyvalerate) fibrous membranes consisting of parallel-aligned fibers or cross-aligned fibers: characterization and biological evaluation. *Journal of Biomaterials Science. Polymer Edition*, 22, 2475-2497.

TRUBIANI, O., ORSINI, G., ZINI, N., DI IORIO, D., PICCIRILLI, M., PIATTELLI, A. & CAPUTI, S. 2008. Regenerative potential of human periodontal ligament derived stem cells on three dimensional biomaterials: A morphological report. *Journal of Biomedical Materials Research Part A*, 87, 986-993.

TRUONG, Y., GLATTAUER, V., LANG, G., HANDS, K., KYRATZIS, I., WERKMEISTER, J. & RAMSHAW, J. 2010. A comparison of the effects of fibre alignment of smooth and textured fibres in electrospun membranes on fibroblast cell adhesion. *Biomedical Materials*, 5, 025005-025012.

TUDORACHE, I., CEBOTARI, S., STURZ, G., KIRSCH, L., HURSCHLER, C., HILFIKER, A., HAVERICH, A. & LICHTENBERG, A. 2007. Tissue engineering of heart valves: biomechanical and morphological properties of decellularized heart valves. *The Journal of Heart Valve Disease*, 16(5), 567-573.

TULLOCH, N. L., MUSKHELI, V., RAZUMOVA, M. V., KORTE, F. S., REGNIER, M., HAUCH, K. D., PABON, L., REINECKE, H. & MURRY, C. E. 2011. Growth of engineered human myocardium with mechanical loading and vascular coculture*Novelty and significance. Circulation Research*, 109, 47-59.

VAN DER PAUW, M. T., VAN DEN BOS, T., EVERTS, V. & BEERTSEN, W. 2000. Enamel matrix-derived protein stimulates attachment of periodontal ligament fibroblasts and enhances alkaline phosphatase activity and transforming growth factor β1 release of periodontal ligament and gingival fibroblasts. *Journal of Periodontology*, 71, 31-43.

VAQUETTE, C., KAHN, C., FROCHOT, C., NOUVEL, C., SIX, J., DE ISLA, N., LUO, L., COOPER WHITE, J., RAHOUADJ, R. & WANG, X. 2010. Aligned poly (L lactic co e caprolactone) electrospun microfibers and knitted structure: A novel composite scaffold for ligament tissue engineering. *Journal of Biomedical Materials Research Part A*, 94, 1270-1282.

VAVKEN, P., JOSHI, S. & MURRAY, M. M. 2009. TRITON-X is most effective among three decellularization agents for ACL tissue engineering. *Journal of Orthopaedic Research*, 27, 1612-1618.

VOROTNIKOVA, E., MCINTOSH, D., DEWILDE, A., ZHANG, J., REING, J. E., ZHANG, L., CORDERO, K., BEDELBAEVA, K., GOUREVITCH, D. & HEBER-KATZ, E. 2010. Extracellular matrix-derived products modulate endothelial and progenitor cell migration and proliferation *in vitro* and stimulate regenerative healing *in vivo*. *Matrix Biology*, 29, 690-700.

WALLIS, J. M., BORG, Z. D., DALY, A. B., DENG, B., BALLIF, B. A., ALLEN, G. B., JAWORSKI, D. M. & WEISS, D. J. 2012. Comparative assessment of detergent-based protocols for mouse lung de-cellularization and re-cellularization. *Tissue Engineering Part C: Methods*, 18, 420-432.

WANG, H. M., NANDA, V. & RAO, L. G. 1980. Specific immunohistochemical localization of type III collagen in porcine periodontal tissues using the peroxidase-antiperoxidase method. *Journal of Histochemistry and Cytochemistry*, 28, 1215-1223.

WANG, H., MULLINS, M., CREGG, J., MCCARTHY, C. & GILBERT, R. 2010. Varying the diameter of aligned electrospun fibers alters neurite outgrowth and Schwann cell migration. *Acta Biomaterialia*, 6, 2970-2978.

WANG, J., YE, R., WEI, Y., WANG, H., XU, X., ZHANG, F., QU, J., ZUO, B. & ZHANG, H. 2012. The effects of electrospun TSF nanofiber diameter and alignment on neuronal differentiation of human embryonic stem cells. *Journal of Biomedical Materials Research Part A*, 100, 632-645.

WANG, Y., LI, Y., FAN, X., ZHANG, Y., WU, J. & ZHAO, Z. 2011. Early proliferation alteration and differential gene expression in human periodontal ligament cells subjected to cyclic tensile stress. *Archives of Oral Biology*, 56, 177-186.

WEBB, K., HITCHCOCK, R. W., SMEAL, R. M., LI, W., GRAY, S. D. & TRESCO, P. A. 2006. Cyclic strain increases fibroblast proliferation, matrix accumulation, and elastic modulus of fibroblast-seeded polyurethane constructs. *Journal of Biomechanics*, 39, 1136-1144.

WEBER, B., DIJKMAN, P. E., SCHERMAN, J., SANDERS, B., EMMERT, M. Y., GRÜNENFELDER, J., VERBEEK, R., BRACHER, M., BLACK, M. & FRANZ, T. 2013. Off-the-shelf human decellularized tissue-engineered heart valves in a non-human primate model. *Biomaterials*, 34(30), 7269-7280.

WEN, W., CHAU, E., JACKSON-BOETERS, L., ELLIOTT, C., DALEY, T. & HAMILTON, D. 2010. TGF-β1 and FAK regulate periostin expression in PDL fibroblasts. *Journal of Dental Research*, 89, 1439-1443.

WEN, Y., YUAN, J.-M., DANG, R.-S., YANG, X.-Q., XIONG, S.-H., SHEN, M.-R., ZHANG, Y.-Z. & ZHANG, C.-S. 2012. Construction of tissue-engineered venous valves *in vitro* using two types of progenitor cells and decellularized scaffolds category: Original. *Open Tissue Engineering and Regenerative Medicine Journal*, 5, 9-16.

WHITED, B. M. & RYLANDER, M. N. 2013. The influence of electrospun scaffold topography on endothelial cell morphology, alignment, and adhesion in response to fluid flow. *Biotechnology and Bioengineering*, 111(1), 184-195.

WOODS, T. & GRATZER, P. F. 2005. Effectiveness of three extraction techniques in the development of a decellularized bone–anterior cruciate ligament–bone graft. *Biomaterials*, 26, 7339-7349.

XIE, J., LI, X., LIPNER, J., MANNING, C., SCHWARTZ, A., THOMOPOULOS, S. & XIA, Y. 2010. “Aligned-to-random” nanofiber scaffolds for mimicking the structure of the tendon-to-bone insertion site. *Nanoscale*, 2, 923-926.

XIE, J., WILLERTH, S., LI, X., MACEWAN, M., RADER, A., SAKIYAMA-ELBERT, S. & XIA, Y. 2009. The differentiation of embryonic stem cells seeded on electrospun nanofibers into neural lineages. *Biomaterials*, 30, 354-362.

XU, C., INAI, R., KOTAKI, M. & RAMAKRISHNA, S. 2004. Aligned biodegradable nanofibrous structure: a potential scaffold for blood vessel engineering. *Biomaterials*, 25, 877-886.

YAMAGUCHI, N., CHIBA, M. & MITANI, H. 2002. The induction of c-fos mRNA expression by mechanical stress in human periodontal ligament cells. *Archives of Oral Biology*, 47, 465-471.

YAMAMOTO, T., KITA, M., KIMURA, I., OSEKO, F., TERAUCHI, R., TAKAHASHI, K., KUBO, T. & KANAMURA, N. 2006. Mechanical stress induces expression of cytokines in human periodontal ligament cells. *Oral Diseases*, 12, 171-175.

YANG, F., MURUGAN, R., RAMAKRISHNA, S., WANG, X., MA, Y.-X. & WANG, S. 2004. Fabrication of nano-structured porous PLLA scaffold intended for nerve tissue engineering. *Biomaterials*, 25, 1891-1900.

YANG, F., MURUGAN, R., WANG, S. & RAMAKRISHNA, S. 2005. Electrospinning of nano/micro scale poly(l-lactic acid) aligned fibers and their potential in neural tissue engineering. *Biomaterials*, 26, 2603-2610.

YANG, Y., LI, X., RABIE, A., FU, M. & ZHANG, D. 2006. Human periodontal ligament cells express osteoblastic phenotypes under intermittent force loading *in vitro*. *Frontiers in Bioscience*, 11, 776-781.

YANG, Y., ROSSI, F. & PUTNINS, E. 2010. Periodontal regeneration using engineered bone marrow mesenchymal stromal cells. Biomaterials, 12, 8574-8582.

YIN, Z., CHEN, X., CHEN, J., SHEN, W., HIEU NGUYEN, T., GAO, L. & OUYANG, H. 2010. The regulation of tendon stem cell differentiation by the alignment of nanofibers. *Biomaterials*, 31, 2163-2175.

YOSHIDA, R., VAVKEN, P. & MURRAY, M. M. 2012. Decellularization of bovine anterior cruciate ligament tissues minimizes immunogenic reactions to alpha-gal epitopes by human peripheral blood mononuclear cells. *The Knee*, 19, 672-675.

YU, B., LI, W., SONG, B. & WU, Y. 2013. Comparative study of the Triton X-100-sodium deoxycholate method and detergent-enzymatic digestion method for decellularization of porcine aortic valves. *European Review for Medical and Pharmacological Sciences*, 17, 2179-2184.

YU, N., PRODANOV, L., RIET, J. T., YANG, F., WALBOOMERS, X. F. & JANSEN, J. A. 2012. Regulation of periodontal ligament cell behaviour by cyclic mechanical loading and substrate nanotexture. *Journal of Periodontology*, 84, 1504-1513.

ZECHNER, D., FUJITA, Y., HÜLSKEN, J., MÜLLER, T., WALTHER, I., TAKETO, M. M., BRYAN CRENSHAW, E., BIRCHMEIER, W. & BIRCHMEIER, C. 2003. β-Catenin signals regulate cell growth and the balance between progenitor cell

expansion and differentiation in the nervous system. *Developmental Biology*, 258, 406-418.

ZEICHNER DAVID, M. 2006. Regeneration of periodontal tissues: cementogenesis revisited. *Periodontology 2000*, 41, 196-217.

ZHANG, X., SCHUPPAN, D., BECKER, J., REICHART, P. & GELDERBLOM, H. R. 1993. Distribution of undulin, tenascin, and fibronectin in the human periodontal ligament and cementum: Comparative immunoelectron microscopy with ultra-thin cryosections. *Journal of Histochemistry and Cytochemistry*, 41, 245-251.

ZHAO, Q., GONG, P., TAN, Z. & YANG, X. 2008. Differentiation control of transplanted mesenchymal stem cells (MSCs): A new possible strategy to promote periodontal regeneration. *Medical Hypotheses*, 70, 944-947.

ZHONG, W., XU, C., ZHANG, F., JIANG, X., ZHANG, X. & YE, D. 2008. Cyclic stretching force-induced early apoptosis in human periodontal ligament cells. *Oral Disease*s, 14, 270-276.

ZHOU, J., FRITZE, O., SCHLEICHER, M., WENDEL, H.-P., SCHENKE-LAYLAND, K., HARASZTOSI, C., HU, S. & STOCK, U. A. 2010. Impact of heart valve decellularization on 3D ultrastructure, immunogenicity and thrombogenicity. *Biomaterial*s, 31, 2549-2554.